January 2014

Synthesis, Selection, And Optimization Of Doped Zeolite Catalyst For The Nonbiological Production Of Lactic Acid Derivatives From Biomass Derived Carbohydrates

Clancy Raymond Rick Kadrmas

SYNTHESIS, SELECTION, AND OPTIMIZATION OF DOPED ZEOLITE CATALYST FOR THE NONBIOLOGICAL PRODUCTION OF LACTIC ACID DERIVATIVES FROM BIOMASS DERIVED CARBOHYDRATES

by

Clancy Raymond Rick Kadrmas
Bachelor of Science, University of North Dakota, 2006
Master of Science, Purdue University, 2010

A Dissertation
Submitted to the Graduate Faculty

of the

University of North Dakota

in partial fulfillment of the requirements

for the degree of

Doctor of Philosophy

Grand Forks, North Dakota
May
2014

This dissertation, submitted by Clancy Kadrmas in partial fulfillment of the requirements for the Degree of Doctor of Philosophy from the University of North Dakota, has been read by the Faculty Advisory Committee under whom the work has been done and is hereby approved.

Dr. Wayne Seames, Chairperson

Dr. Robert Wills, Committee Member

Dr. Yun Ji, Committee Member

Dr. Alena Kubatova, Committee Member

Dr. Evguenii Kozliak, Member-at-Large

This dissertation meets the standards for appearance, conforms to the style and format requirements of the Graduate School of the University of North Dakota, and is hereby approved.

Dean of the Graduate School

May 7, 2014

Date

PERMISSION

Title Synthesis, Selection, and Optimization of Doped Zeolite Catalyst for the Nonbiological Production of Lactic Acid Derivatives from Biomass Derived Carbohydrates

Department Chemical Engineering

Degree Doctor of Philosophy

In presenting this dissertation in partial fulfillment of the requirements for a graduate degree from the University of North Dakota, I agree that the library of this University shall make it freely available for inspection. I further agree that permission for extensive copying for scholarly purposes may be granted by the professor who supervised my dissertation work or, in his absence, by the chairperson of the department or the dean of the Graduate School. It is understood that any copying or publication or other use of this dissertation or part thereof for financial gain shall not be allowed without my written permission. It is also understood that due recognition shall be given to me and to the University of North Dakota in any scholarly use which may be made of any material in my dissertation.

Signature Clancy Kadrmas

Date April 30th, 2014

TABLE OF CONTENTS

LIST OF FIGURES

LIST OF TABLES

ACKNOWLEDGEMENTS

I would first like to thank my family and friends for all their support over the years. Especially my supportive wife, Lisa, who has always given her all so I may do the same. Also a special thanks to the Department of Chemical Engineering of UND for giving me this exciting opportunity. As a native of North Dakota and having spent my undergraduate years at UND, it is a real honor to achieve this lifetime goal at UND with this exceptional faculty. Additionally, I must thank my advisory committee for their encouragement, knowledge, resources, and opportunity to work on this challenging research. Finally, I need to thank my advisor, Dr. Wayne Seames, for his continuous support and understanding who has helped guide me to become an independent scholar. I will always be grateful for this life changing experience as I continue to strive to appreciate and comprehend what has yet to be known.

ABSTRACT

The objective of the overall project is to chemically synthesize fatty acids, hydrocarbons, other fuel constituents, or high value chemicals directly from biomass-derived carbohydrates (e.g. sugars generated using processes developed for the cellulosic ethanol industry). This work will look specifically at synthesizing lactic acid and its derivatives for later use to build chemically identical fuel components or high value chemicals.

We have built upon recent advancements in the literature using Sn-doped beta zeolite catalysts. Previous work has demonstrated that glucose can be chemically transformed into fructose then reduced to methyl lactate in a methanol solution. Since these reactions are not biochemical, increased reaction rates can be realized by increasing temperatures above those tolerated by biological entities. This should result in substantial savings in time and resources required to achieve the final end product. These savings can translate into more cost effective pathways to renewable fuels and chemicals.

The literature's reported best results focused on sucrose substrate with a methanol solvent and achieved overall methyl lactate yields of 64%, with >99% conversion of the feedstock. The challenge this research undertook was to maximize selective conversion of glucose substrate, the main product from the breakdown of biomass, in a water solvent as an economical and "green" universal solvent. An important part of this work was to carefully characterize side reaction constituents so that we can identify ways to transform these constituents into valuable co-products in the future.

When operating conditions were optimized roughly 80% of all products were determined utilizing GC-MS analysis technique, greatly increasing the known product yields reported in the literature. Lactic acid was maximized at 47% using Sn^{+4}-doped beta zeolite in pure water. Levulinic acid was maximized at 53% recovered using Sn^{+2}-doped beta zeolite in pure water. Methyl lactate, 22%, and methyl levulinate, 49%, were produced using Sn^{+4}-doped beta zeolite in methanol. These results are a key step in the overall project to produce fuel components and value chemicals from cellulosic biomass.

CHAPTER I
INTRODUCTION

Energy and food demands are projected to increase significantly with the steady increase in population and quality of life worldwide [1-5]. Taking into account the limited supply of fossil fuels and their associated enviromental concerns, the demand for renewable resources for fuels and chemicals is greatly increasing [2]. With a finite availability of landmass and water supply, production of renewable raw materials may impinge upon food production.

The efficient conversion of lignocellulosic biomass to fuel and high value chemicals would be useful to address the emerging food versus fuel/chemical dilemma for an ever increasing global population while minimizing environmental degradation [5]. Greater than one billion dry tons of non-food based biomass can be sustainably produced annually in the US [6]. These current untapped renewable resourses will provide an ecomoical feedstock for the production of renewable fuel componants and value chemicals. This disseratation concentrates on utilizing glucose, which is the main product from the breakdown of biomass.

Most notably, biomass is a carbon neutral process. By contrast, crude oil consumption has harmful effects, mainly the increase emission of greenhouse gases, specifically CO2. Increased CO2 in the atmosphere is the leading cause of global climate change [7]. Climate change and other environmental health concerns related to burning fossil fuels have also become prevalent in today's society [8-10]. The earth's surface temperature has been increasing due to trapped radiant heat caused by increased concentrations of carbon dioxide, methane, nitrous oxide, ozone, halons, peroxyacetylnitrate, and CFCs [11, 12]. Table 1 shows the increase in

greenhouse gas concentration attributed to industrialization [12, 13]. Total emissions have grown 65% since 1971 [14]. Surface temperatures have already increased by 0.4-0.8 °C over the last century, causing an annual sea rise of 1-2mm, and 40% thinning of arctic ice since the 1950's [15].

Table 1: Global warming effects of common greenhouse gases

Substance	Ability to retain infrared radiations compared to CO_2	Pre industrial concentration	Present concentration	Annual growth rate (%)	Share in the greenhouse effect due to human activity (%)	Share in the greenhouse increase due to human activity (%)
CO_2	1	275	346	0.4	71	50 ± 5
CH_4	25	0.75	1.65	1.0	8	15 ± 5
N_2O	250	0.25	0.35	0.2	18	9 ± 2
R-11	17,500	0	0.00023	5.0	1	13 ± 3
R-12	20,000	0	0.00040	5.0	2	13 ± 3

It is important to look at economically maximizing all products and byproducts from renewable resources to create cost-effective alternatives to fossil fuels. Fossil fuels have been driving economic growth through fuel for trade and manufactured goods since the beginning of the industrial era [16]. However, concerns about environmental effects and limited reserve capacity grow as demand continues to surge and population increases [17-21]. Available data suggest that current oil production techniques have a finite capacity to supply the growing demand, and unconventional sources will need to be implemented to avoid negative economic and environmental consequences [22]. Figure 1 shows the reduced frequency of new oil field discoveries along with the projected increase in demand, with an expected depletion within the century [23]. With the implementation of fracking techniques to access tight oil there is controversial data on when "peak oil" or crude oil depletion will actually occur [24]. Figure 2 shows the expected increase of fracked oil, but only roughly matching traditional crude oil

production. The crude oil supply is finite and one day will be unable to economically meet our increasing demand and the era of low cost petroleum will come to an end [17-27]. Although access to fracked oil helps relieve oil demand, it does amplify the amount of carbon released into the atmosphere. This is of interest for our work as lactic acid and levulinic acid have functional groups that will facilitate the building carbon neutral fuel components.

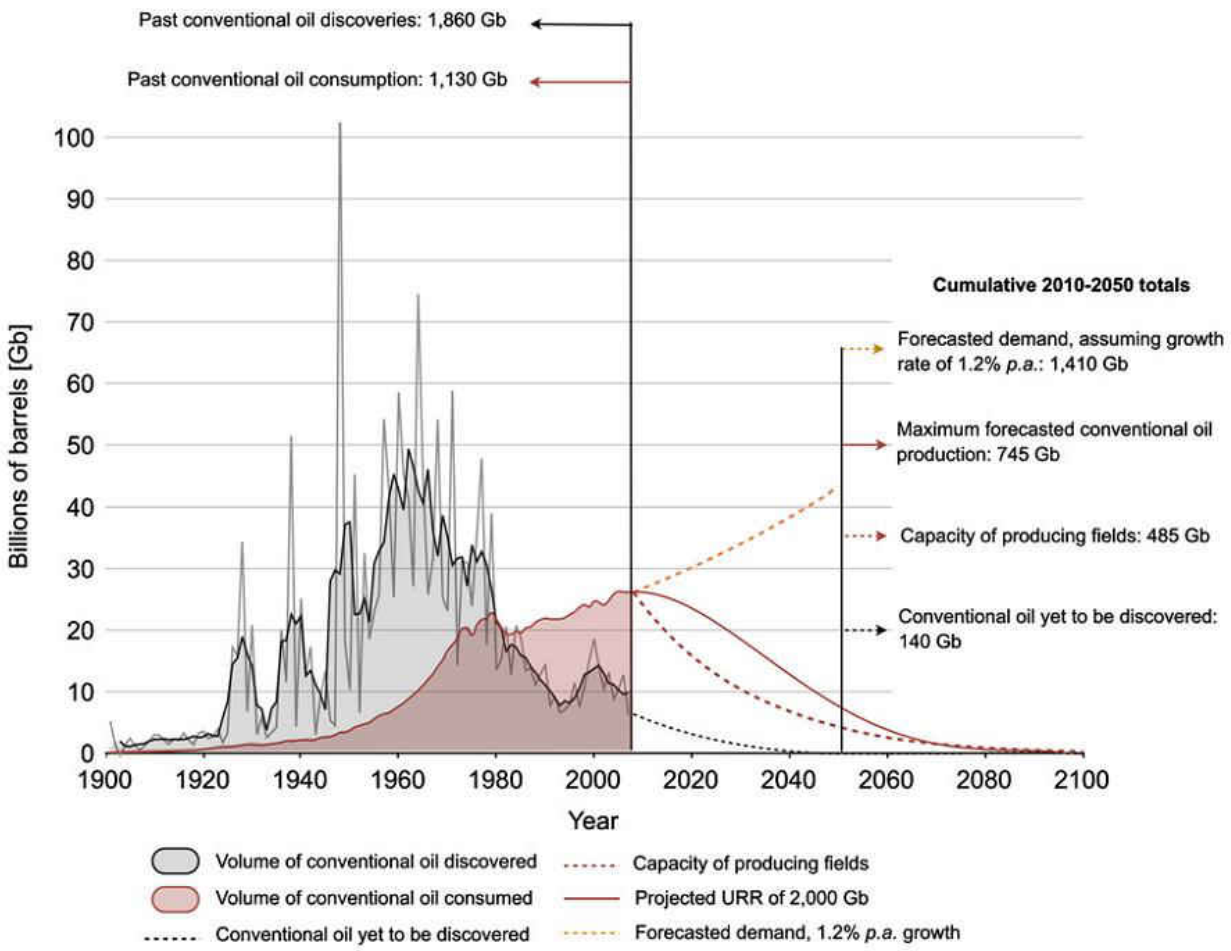

Figure 1. Declining crude oil reserves shown by historical oil discovery, consumption, and forecasted production

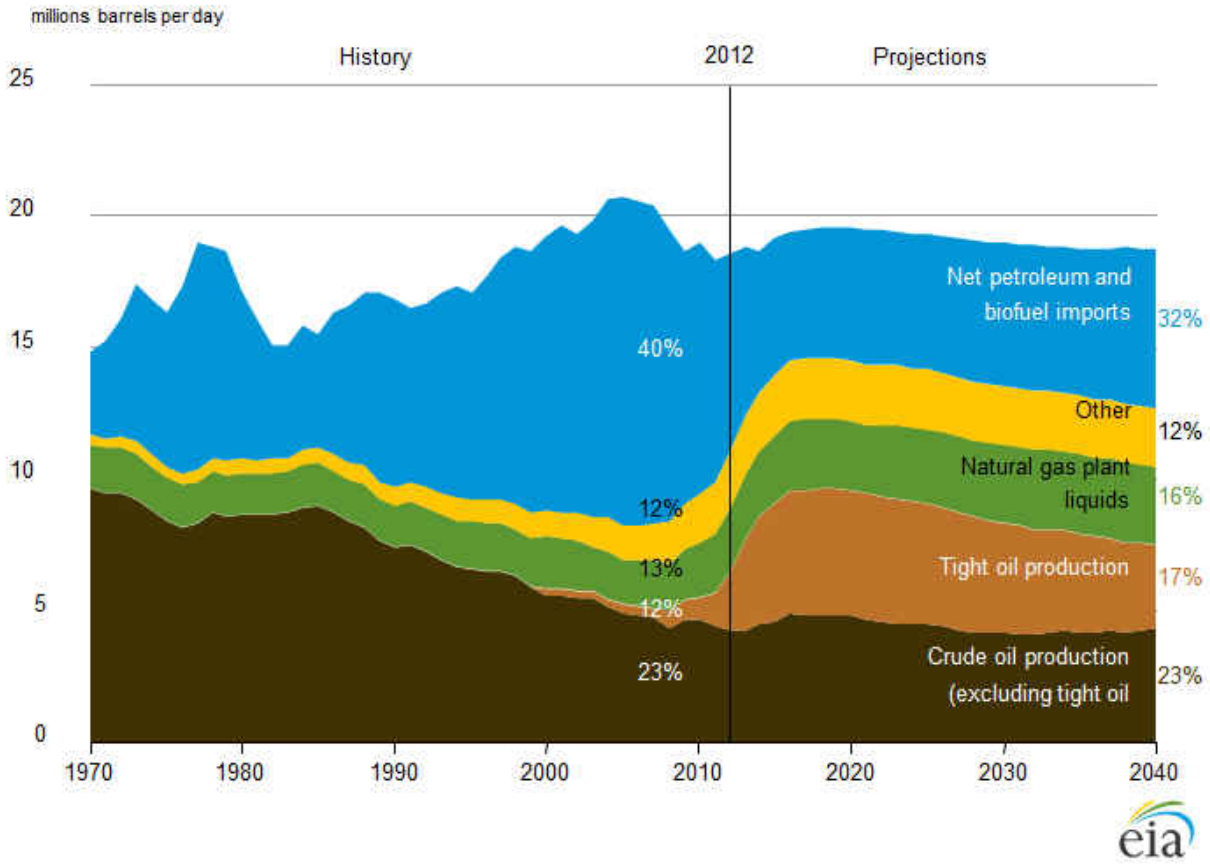

Figure 2: Petroleum and other liquid fuel history and projections including tight oil production

Researching and utilizing renewable technologies can help to mitigate the damaging effects from greenhouse emissions by developing carbon neutral technologies to minimize current fossil fuel uses; conversion of biomass to fuel and high value chemicals is one such technology [28]. Developing renewable transportation fuels is attractive because 85% of all crude oil consumed is for production of transportation fuels [29].

Additionally, lactic acid and levulinic acid have multiple functional groups that can be utilized for synthesis of polymers, solvents, and other value chemicals. These uses are also important, as 10% of crude oil is used for the production of industrial chemicals which are inherently more valuable than fuel [29, 30]. Historically, little attention has been given to

biomass based industrial chemicals [31]. Innovative developments are providing an argument that renewable feedstocks can be optimal for the chemical industry [32]. Renewable feedstocks are typically highly functionalized molecules, unlike fossil fuels, creating the challenge to develop a new set of tools to economically produce biomass based industrial chemicals [33,34].

This body of work concentrated on the production of lactic acid/derivatives and levulinic acid/derivatives from biomass derived glucose. Lactic acid and levulinic acid were optimized from glucose using Sn-doped beta zeolite type catalysts. Economic versatility can be achieved through selectivity of the glucose towards either lactic or levulinic products, conversion of lactic or levulinic products toward fuel components, and/or conversion of levulinic products towards high value chemicals. The combination of uses for fuel or value chemicals makes this research an important economic step in reducing fossil fuel consumption. Implementation of these technologies would decrease greenhouse emissions and reduce crude oil demand.

CHAPTER II
LACTIC/LEVULINIC ACID

1.1 Lactic Acid Literature Review

Lactic acid was first discovered in 1780 in sour milk and was produced commercially by 1881 [35]. Lactic acid is still largely used as a buffering agent, acidic flavoring agent, acidulant, and bacterial growth inhibitor within the food industry [36, 37]. The majority of the world's production of lactic acid is from batch bacterial fermentations of carbohydrates [38]. Lactobacilli can convert more than 90% of glucose to lactic acid, however there are multiple limitations to this biological reaction that limit its efficiency. The reaction requires low to neutral pH, temperatures near 40 °C, low oxygen concentrations and large amounts of water [39]. In addition to specific carbohydrate feedstocks, the living organisms require complex nutrients, amino acids, and nucleotides [40]. Commercial fermentation is usually completed in three to six day batches with feedstock of up to only 10% saccharides, requiring a relatively large reaction vessel. High lactic acid concentrations are desired for efficiency but lead to toxicity and growth inhibition of the lactobacilli [41].

Recent discoveries have demonstrated non-biological pathways to produce lactic acid which may increase process efficiency by removing the limitations of living organisms such as low concentration of products, long fermentation times, requirements for nutrients, and moderate temperatures [42]. In 2005, Bicker et al. reported the thermal degradation of saccharides to produce 40% lactic acid when metal ions such as cobalt, nickel, copper and zinc were used as catalysts [43]. Five years later Homl and coworkers reported using metal doped zeolites to

convert triose saccharides to methyl lactate in a methanol solvent [44,45]. Further work from the Holm group showed that tin doped beta zeolites facilitated isomerization from glucose to fructose at 100 °C [46]. When reaction times were increased to 16 hours and temperature increased to 160 °C, the saccharides in a methanol solution would produce methyl lactate at a 52% concentration from glucose and 64% from sucrose [42, 47, 48]. Yang and Liu found that three hours of microwave irradiation with zinc powder produced 40% lactic acid from an aqueous solution [49].

Most recent publications show that equal additions of alkaline compounds converted glucose to 50% lactic acid with the best results from barium hydroxide under supercritical conditions [50]. Recent patents describe methods to produce 23% molar yield of lactic acid from cellulose using Al/Sn catalyst and 50% methyl lactate yield from fructose using tin containing compounds [51, 52].

While the literature documents partial selectivity toward lactic acid derivatives there is still an information gap regarding ideal conditions for conversion of glucose to lactic acid in an aqueous solvent. With the overall project goal to convert cellulosic biomass to valuable chemicals, the biomass glucose feedstock will be in an aqueous solution and it would be costly to transfer to methanol. The best published results for a water solvent show only 27% lactic acid from sucrose, while the same substrate produced 64% methyl lactate in methanol [47]. Table 2 shows the results Holm et al. published using sucrose and glucose with various catalysts to produce lactic acid or methyl lactate [42, 47, 53]. In our work we endeavor to optimize glucose to lactic acid conversion within an aqueous solvent. Table 3 shows our best results for comparison to the current literature.

Table 2: A summary of published results for lactic acid and methyl lactate production from sugars with various catalysts and solvents

Feed/ Solvent/ Catalyst	Unreacted	Lactic acid or methyl lactate	Other	Coke	Unaccounted product	Ref.
Sucrose/ Methanol/ None	46%	6%	n/a	n/a	48%	[42]
Sucrose/ Methanol/ Si-Beta	37%	6%	n/a	n/a	57%	[42]
Sucrose/ Methanol/ Sn^{+4}-Beta	<1%	64%	10%	1.3%	24%	[53]
Sucrose/ Methanol/ $SnCl_4$	1%	31%	n/a	n/a	68%	[42]
Sucrose/ Methanol/ $SnCl_2$	19%	4%	n/a	n/a	77%	[42]
Sucrose/ Water/ Sn^{+4}-Beta	<1%	27%	7%	7%	58%	[53]
Glucose/ Methanol/ None	47%	5%	n/a	n/a	48%	[42]
Glucose/ Methanol/ Si-Beta	39%	5%	n/a	n/a	56%	[42]
Glucose/ Methanol/ Sn^{+4}-Beta	2%	51%	12%	n/a	35%	[47]

Table 3: Summary of our best results for lactic acid and methyl lactate production from glucose with various catalysts and solvents

Feed/ Solvent/ Catalyst	Unreacted	Lactic acid or methyl lactate	Levulinic acid or methyl levulinate	Other	Coke	Unaccounted product
Glucose/ Methanol/ Sn^{+4}-Beta	4.4%	22%	49.2%	2.4%	2.7%	16.2%
Glucose/ Water/ Sn^{+4}-Beta	2.3%	47.8%	0%	0%	24.2%	25.8%
Glucose/ Methanol/ Sn^{+2}-Beta	1.8%	4.4%	52.8%	0%	13.7%	27.3%

1.2 Levulinic Acid Production Literature Review

Levulinic acid has been identified by the National Renewable Energy Laboratory (NREL) as one of the top ten molecules for the production of value-added chemicals and liquid transportation fuels from renewable sources [54]. Levulinic acid has several applications as a value chemical, including polymers, lubricants, adsorbents, coatings, batteries, drug delivery, corrosion inhibitors and many others [55-71]. The most common process for the production of levulinic acid from biomass used LZY zeolite catalyst or micro-porous acidic clay [72-74]. Currently, the majority of commercial quantity production of renewable levulinic acid is from Biofine Corporation's pilot plant at 1 ton/day. The plant converts >60% hexoses to levulinic acid with minimal side products [75-76].

Our work shows high percentages of levulinic acid production from glucose, dependent on reaction conditions. This is of great interest as it allows for the selectivity of either valuable product to produce, levulinic or lactic acid, within the same system depending on the current demand. The following sections will show the optimization of lactic and levulinic acid production with the same equipment using slightly different catalysts.

1.3 Catalyst Selection

The literature shows that Sn-beta zeolite has the highest selectivity towards lactic acid in methanol [42]. In our study, several readily available commercial catalysts were screened to confirm published results. Table 4 shows the results of catalyst screening conducted for glucose at 140 °C in methanol, matching the ideal conditions in the literature. While some of the results were better than no catalyst, the results did not come near to published results for methyl lactate and further efforts were spent towards production of Sn-doped beta zeolite for the degradation of glucose.

Table 4: Methyl lactate and methyl levulinate results from catalyst screening experiments

Catalyst	Methyl Lactate	Methyl Levulinate
No Catalyst	4%	2%
Sn(II)Cl 5·H2O	23%	10%
Sn(IV) Acetate	5%	5%
Zinc Acetate	14%	4%
Montmorillonite	8%	7%
Boron Tribromide	20%	24%
Ag(II) Oxide	4%	2%
Zr(IV)Hydroxide	4%	2%
Titanium on Alumina	8%	2%
Palladium on Activated Carbon	2%	2%
Ni 55/5 commercial catalyst	10%	2%

The best catalyst from the literature, results shown in Table 2, is tin beta zeolite and was produced from tetraethyl orthoxilacted, tetraethyl ammonium, tin (IV) chloride, hydrogen fluoride, and dealuminated beta seeds [53]. The procedure requires up to forty days for completion. We were able to take advantage of recent zeolite doping procedures that allowed us to purchase beta zeolite and dope the zeolite with our desired metal ion, allowing catalyst production in under 48 hours [77, 78]. This work expands on previously published results for

doping HZSM-5 zeolites to beta zeolites doped with tin. The optimization of this procedure is a previously undocumented advancement over any other published results dealing with this given metal dopant and zeolite.

1.4 Experimental Setup

1.4.1 Reactants, Standards and Catalysts

Glucose (99.5% purity), methanol (99.8% purity), tin(II) chloride (98% purity), tin(IV) pentahydrate (98% purity), lactic acid (98% purity), methyl lactate (98% purity), levulinic acid (98% purity), methyl lactate (98% purity), furfural (99% purity), and 5-(hydroxymethyl)furfural (99% purity) were purchased from Sigma-Aldrich. Beta zeolites with SiO2/Al2O3 ratios of 25, 38, and 300 were purchased from Zeolyst International. Ion free water was obtained from an in-house ultra milli-Q filter system. Compressed nitrogen gas (99.99% purity) and hydrogen (99.95% purity) were purchased from Praxair.

1.4.2 Catalyst Doping

The purchased beta zeolite was calcined in a 600 °C oven for 8 hours to remove any possible settlement on the catalyst from shipping and storage. The calcined beta zeolite was then dispersed in an aqueous solution of ultrapure water and mixed with the required amount of tin ion. The solution was then sonicated overnight at 60 °C. The doped zeolite was separated from the water with a gravity filter and placed in an oven at 150 °C to dry, followed by another calcine stage for 8 hours. The calcined, doped zeolite was stored in sealed containers or used immediately in an experiment. A detailed procedure is presented in Appendix A.

1.4.3 Autoclave Reactor

All experiments were conducted in a 500 ml, high temperature, high pressure batch reactor (Parr 4575 series HP/HT reactor, manufacturing code: 4575A-G-GP-SS-115-VS.25-5000-4857-TDM-MCM-PDM-HTMA1925E2-SVM) [79]. This code fully explains the reactor configuration and is explained as follows: 4575A is the base model number. G is the material of gasket used to seal the vessel to the head and is the code for graphite which is a compressed flexible gasket that can withstand up to 500 °C. GP indicates a general purpose magnetic stirrer drive. The material of construction of the head and the vessel is SS 316 and is indicated by SS. The system runs at 115 V and was indicated by the code 115. VS.25 specifies that the magnetic motor drive is a 190 watt (0.25 hp) motor. The reactor has a pressure gauge with a range of 0 – 34.5 MPa (5000 psig) indicated by the code 5000. The controller code is a model 4857 and is equipped with a tachometer display module (TDM), motor control module (MCM), pressure display module (PDM), high temperature cut off module (HTM), and a solenoid valve module (SVM). The overall setup includes the reactor, a controller, a condenser, and a collection cylinder. Figure 3 shows a schematic of the 500 ml Parr autoclave used for all experiments.

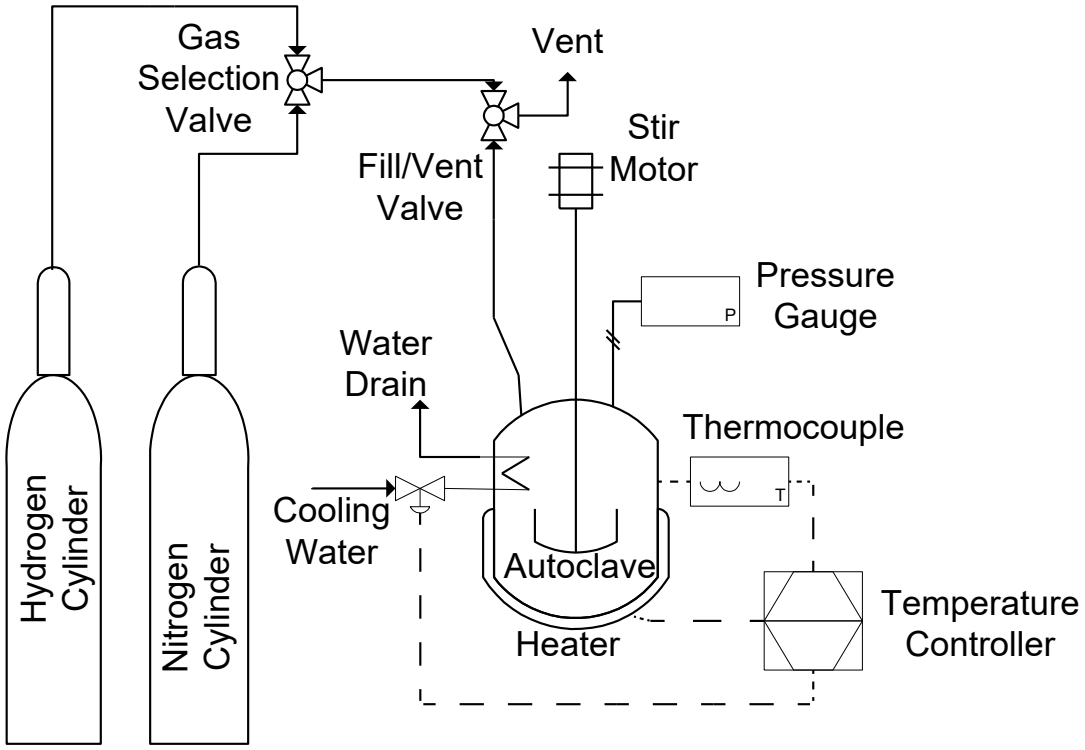

Figure 3: Simplified schematic of autoclave reactor used for all experiments

Agitation was provided by a variable speed electric DC motor using a magnetic drive. It was capable of mixing at 600 RPM. This magnetic drive is connected to the head of the reactor by a threaded pipe connection. The magnetic stirring drive has two o-rings which seal the sleeve onto the stem of the drive housing preventing leaks at high pressure. Because the autoclave ran at high temperatures (>100 °C) for all the reaction runs, it was necessary to have cooling water flow continuously to the jacket between the two o-rings to ensure proper operation of the magnetic drive. The pressure transducer was also subjected to high temperatures and was equipped with a cooling jacket around it to ensure proper functioning.

A 4843 Parr controller was used to display and control the temperature and stirring rate and to display the pressure transducer output. The controller also had a cut off module which worked as a safety feature to terminate power to the heater if it exceeded a set temperature. A

safety cut-off feature also offered protection against accidental over-pressure by allowing the user to set a maximum pressure which, if reached, activates the high limit relay and turns the heater off.

1.4.4 Experimental Reaction

The specified amount of powdered beta zeolite catalyst was added to the reaction vessel, followed by the required amount of reactant glucose, and then dispersed in the specified volume of solvent. Depending on the variables being tested, the exact quantity of catalyst, glucose, methanol, and water were varied and are specified for each experiment discussed in the experimental methods section. Once the vessel was charged it was sealed in the Parr reactor and purged 5 times with nitrogen gas. After passing an initial pressure test the heater was turned on and set to the specified temperature and the stirrer was turned on.

Once the required reaction time was completed the heater was removed and cooling water was turned on to rapidly cool the mixture to room temperature. The mixture was gravity filtered to separate the catalyst from solution. All the coked catalyst was carefully collected from the agitator blades, cooling coil, thermocouple thermowell, all other internal parts of the reactor, and the reactor vessel. The difference in the weight of the catalyst before and after the reaction was measured to calculate the amount of coke produced. Coke was the general term used for all organic solids on the catalyst and may be deposited carbon or insoluble byproducts. The product solution was collected for future GC-MS analysis. All parts of the reactor were cleaned and prepared for the next experiment. A detailed procedure is presented in Appendix B.

1.4.5 GC-MS Analysis

GC-MS analyses were performed following the method developed by Kubatova and coworkers [80, 81]. This method uses GC separation and an MS detector (Agilent 6890GC-MS)

equipped with an autosampler (7386B series) and a split/splitless injector. Separation was accomplished using a 30-m long DB-5 capillary column, 0.25mm internal diameter (I.D.) and 0.25µm film thickness with a constant helium flow rate. Analysis of acids was accomplished after derivation with BTSFA in pyridine solvent. Detailed procedures for analysis and data processing are presented in Appendix C and Appendix D, respectively.

1.5 Experimental Methods

1.5.1 Design of Experiments – Screening Study

A twelve run Plackett-Burman design was employed to test for any significant effects from eleven factors. As this project's catalyst synthesis was different from the published literature, seven of these factors were associated with the doping of the beta zeolite catalyst. The other four factors optimized reaction conditions.

Table 5 lists the low and high values for all eleven factors examined in the Plackett-Burman screening study.

Table 5: Low and high values for eleven factors tested in the screening study

Factor	Low (-)	High (+)
SiO2/Al2O3 Ratio	25	300
Calcine New Zeolite	0 °C	600 °C
Intermediate H-doping	No	Yes
Calcine H Doped Zeolite	0 °C	600 °C
Tin Charge	Sn^{+2}	Sn^{+4}
Tin Added Mol Ratio	150%	300%
Calcine Sn Doped Zeolite	400 °C	600 °C
Water-to-Methanol Ratio	25%	75%
Sn-beta zeolite	3 grams	6 grams
Glucose	5 grams	10 grams
Temperature	135 °C	165 °C

Factor one studied the effect of the SiO2/Al2O3 ratio of commercially available beta zeolites. The 25 SiO2/Al2O3 ratio chosen will be slightly more hydrophobic than the 300, which will be more hydrophilic. Both have similar surface areas of 680 and 620 m2/g, respectively. The second factor looked at the need for precalcining of the purchased catalyst. The catalyst was submersed in a doping fluid and would remove any absorbed water or other contaminates and a precalcine at 600 °C may be unnecessary. The third factor considered the effect of an intermediate H-doping step using ammonium nitrate. This intermediate step has shown a favorable effect on other zeolite doping performed in our labs for the production of Zn-ZSM-5 and Ga-ZSM-5 [82]. The fourth factor concerned calcining the intermediate H-beta catalyst at 600 °C for the same reason as factor two. Factor five studied the effect of the tin charge, Sn^{+2} verses Sn^{+4}. Studies of Sn^{+2}-doped beta zeolite have not been reported in the literature. Factor six looked at the effect of adding different amounts of tin to the catalyst. Both 150% and 300% were evaluated to determine if there were any equilibrium effects occurring when displacing the sodium ions. The seventh factor addressed the final calcine temperature of the Sn-doped beta zeolite. Temperatures of 400 °C and 600 °C were tested to see if any thermal effects changed the novel Sn-doped beta zeolite.

The other four factors were used to explore the operating conditions for the catalytic degradation of glucose to levulinic and lactic acids. The eighth factor looked at the effect of water-to-methanol ratio. Ratios of 25% and 75% were tested to study the effect of each solvent on the production of levulinic and lactic acids or their ester derivatives. The ninth and tenth factors studied the effect of the catalyst-to-glucose ratio, as well as the effect of the concentration of reactants in the solution. Factor nine varied between 3 to 6 grams of Sn-doped beta zeolite

and factor ten varied between 5 to 10 grams of glucose. The last factor looked at the reaction temperature. The literature has shown the highest conversion of sucrose at ~140 °C and preliminary experiments with glucose were performed to determine the temperature range. The parameter range of 135 °C to 165 °C was selected based on these preliminary experiments.

The twelve run Plackett-Burman design was studied in two blocks, with the twelve runs randomized in each block to screen for significant factors and begin optimization. Six samples were taken from each of the 24 runs. Three samples were taken near the beginning of the reaction at zero, one, and two hours to observe early reaction products. Three samples were taken towards the end at 20, 21, and 22 hours to verify that the reaction had reached completion and to observe any potential product degradation. Table 6 shows the run order and low/high factors studied in each run.

Table 6: Design of experiments screening study run order showing high and low values of each of the eleven factors tested

Standard order	Experimental order	F1	F2	F3	F4	F5	F6	F7	F8	F9	F10	F11
1-1	1	+	+	-	+	+	+	-	-	+	+	+
1-2	7	+	-	+	+	+	-	-	+	-	+	+
1-3	10	-	+	+	+	-	-	-	-	-	-	-
1-4	11	+	+	+	-	-	-	+	-	-	+	-
1-5	2	+	+	-	-	-	+	-	+	+	-	-
1-6	6	+	-	-	-	+	-	+	+	+	-	+
1-7	4	-	-	-	+	-	+	+	-	+	-	+
1-8	8	-	-	+	-	+	+	-	+	-	+	+
1-9	5	-	+	-	+	+	-	+	-	+	+	-
1-10	9	+	-	+	+	-	+	+	+	+	+	-
1-11	12	-	+	+	-	+	+	+	+	-	-	-
1-12	3	-	-	-	-	-	-	-	-	-	-	+
2-1	23	+	+	-	+	+	+	-	-	+	+	+
2-2	13	+	-	+	+	+	-	-	+	-	+	+
2-3	21	-	+	+	+	-	-	-	-	-	-	-
2-4	18	+	+	+	-	-	-	+	-	-	+	-
2-5	14	+	+	-	-	-	+	-	+	+	-	-
2-6	16	+	-	-	-	+	-	+	+	+	-	+
2-7	24	-	-	-	+	-	+	+	-	+	-	+
2-8	20	-	-	+	-	+	+	-	+	-	+	+
2-9	22	-	+	-	+	+	-	+	-	+	+	-
2-10	15	+	-	+	+	-	+	+	+	+	+	-
2-11	19	-	+	+	-	+	+	+	+	-	-	-
2-12	17	-	-	-	-	-	-	-	-	-	-	+

1.6 Screening Study Results Based on Chemical Analysis

The reaction begins slowly with little or no reaction during the first two hours. Levulinic acid was typically the first product to form. In over half the runs there was no sign of any products during the early stages. The reaction was complete by hour twenty with no signs of loss

of product over the next two hours until the experiment was halted. Figure 4 shows the time results for experiment 2-7 as it had the highest results for all target products.

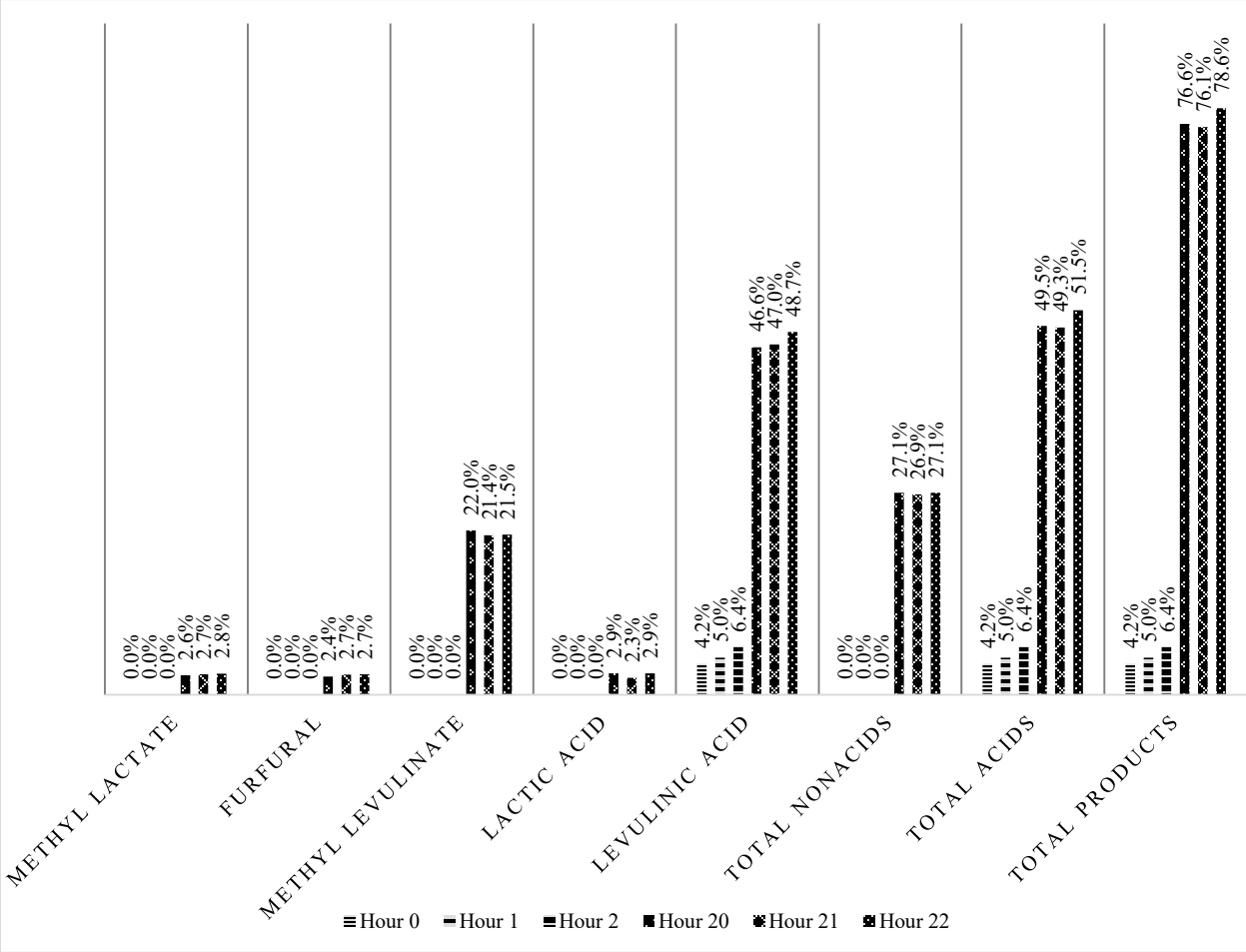

Figure 4: Experiment 2-7 showing the typical trend of product yields over time

The last three samples, results at hours 20, 21, and 22 were averaged to represent the amount of product converted for that given run. This was done to compensate for any possible variation in GC-MS analysis between injections. The two repeat runs from each DOE block were averaged and the standard deviation was added to show repeatability. Table 7 and Table 8 show the analytical results of each product and congregated results, respectively. Appendix E

shows the results from all experiments related to the degradation of glucose and Appendix F shoes all the data from the DOE statistical analysis.

Table 7: Averaged analytical results of products from screening study

Combined Run	Methyl Lactate	Furfural	Methyl Levulinate	Lactic Acid	Levulinic Acid
1	3.34% ± 0.59%	1.68% ± 0.75%	22.51% ± 0.57%	2.43% ± 0.11%	47.88% ± 2.59%
2	0% ± 0%	0.55% ± 0.78%	1.56% ± 0.82%	0.61% ± 0.86%	16.50% ± 8.76%
3	0% ± 0%	0% ± 0%	0% ± 0%	0% ± 0%	5.95% ± 2.02%
4	0% ± 0%	0.38% ± 0.54%	0% ± 0%	0% ± 0%	5.59% ± 2.46%
5	0% ± 0%	0% ± 0%	0% ± 0%	0% ± 0%	6.72% ± 0.96%
6	1.96% ± 2.78%	0.89% ± 1.25%	4.76% ± 0.43%	12.01% ± 4.48%	8.46% ± 1.31%
7	3.58% ± 1.18%	2.18% ± 0.63%	22.07% ± 0.59%	2.51% ± 0.23%	44.00% ± 4.83%
8	0% ± 0%	0.85% ± 0.28%	2.75% ± 0.41%	0% ± 0%	43.38% ± 3.41%
9	0% ± 0%	0% ± 0%	0.56% ± 0.8%	0% ± 0%	6.84% ± 4.53%
10	0% ± 0%	0.37% ± 0.52%	0% ± 0%	1.47% ± 0.74%	9.92% ± 3.38%
11	0% ± 0%	0% ± 0%	0% ± 0%	0% ± 0%	5.42% ± 1.00%
12	0.71% ± 1.01%	0.94% ± 1.33%	11.77% ± 2.73%	0.9% ± 1.27%	29.46% ± 5.29%

Table 8: Summary of total products, unreacted glucose, and unaccounted products from screening study

Combined Run	Total Non-Acids	Total Acids	Total Products	Unreacted Glucose	Unaccounted product
1	27.53% ± 0.73%	50.31% ± 2.7%	77.84% ± 3.43%	4.85% ± 0.03%	17.31% ± 3.40%
2	2.12% ± 1.60%	17.11% ± 7.89%	19.22% ± 9.50%	26.99% ± 4.65%	53.78% ± 4.84%
3	0% ± 0%	5.95% ± 2.02%	5.95% ± 2.02%	43.1% ± 1.24%	50.95% ± 3.25%
4	0.38% ± 0.54%	5.59% ± 2.46%	5.98% ± 1.92%	57.46% ± 1.28%	36.56% ± 3.20%
5	0% ± 0%	6.72% ± 0.96%	6.72% ± 0.96%	53.53% ± 0.25%	39.75% ± 0.71%
6	7.61% ± 1.09%	20.47% ± 3.17%	28.08% ± 2.08%	6.56% ± 1.82%	65.35% ± 0.26%
7	27.83% ± 1.14%	46.51% ± 5.06%	74.34% ± 3.92%	12.45% ± 7.61%	13.21% ± 3.69%
8	3.60% ± 0.13%	43.38% ± 3.41%	46.98% ± 3.54%	23.79% ± 3.04%	29.23% ± 0.50%
9	0.56% ± 0.80%	6.84% ± 4.53%	7.40% ± 5.33%	53.01% ± 0.76%	39.59% ± 6.08%
10	0.37% ± 0.52%	11.39% ± 4.11%	11.76% ± 4.63%	57.19% ± 0.60%	31.05% ± 4.03%
11	0% ± 0%	5.42% ± 1.00%	5.42% ± 1.00%	82.44% ± 3.75%	12.14% ± 4.75%
12	13.42% ± 3.06%	30.36% ± 6.56%	43.79% ± 3.5%	8.29% ± 0.37%	47.92% ± 3.87%

1.6.1 Statistical Analysis of Screening Study

Glucose conversion increased with higher temperatures, increased catalyst-to-reactant ratio, and decreased water-to-methanol ratio. Higher temperatures are known to increase reaction rates so this effect was expected. The increased presence of catalyst helped facilitate the breakdown of glucose to target products. The reduced amount of initial glucose apparently allowed a higher percentage of available glucose to react before possible coking or deactivation of the catalyst. The increased conversion with higher methanol percentage supports literature findings that more coking was observed in aqueous solvents compared to methanol [48]. Figure

5 and Figure 6 show the glucose conversion Pareto chart with 90% confidence for the evaluated factors and the main effects plot, respectively.

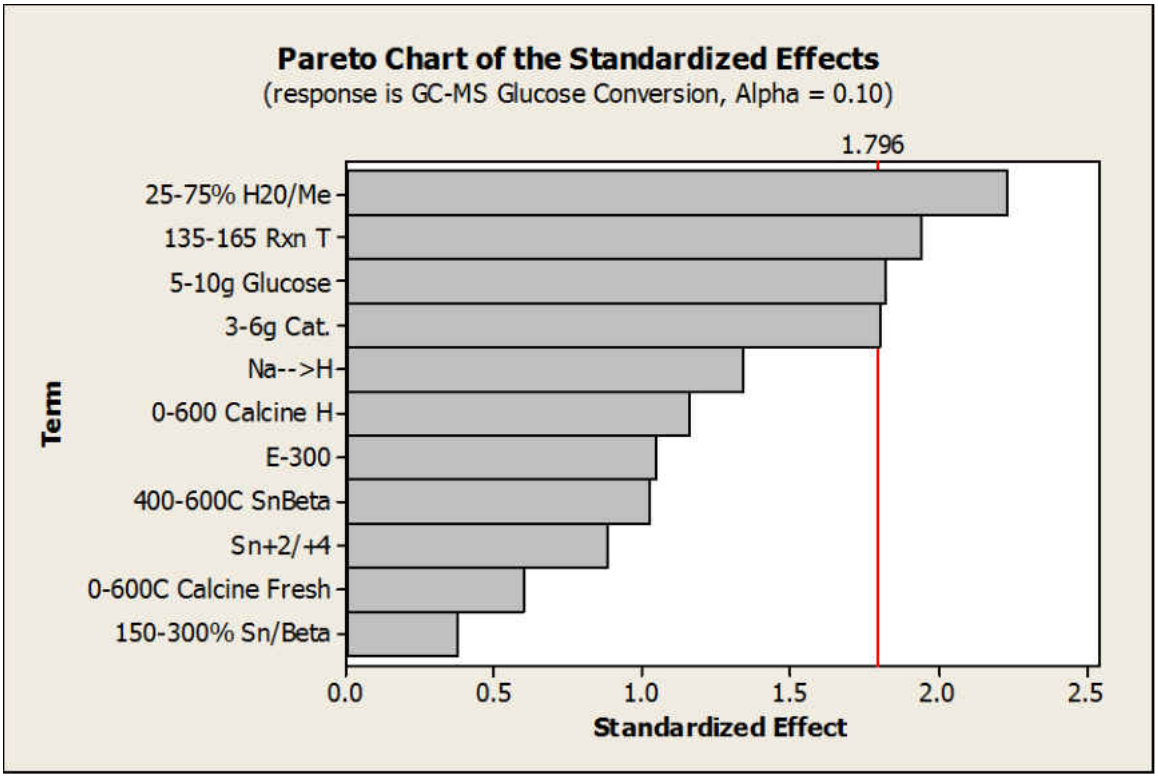

Figure 5: Screening study Pareto chart for glucose conversion

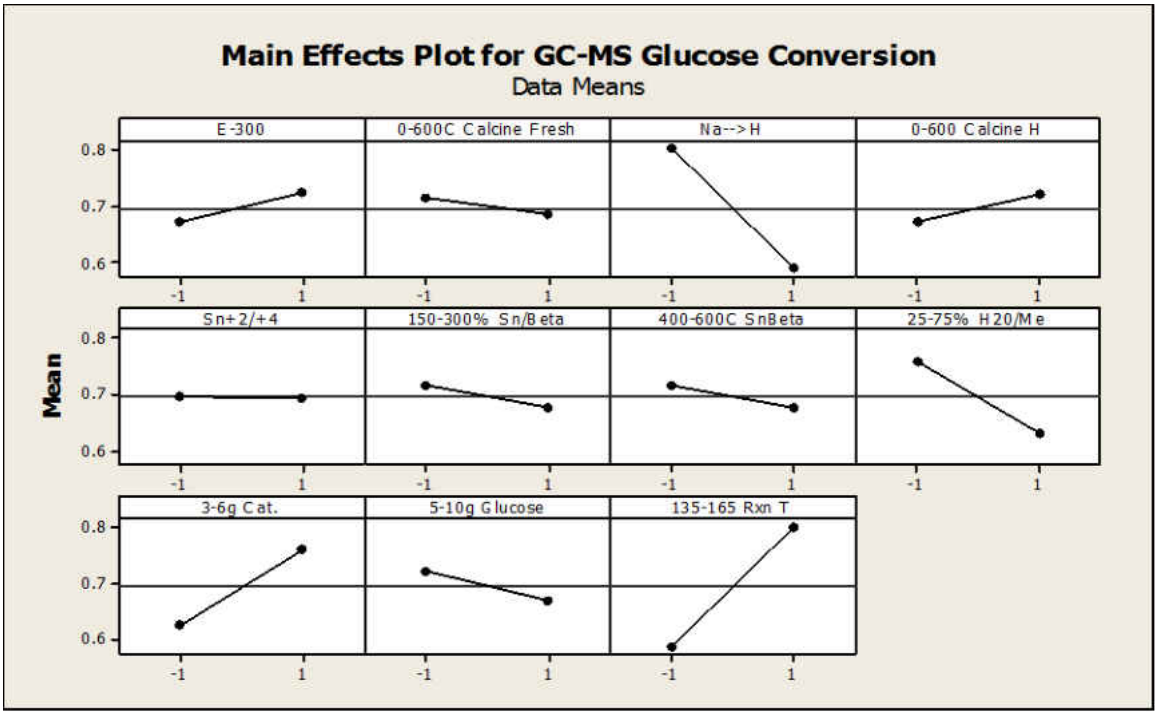

Figure 6: Screening study main effects plot for glucose conversion

Methyl lactate production was aided by decreased water-to-methanol ratio, higher temperature, and small glucose amount. The increase of available methanol content in the solvent promotes the ester formation over the acid which uses the available water. The increased production of methyl lactate with higher temperature suggests a higher activity of the catalyst at higher temperatures. The preference for reduced glucose concentration may suggest more coking or deactivation at higher concentrations. Figure 7 and Figure 8 show the methyl lactate production Pareto chart with 90% confidence for the evaluated factors and the main effects plot, respectively.

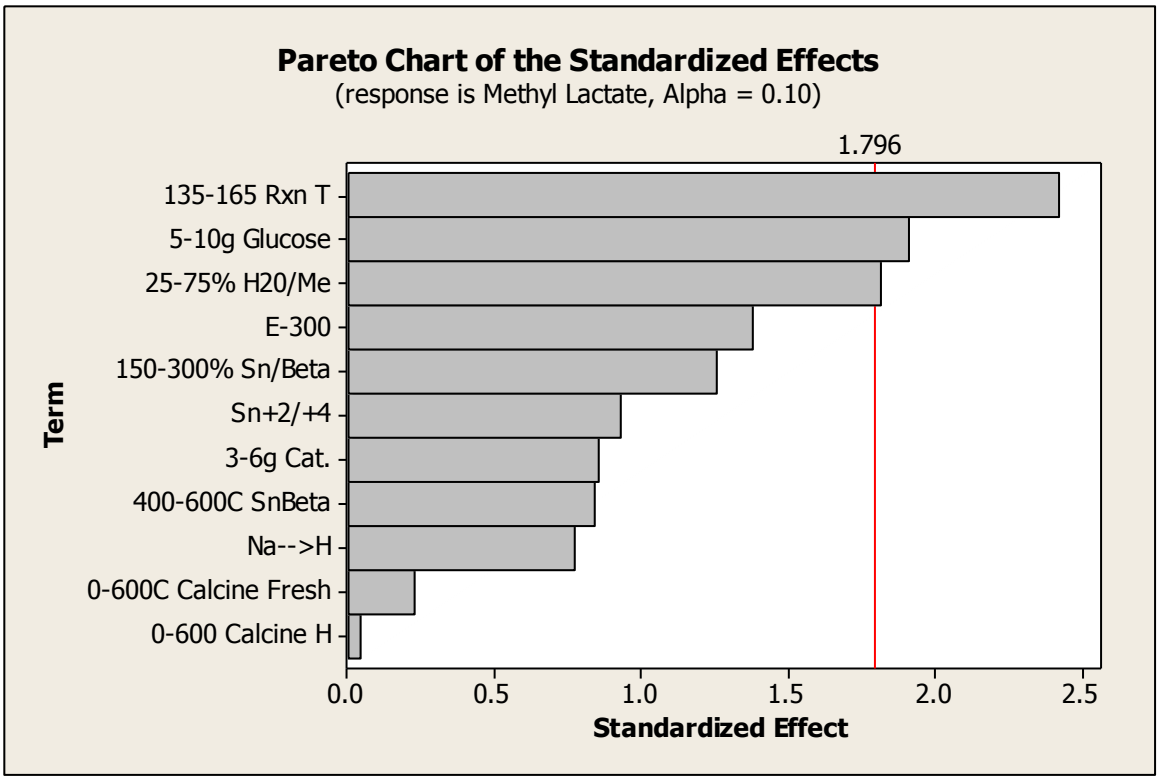

Figure 7: Screening study Pareto chart for methyl lactate production

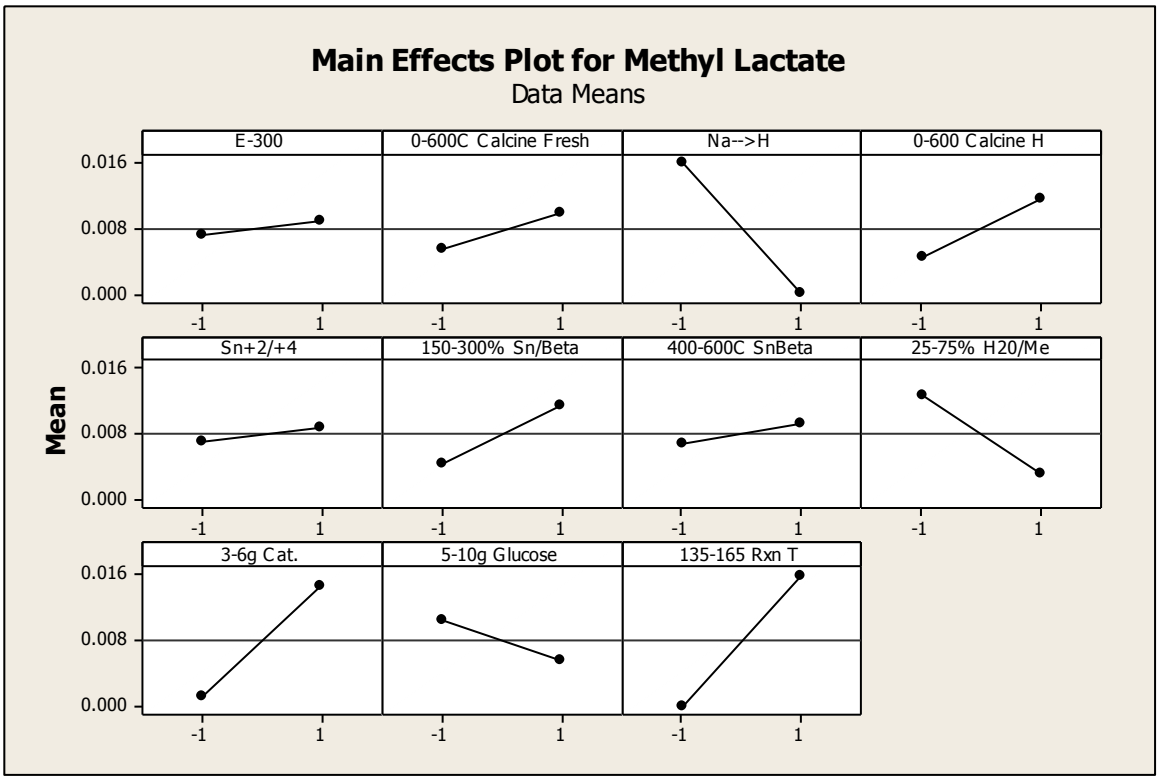

Figure 8: Screening study main effects plot for methyl lactate production

Lactic acid production was increased with higher catalyst-to-glucose ratio, higher temperature, increased water solvent percentage, no H-doped beta intermediate, and use of increased Sn^{+4} for doping. The higher temperature and increased catalyst-to-glucose ratio shows the selectivity of the catalyst for lactic acid. A higher percentage of water allows for more acid production as compared to methyl esters. The H-doped beta intermediate appeared to prevent full doping with tin. Lewis acids have demonstrated selectivity for lactic acids [40]. Sn^{+4} is an oxidant and a slightly stronger Lewis acid than Sn^{+2}; this may be essential for reactivity. The higher SiO2/Al2O3 ratio will be more hydrophilic, promoting the reaction with water instead of methanol. Figure 9 and Figure 10 show the lactic acid production Pareto chart with 90% confidence for the evaluated factors and the main effects plot, respectively.

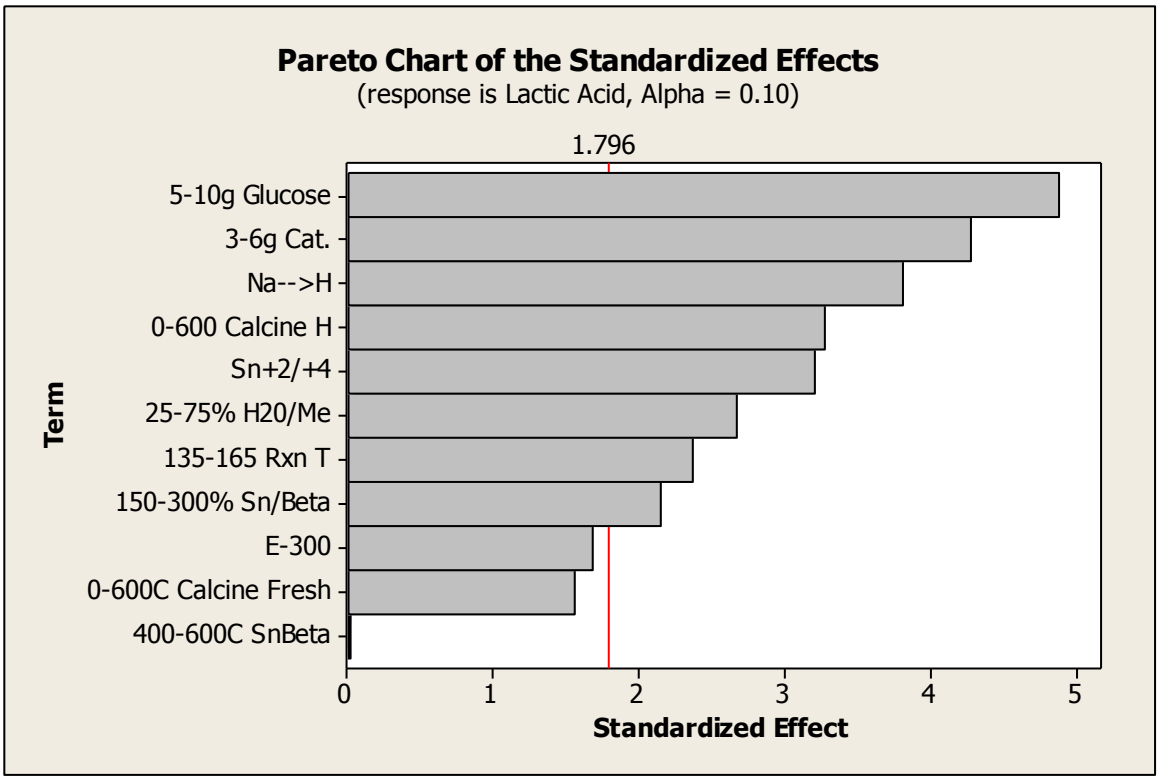

Figure 9: Screening study Pareto chart for lactic acid production

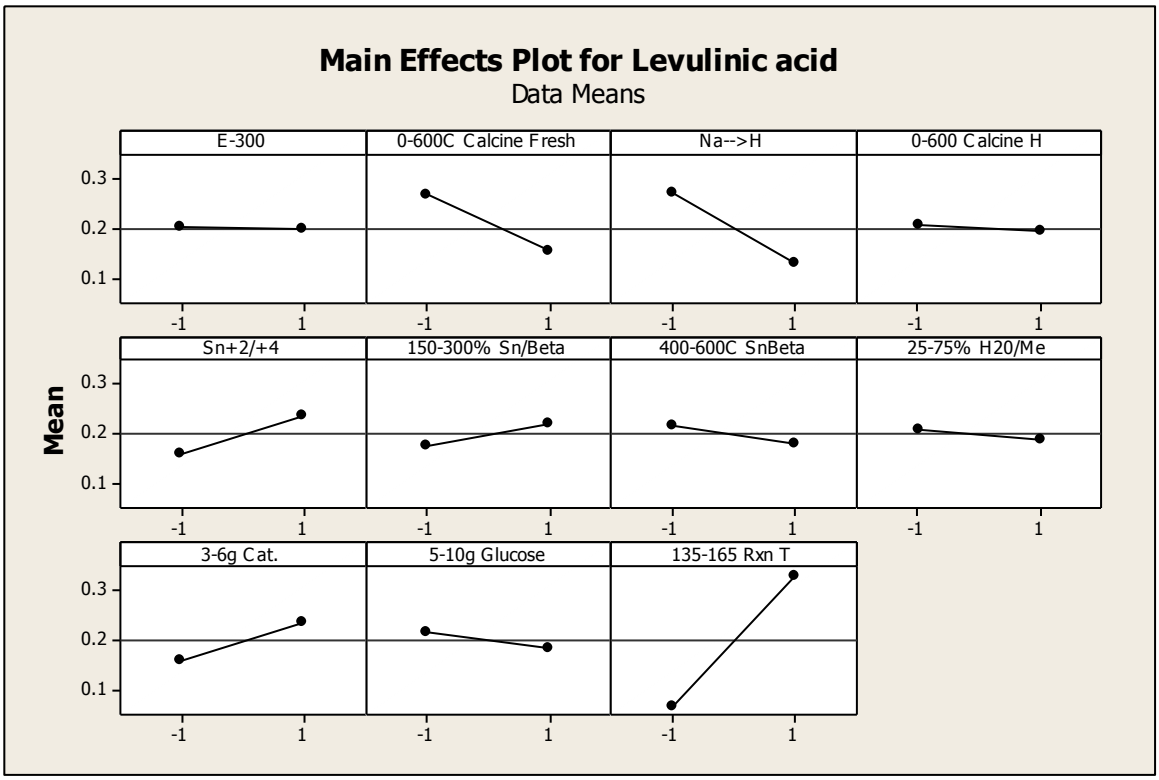

Figure 10: Screening study main effects plot for lactic acid production

Methyl levulinate was produced in most of the experiments and was significantly affected by all the factors studied. Higher temperatures, increased methanol, higher catalyst-to-glucose ratio, and no H-doped beta intermediate caused the higher production for the same reasons as stated earlier. The preference for increased methyl levulinate production with Sn^{+2} can be explained by Sn^{+2} not being an oxidant; as noted above, Sn^{+4} preferred methyl lactate production. Methyl levulinate can also be formed from a non-catalytic reaction. The results show that this is a process competing with the formation of methyl lactate. If methyl lactate is not formed, methyl levulinate is. The increased production with a lower SiO2/Al2O3 ratio, which is relatively more hydrophobic, is most likely a combined effect with the increased methanol solvent promoting

methyl esters. Figure 11 and Figure 12 show the methyl levulinate production Pareto chart with 90% confidence for the evaluated factors and the main effects plot, respectively.

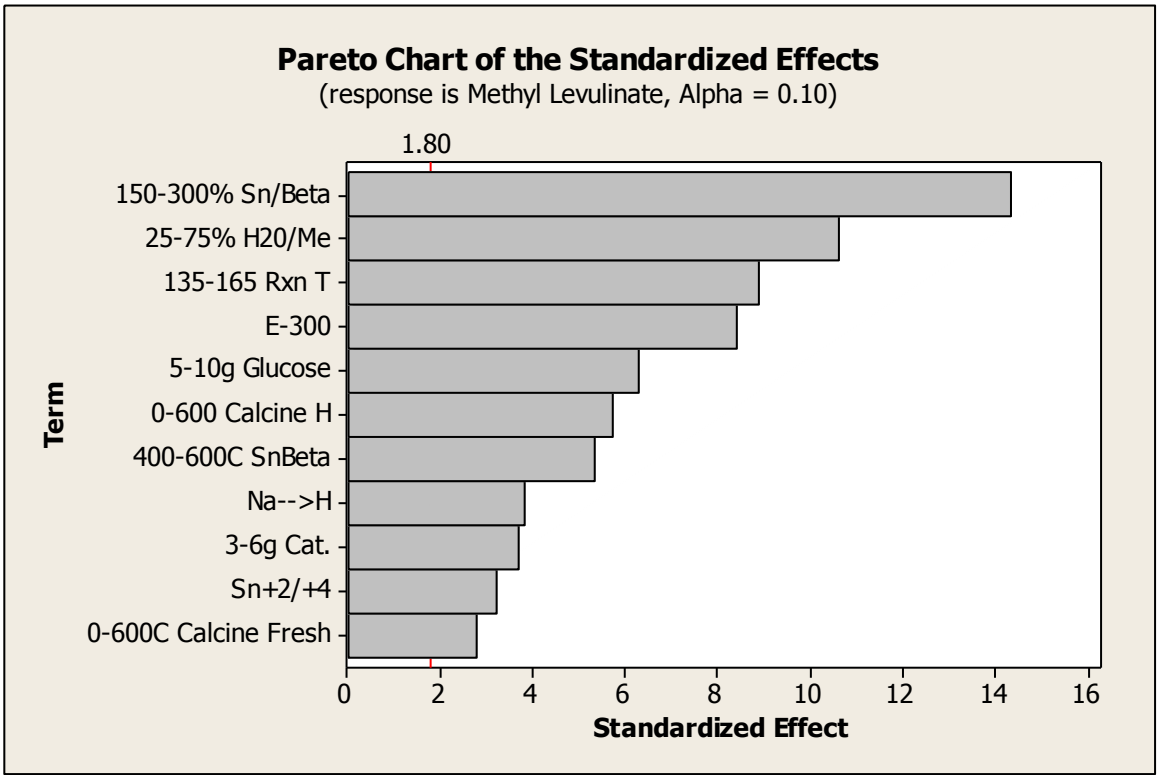

Figure 11: Screening study Pareto chart for methyl levulinate production

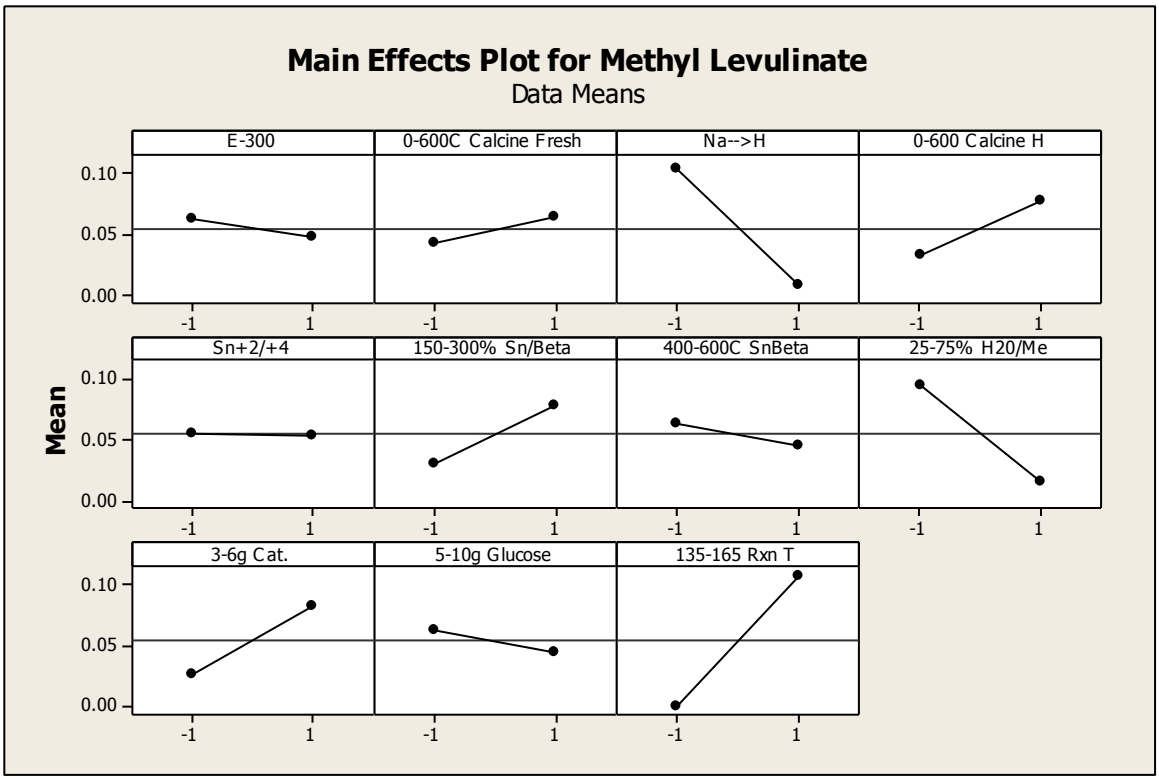

Figure 12: Screening study main effects plot for methyl levulinate production

Levulinic acid production was only increased with higher temperatures. This is interesting in that increased water percentage did not have an effect and suggests that water solvent promotes production of lactic acid over levulinic acid when Sn^{+4} is present. Figure 13 and Figure 14 show the levulinic acid production Pareto chart with 90% confidence for the evaluated factors and the main effects plot, respectively.

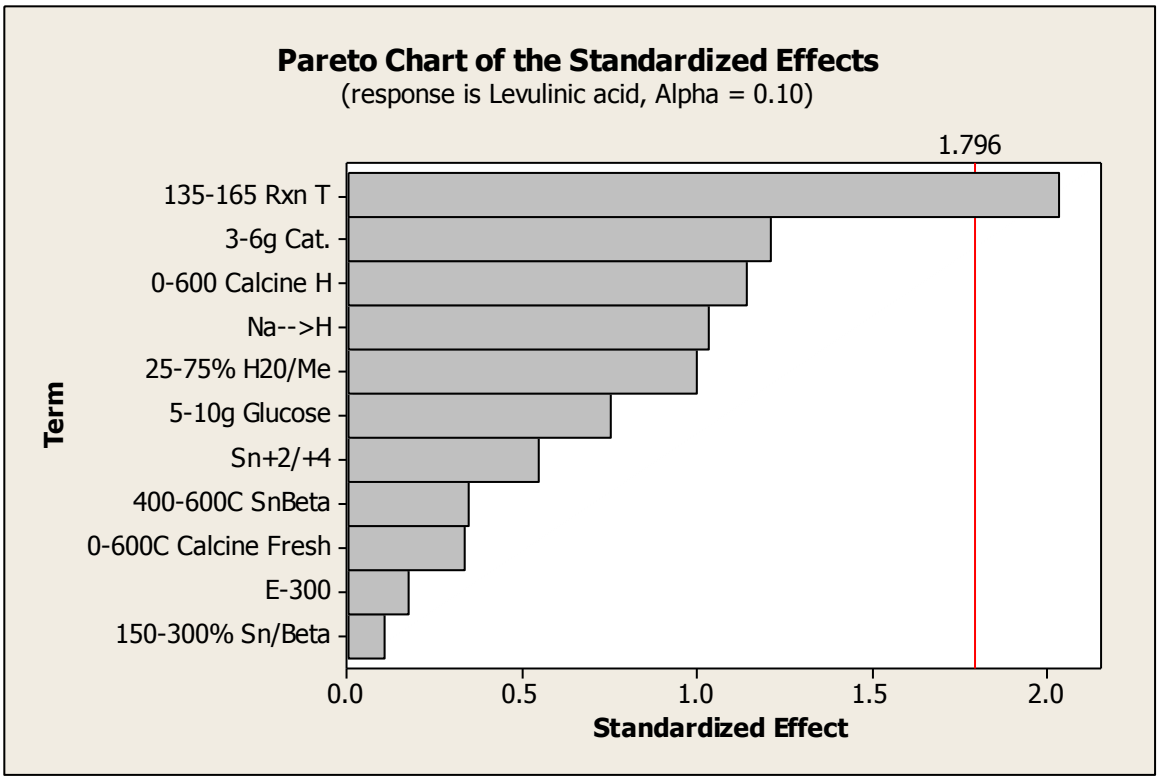

Figure 13: Screening study Pareto chart for levulinic acid production

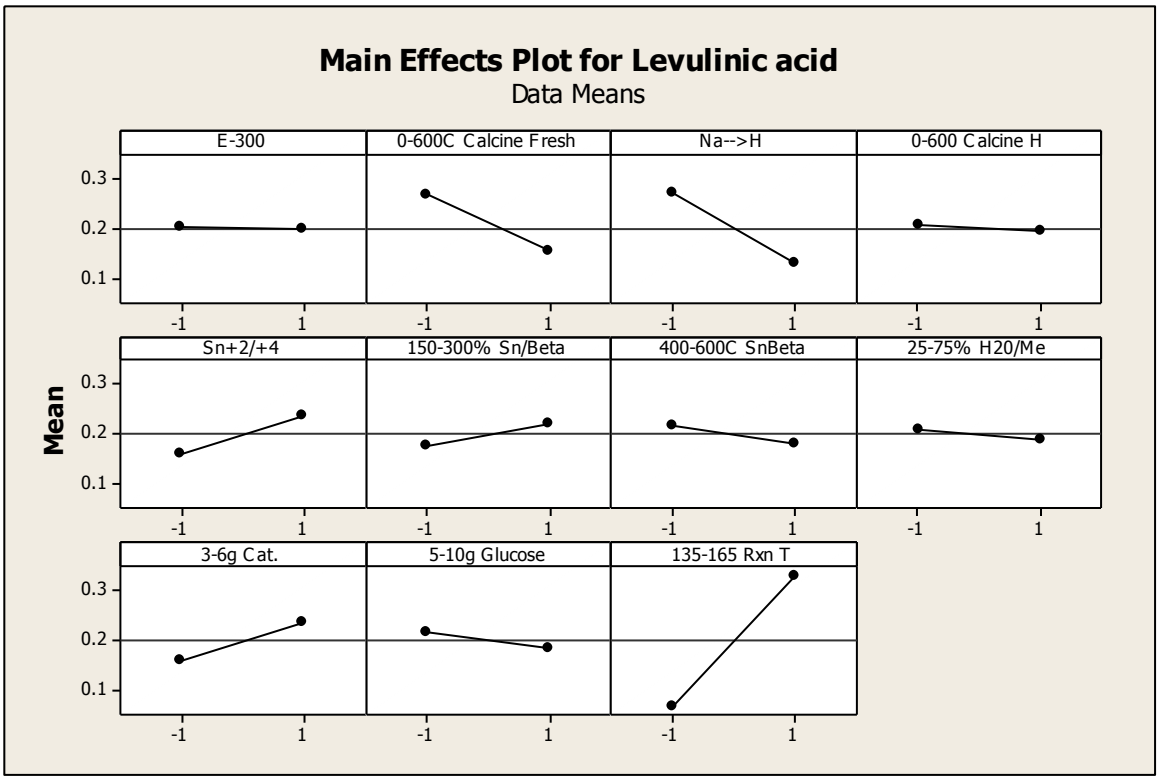

Figure 14: Screening study main effects plot for levulinic acid production

As this was a screening study, interactions between factors were not analyzed as the high number of tested factors and relatively low number of runs would cause heavy convolution of all interactions. The main goal of this project was to produce lactic acid and valuable byproducts, and further explorations to bound significant factors were conducted at higher temperatures, higher water content, and increased catalyst-to-glucose ratio. Table 9 shows the summary of the significant factors for each product analyzed.

Table 9: Significant factors discovered in the Plackett-Burman screening study

	Methanol	Temp.	Glucose	Catalyst	H Doped	Sn^{+2}/ Sn^{+4}	25/300 Beta	Tin wt.%
Glucose	+	+	-	+				
Methyl Lactate	+	+	-					
Lactic Acid	-	+	-	+	-	+	+	
Methyl Levulinate	+	+	-	+	-	-	-	+
Levulinic Acid		+						

"+" indicates an increased effect on production "-" indicates a decreased effect on production

Increased temperature, increased catalyst-to-glucose ratio, and pure solvents favored target products. Further studies were then performed for higher temperatures and with an increased catalyst-to-glucose ratio. Pure methanol was used to target methyl lactate and methyl levulinate. Pure water was used to target lactic acid using Sn^{+4}-doped beta zeolite.

1.6.2 Temperature Bounding Studies

Increased temperatures were found to favor production of all target products therefore a one-variable-at-a-time set of experiments was conducted. All operating conditions, except for temperature, were set identically to the screening study experiments. Lactic acid production was increased with higher temperature, increased water solvent percentage, and use of increased Sn^{+4} for doping on the zeolite with a 300 SiO2/Al2O3 ratio. Figure 15 shows the temperature bounding experiments for maximum lactic acid production at 200 °C. Moderate amounts of levulinic acid and lactic acid were still reported above 200 °C, however the amounts of unaccounted products grow substantially. This signifies unwanted thermal degradation of glucose before any conversion to target products. If there was thermal degradation of target products past 200 °C, they would not be present during analysis, like unreacted glucose.

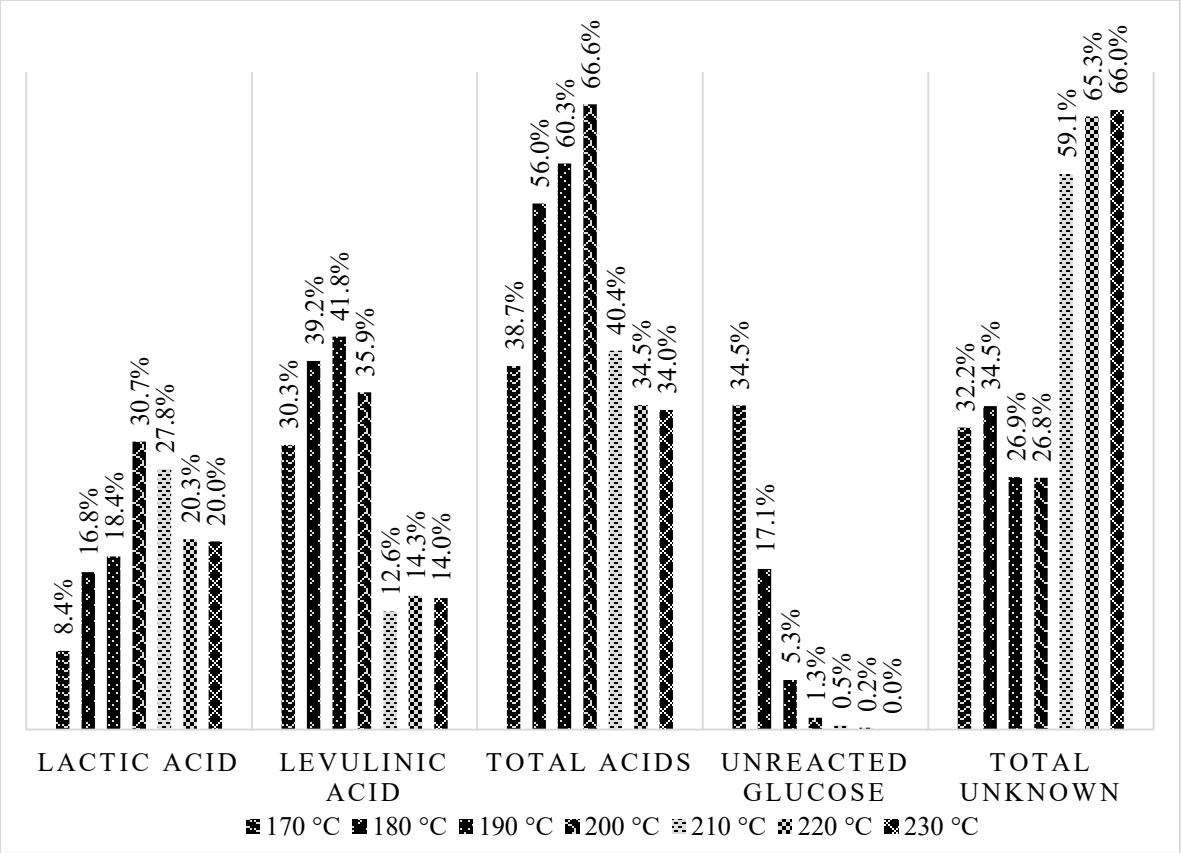

Figure 15: Temperature experiments in pure water solvent using Sn^{+4}-doped beta zeolite

Levulinic acid production was only increased with higher temperatures. Further temperature studies were performed on Sn^{+2}-doped beta zeolite. Figure 16 shows the temperature bounding experiments for maximum levulinic acid with moderate lactic acid production at 200 °C. The upper limit of 200 °C was chosen as the previous study showed significant thermal degradation of the glucose feedstock.

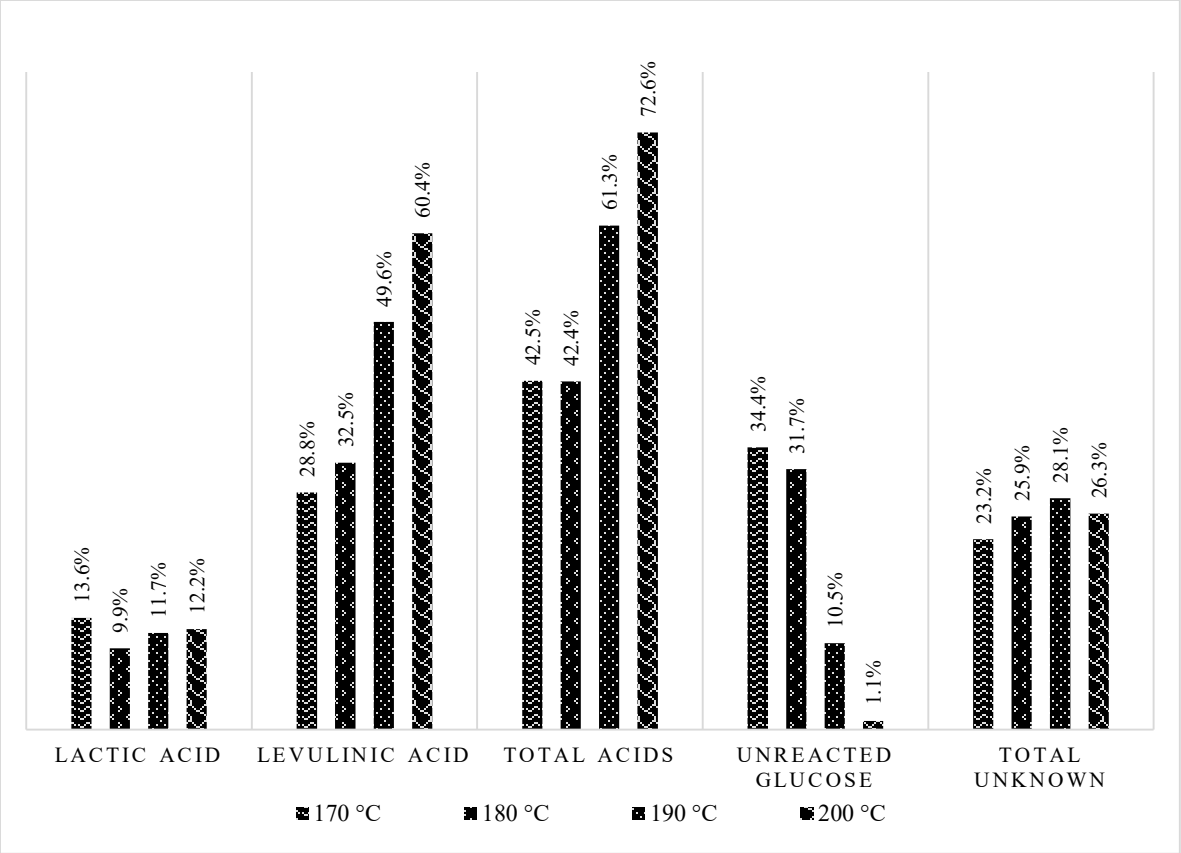

Figure 16: Temperature experiments in pure water solvent using Sn^{+2}-doped beta zeolite

1.6.3 Triplicate Results Under Optimized Conditions

Lactic acid production was maximized at 200 °C using Sn^{+4}-doped beta zeolite in pure water. Three identical experiments were conducted using the procedure previously described. Of the five grams of glucose added, 26.7% and 37.2% successfully converted to lactic acid and levulinic acid, respectively. Under these operating conditions glucose also undergoes isomerization to fructose and mannose. As these three monosaccharides are known isomers at elevated temperatures they are grouped together to account for 11.2% unreacted feed. Visible blackening and increased weight of the collected catalyst is assumed coke, which accounted for 9.2% of the reacted feed. 15.8% of the glucose is still unaccounted for and assumed to be

random caramelized products that are soluble but not eluted during GC-MS analysis. Figure 17 shows the target products, unreacted feed, coke, and combined analysis results with standard deviation for the three runs.

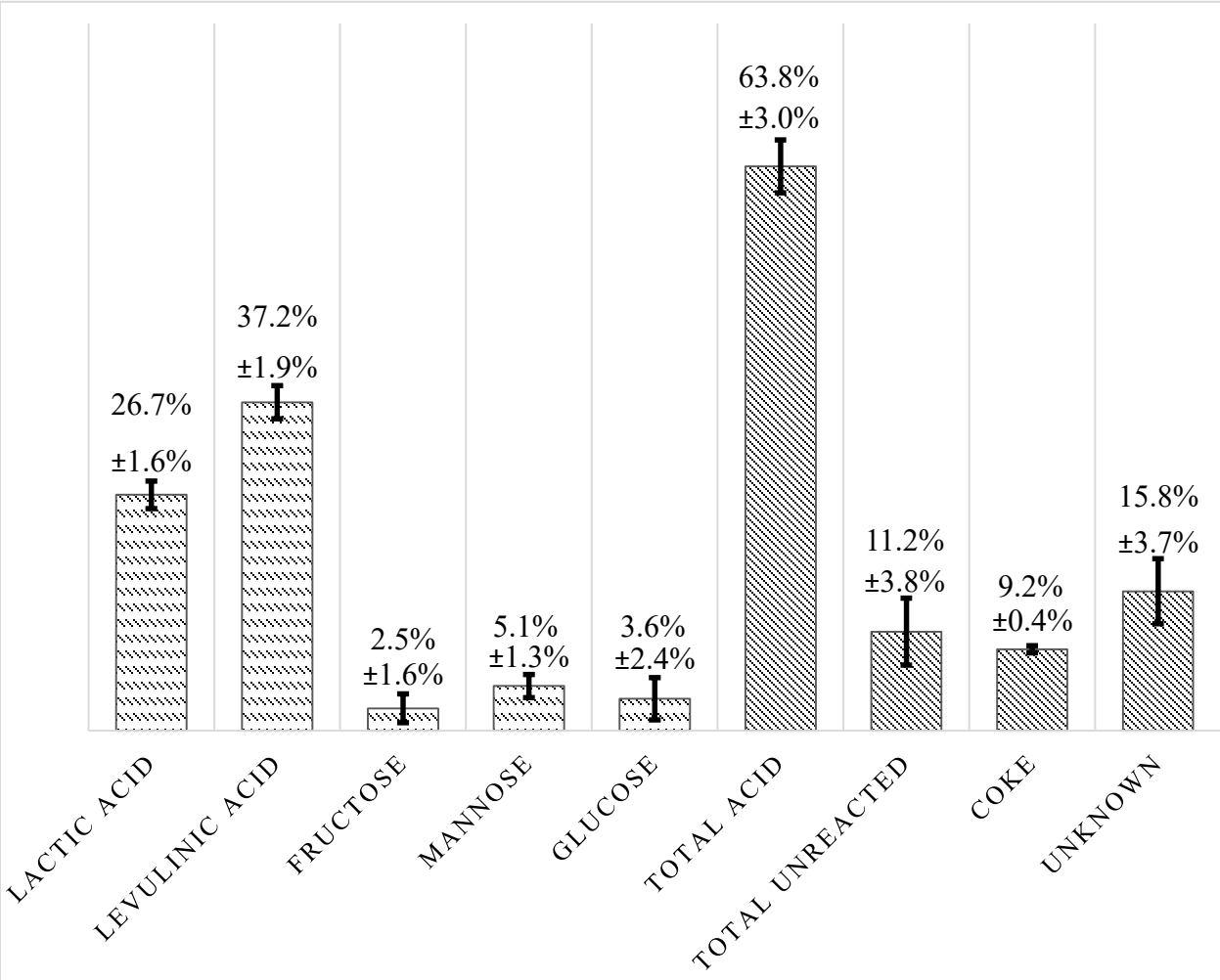

Figure 17: Results from triplicate experiments at 200 °C using Sn^{+4} beta zeolite in pure water

Levulinic acid production was maximized at 200 °C using Sn^{+2}-doped beta zeolite in pure water. Triplicate runs showed an increase of ~15% levulinic acid for a total production of 52.8%. The increase in levulinic acid yields came at the expense of lactic acid production with only 4.4% selectivity toward lactic acid. The competition for reactant favors levulinic acid

without the presence of Sn^{+4}. Coke production was slightly increased which may be due to the almost complete consumption of glucose leading to lower selectivity. The yield of unaccounted products were also increased, which may also be caused by the high glucose consumption. A portion of the unaccounted products should also be formic acid, a known co-product of levulinic acid. Based on molecular weight comparison of formic acid and levulinic acid, there could be up to 10% weight production of formic acid. However, due to the drying process that was needed to derivatize the samples for GC-MS analysis, formic acid was absent. Even the formic acid placed in the calibration standards was not observed in the calibration analysis. Figure 18 shows the full recoverable analyte results along with standard deviations for the three runs with Sn^{+2}-doped beta zeolite in pure water.

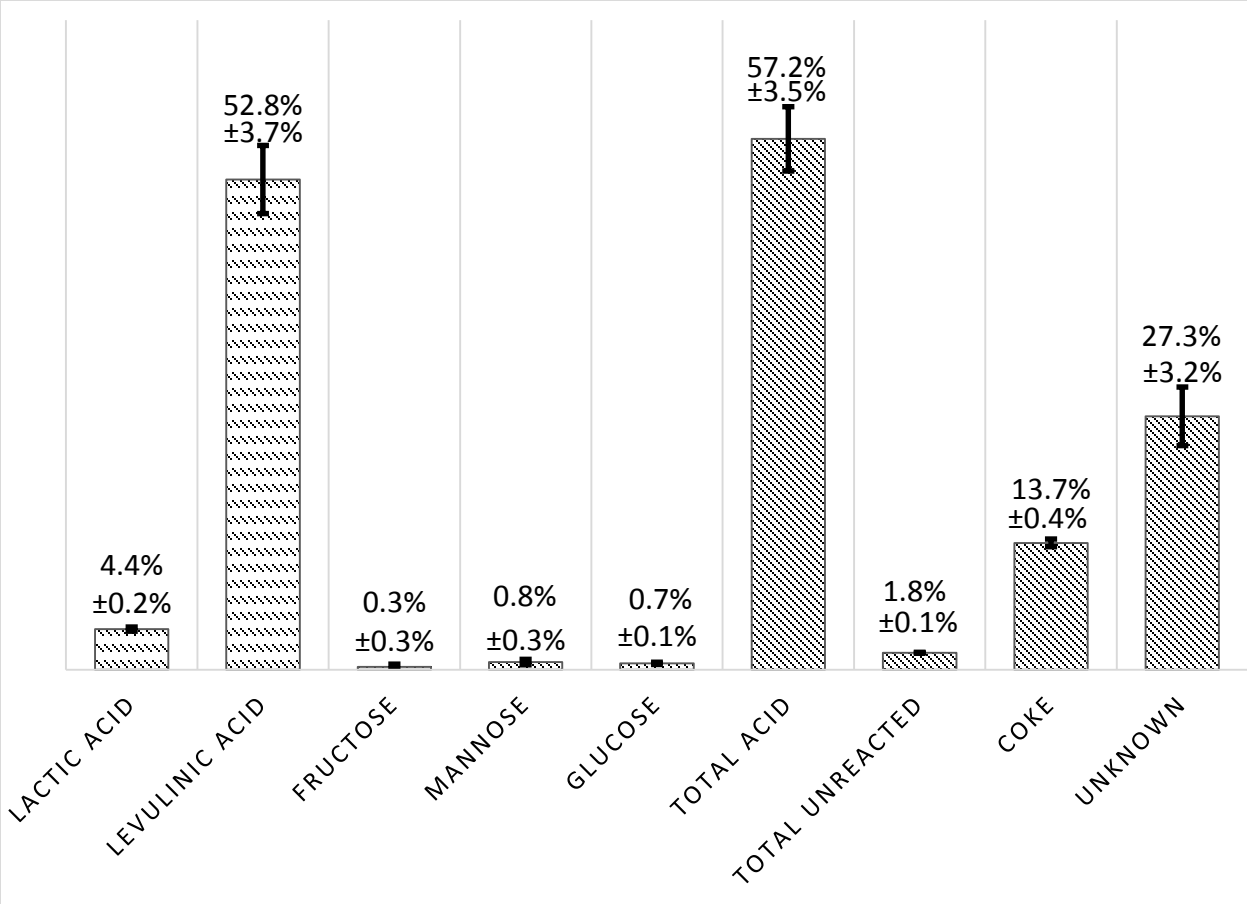

Figure 18: Results from triplicate experiments at 200 °C using Sn^{+2}-doped beta zeolite in pure water

Methyl lactate and methyl levulinate were maximized at 200 °C using Sn^{+4}-doped beta zeolite in methanol. Triplicate results showed 49.2% methyl levulinate, 22.0% methyl lactate, and 2.4% methyl vinyl glycolate. It is important to note that these results are based on weight of corresponding atoms from glucose. The methyl group was contributed from the methanol solvent, so its weight was subtracted as to not skew the results of feed converted. Although most of the glucose was consumed, use of the methanol solvent resulted in significantly less coking. The less polar solvent may be able to remove any formed precursors of coke and keep the catalyst active for a longer period of time. Figure 19 and Figure 20 show the analyte results and

grouped products from triplicate experiments at 200 °C using Sn^{+4}-doped beta zeolite in methanol.

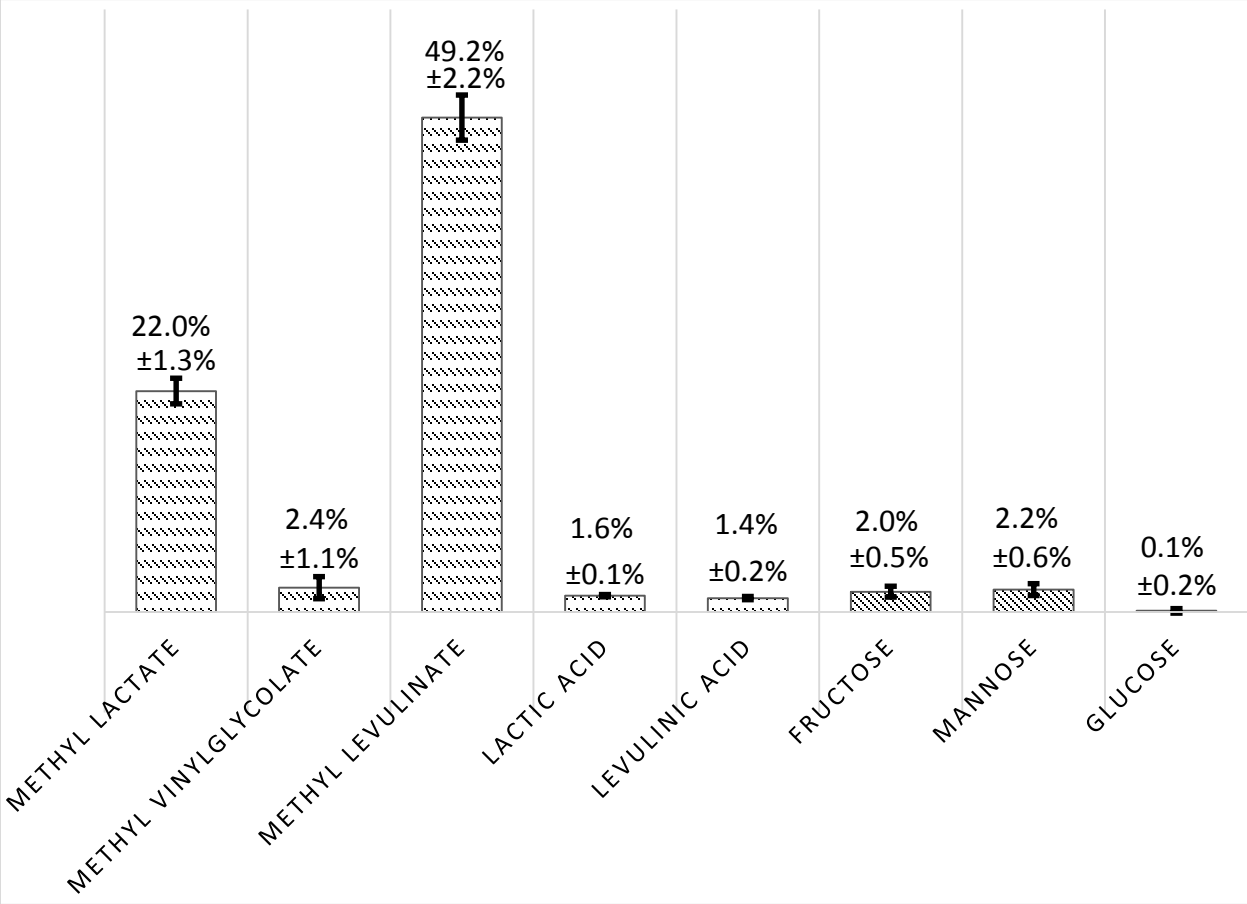

Figure 19: Results from triplicate experiments at 200 °C using Sn^{+4}-doped beta zeolite in methanol

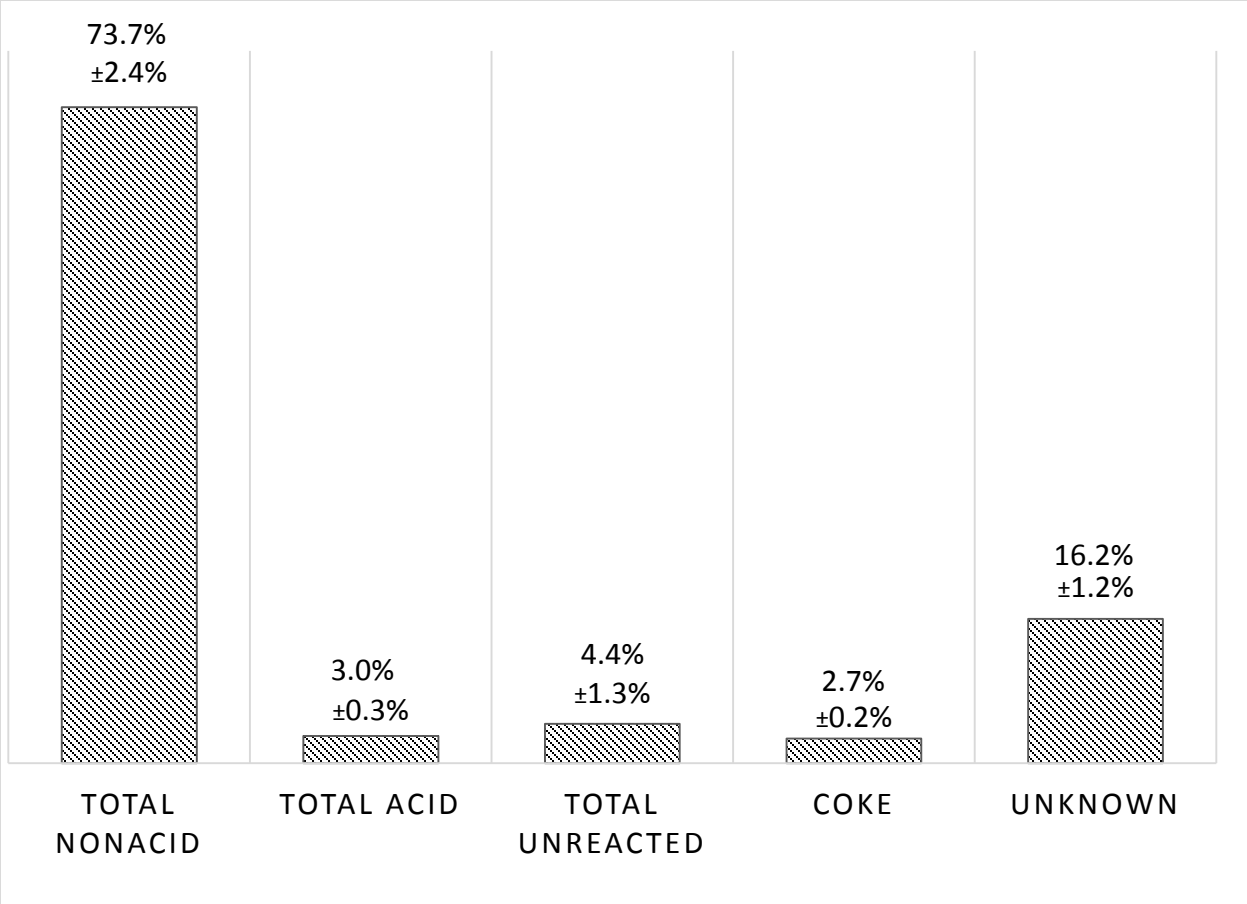

Figure 20: Grouped results from triplicate experiments at 200 °C using Sn^{+4}-doped beta zeolite in methanol

With the main goal of lactic acid production, one more set of triplicates was performed with Sn^{+4}-doped beta zeolite in pure water. For these reactions, the amount of glucose was reduced from five grams to only two grams with only 200 ml of water. This was done to increase the catalyst-to-glucose ratio and keep the overall concentration similar to prior experiments. The increased catalyst amount had a great effect on lactic acid production, with 47.8% selectivity. Surprisingly, there was no levulinic acid measured in these runs, however unaccounted products also increased to 25.8%. A similar total amount of coke was recovered in both the two and five gram experiments, which represents a higher percentage of coke formed

due to the smaller initial feed weight. Apparently, higher catalyst amounts, while increasing reactivity also decrease the selectivity of the catalytic process. Figure 21 shows the lactic acid production, unreacted feed, coke, and combined analysis results along with standard deviation for the three runs.

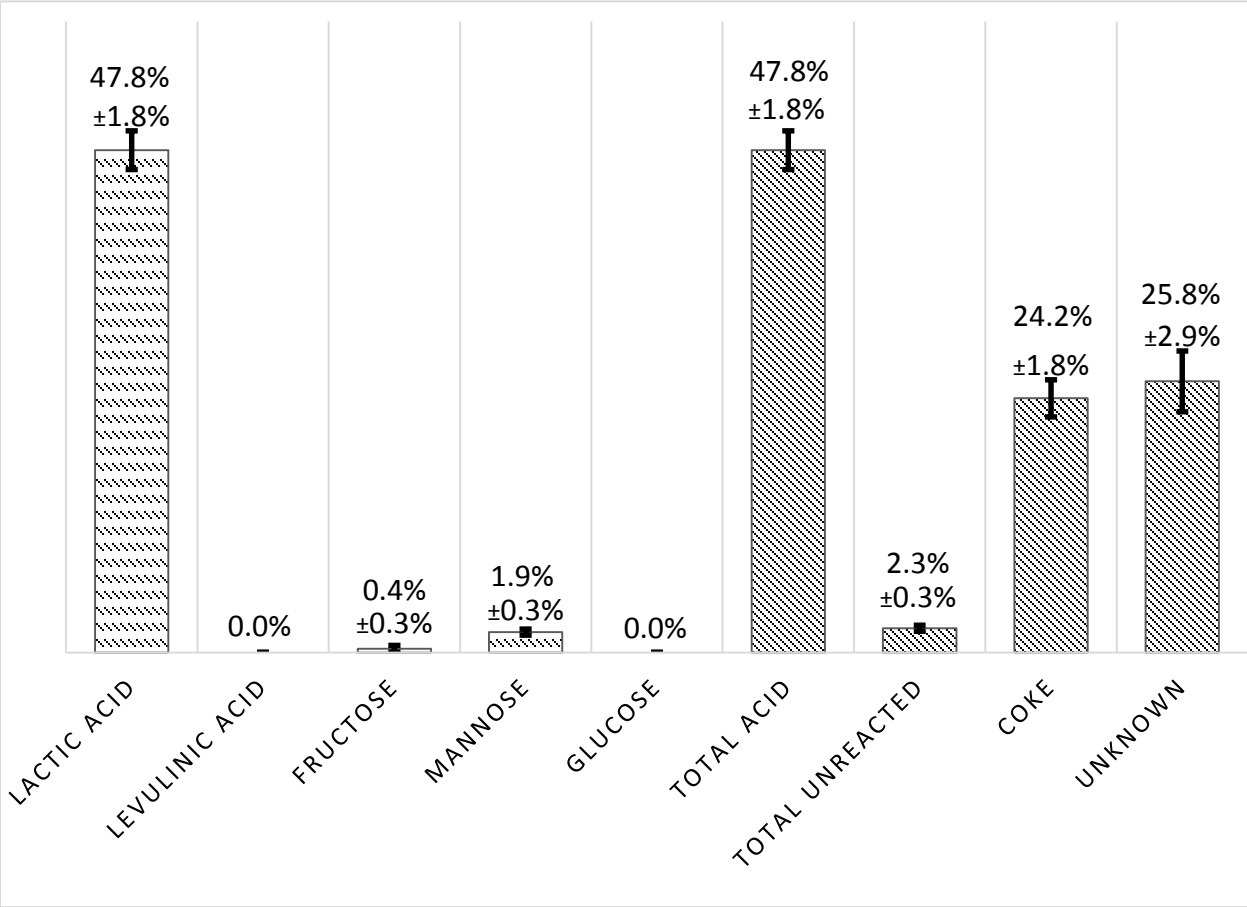

Figure 21: Results from triplicate experiments at 200 °C using Sn^{+4}-doped beta zeolite in pure water with increased catalyst-to-glucose ratio

1.7 Lactic Acid and Levulinic Production Recommendations

Lactic acid was maximized with Sn^{+4}-doped beta zeolite in pure water. Since glucose is readily soluble in water, increased conversion or processing efficiency could be implemented with a continuous process. Future work should look at setting up a bench scale packed bed reactor. Feed flow rate, glucose concentration, temperature, and pressure can be optimized with

the new reactor. Sampling at specified time intervals will provide kinetic information as well as information about catalyst deactivation. Once optimized with a glucose solution, the reactor should be tested on glucose solutions made from biomass degradation. This step will determine whether any purification processing would be needed to protect the catalyst.

Commercial processing for conversion of biomass to fuel components would start with production of glucose from the biomass feedstock. This could be accomplished using technology that is currently in place for glucose production in cellulosic ethanol plants, or preferentially utilizing current UND research on maximizing glucose production from biomass. The biomass degradation product stream would then be fed to a purification system if needed. The purified stream could then be fed into a packed bed reactor with Sn^{+4}-doped beta zeolite for lactic acid or Sn^{+2}-doped beta zeolite for levulinic acid. The lactic acid or levulinic acid solution would then be separated, most likely a distillation tower. The concentrated lactic acid or levulinic acid stream would be fed into another catalytic reactor to utilize their functional groups to make fuel components or value chemicals.

Depending on market demand, the Sn-doped beta zeolite reactor can be switched between Sn^{+4}-doped beta zeolite for lactic acid or Sn^{+2}-doped for levulinic acid. The conversion of the acids to fuel components or value chemicals can also be selected for maximum profit. Assuming high conversion of glucose from the biomass and high conversion of lactic acid or levulinic acid to fuel components or value chemicals, up to 50% of renewable biomass could be converted into valuable products using Sn-doped beta zeolite catalyst that was maximized with this research.

1.8 Methyl Lactate or Methyl Levulinate Production Recommendations

The catalyst to glucose ratio should be explored in greater detail. Future experiments would focus on increasing the added catalyst amount instead of decreasing the substrate. Reducing the overall solvent amount is another area of interest, by increasing the substrate concentration above lactobacilli limitations will demonstrate one of the main advantages over biological processes.

Overall conversion of glucose was maximized with Sn^{+4}-doped beta zeolite in pure methanol, producing 22% methyl lactate and 49% methyl levulinate. However, as glucose solubility in methanol is only 0.037 M, a continuous stir fed reactor (CSTR) would be more efficient. A bench scale CSTR system could be set up with catalyst and glucose charged in the CSTR, and pure methanol would be introduced. As methyl lactate and methyl levulinate are readily soluble in methanol, the product stream from the CSTR would contain the target compounds. Initial glucose concentration, temperature, and pressure can be optimized with the CSTR. Sampling at specified time intervals will provide kinetic information as well as information about catalyst deactivation.

Commercial processing for conversion of biomass to fuel components would start with the same technique as above to maximize glucose from biomass. However since methanol will be the new solvent, there will need to be a separation process to crystalize the glucose and transfer it to the CSTR. Once the CSTR is charged with biomass derived glucose and Sn^{+4}-doped beta zeolite, the reactor would be filled with methanol and heated to reaction temperature. The product stream containing both methyl lactate and methyl levulinate would then be separated, most likely in a distillation tower. The separated methyl lactate and methyl levulinate

streams would be fed into their respective catalytic reactors to utilize their functional groups to make fuel components or value chemicals.

There may be a cost prohibitive step of transferring the biomass derived glucose to methanol. In addition, this setup does not have the same versatility to target methyl levulinate or methyl lactate, although it has a higher overall conversion of glucose and less coke formation. Assuming high conversion of glucose from the biomass and high conversion methyl lactate and methyl levulinate to fuel components or value chemicals, up to 70% of renewable biomass could be converted into valuable products.

CHAPTER III
CONCLUSIONS

Lactic acid and levulinic acids along with their methyl ester derivatives were selectively produced using a novel Sn-doped beta zeolite. A twelve run Plackett-Burman design of experiments study was implemented to study catalyst synthesis as well as operating conditions. The DOE for catalyst synthesis showed Sn^{+4} was selective towards lactic acid and its derivatives while the Sn^{+2} was selective towards levulinic acid and its derivatives. The intermediate step of H-beta showed a negative effect on total Sn doping and was removed from all future synthesis.

The solvent factor from the DOE showed simultaneous production of both the acids and methyl esters. However, preference for the related products was dependent on which solvent, water or methanol, was dominant. For example higher methanol solvent promoted methyl lactate over lactic acid. As there was no increase on overall conversion with the mixed solvents all future runs were conducted in pure methanol or water solvent.

The DOE on operating conditions also showed that increased temperature promoted production of target products and the next set of experiments concentrated on bounding the temperature limit. There was an increase of target products up to 200 °C. After 200 °C there was a moderate decrease in target products but a significant increase in unaccounted products. All future experiments were conducted at the optimal 200 °C.

Triplicate runs were conducted under the experimental conditions that maximized target product yields. When using Sn^{+4}-doped beta zeolite in pure water with a high catalyst-to-glucose ratio 47% lactic acid was produced with 26% unaccounted product. Levulinic acid yield was

maximized with 53% selectivity and 27% unaccounted product using Sn^{+2}-doped beta zeolite. Methyl lactate, 22%, and methyl levulinate, 49%, were produced using Sn^{+4}-doped beta zeolite in methanol, with only 16% unaccounted product. All triplicate results were successful in defining a large majority of the products. The experiments also showed that the yield of each targeted product could be maximized by changing the dopant or solvent.

Current UND research is focused on maximizing glucose recovery from biomass degradation and future research will look at utilizing lactic acid, levulinic acid, methyl lactate, and methyl levulinate for conversion to fuel components or value products. While this body of work shows just one step in the process, it was significant in showing that up to 50% lactic acid or levulinic acid can be recovered from an aqueous system, where previous publications only produced 27%. Utilizing glucose in an aqueous system will provide substantial cost savings in preprocessing the biomass derived glucose. If the methanol solvent route is preferred, our work showed an increase of recovered products to 70% including the unreported methyl levulinate. This is a 20% increase compared to literature results for glucose conversion in a methanol solution. Our research fills an information gap in the literature as well as provides essential information for continuing research to allow further processing towards either fuels or value chemicals from renewable biomass.

APPENDIX A
ZEOLITE DOPING

The procedure for doping was identical whether using the 25 or 300 SiO_2/Al_2O_3 ratio beta zeolite. Thirty grams of the purchased zeolite was calcined at 600 °C for 8 hours. When the zeolite was cooled to room temperature it was dispersed in a doping solution and stirred until well dispersed. The doping solution was prepared with 1 gram $SnCl_4 \cdot 5H_2O$ or 0.5 grams $SnCl_2$ in 50 ml of 1 mol HCl to help dissolve the salt. Parafilm was placed over the opening of the glass container and the container was then place in a sonicator. It was sonicated overnight; note that the sonicator fluid warms to about 60 °C from normal operation without the need to turn on the heater. The next day a funnel with filter paper was set up to collect the doped zeolite. The sonicated solution was carefully poured into the filter paper and let set overnight. When the contents of the filter paper was a thick paste all contents were scraped off the filter paper into a ceramic dish and calcined at 400 °C for 8 hours. When the Sn-doped zeolite was cooled it was sealed in a glass container for future use.

APPENDIX B
AUTOCLAVE EXPERIMENT SETUP

Using a mass balance and weigh dish ten grams of Sn-doped beta zeolite were measured and all contents of the weigh dish were placed into the clean reactor vessel. Five grams of glucose were measured and placed in the reactor vessel. 300 ml ultra-pure water from the millipore purifying system was measured in a clean graduated cylinder then slowly added to the reactor vessel. A thin layer of vacuum grease was placed on the reactor vessel lip to ensure a complete seal was formed and to protect the high pressure gasket from sticking to the vessel.

The reaction vessel was then ready to be connected to the rest of the Parr reactor. Both halves of the reactor vessel clamp were placed and the safety clasps were connected to hold the reactor in place. The eight bolts sealing the vessel were tightened with a torque wrench set to 20 foot-pounds to protect the gasket from over tightening. Bolts were tightened, alternating between opposite sides to prevent over tightening of one side and to ensure an even sealing of the reactor. Once all bolts were tightened to 20 foot-pounds, the torque wrench was set to 35 foot-pounds and the alternating tightening procedure was repeated. The 35 foot-pounds tightening sequence was done twice to ensure all the bolts were correctly tightened and a proper seal was formed.

Once the reactor was sealed, the gas phase needed to be purged to remove atmospheric gasses. The nitrogen input line was slowly opened to increase the pressure of the reactor to 300 psig. Then the vent was slowly opened to relieve the built up pressure. This procedure was used

to purge the reactor with nitrogen five times. After purging the vessel the reactor was charged one last time with nitrogen to 300 psi and all inlet valves on the reactor were closed.

Once the reactor was sealed and charged the Parr heater was raised and locked into place around the reactor vessel. The cooling water line was opened and the bypass line was closed, to ensure the cooling water was only used for temperature control. The heater was turned on and set to 200 °C. If the temperature raised above 200 °C the cooling water bypass valve was opened shortly until 200 °C was achieved. The temperature was maintained at 200±1 °C. The stirring motor was set to 400 RPMs and signified the start of the reaction.

After 20 hours the reaction was considered complete and the heater was turned off and lowered, the cooling water bypass valve was opened, and a small fan was placed to blow over the reactor vessel. When the reactor was cooled to room temperature the gas vent was slowly opened, bringing the reaction mixture back to atmospheric pressure.

The bolts on the seal clamp were loosened in the same order as they were tightened. The clasps on the clamp were opened and the vessel was removed from the rest of the Parr reactor. Using a 2 ml syringe a small volume of the reactor fluid was removed, filtered through a micron, and collected in a small container for later analysis. A funnel with filter paper was set up to separate the solids from the liquid reactor solution. The reactor fluid was carefully poured into the filter paper to collect the used catalyst. All solids were removed from the agitator blades, cooling coil, thermocouple thermowell, all other internal parts of the reactor, and the reactor vessel and placed in the filter paper. When all the fluid had drained the liquid was placed in a large storage vessel. The filter paper with the collected used catalyst was set aside to let dry. When completely dry and the used catalyst was again in powder form it was weighed to calculate the amount of coke formed.

APPENDIX C
GC-MS ANALYSIS

Exactly 20 µl of the micron filtered collected sample from the completed reaction was placed in a new two ml autosampler vial. The vial was placed under a slow nitrogen flow to dry the sample. When the sample was dry 60 µl pyridine and 60 µl BTSFA derivatizing solution were added. The autosampler vial was capped using a crimping tool. The sample was vortexed and placed in a 70 °C oven overnight. The next day the autosampler vial was opened and one ml of dilute internal standard solution was added and resealed. The internal standard solution was made with 4 mg of o-terphenyl in 100 ml of DCM.

Calibration samples were prepared using purchased stock chemicals. Calibration solution was prepared by accurately measuring approximately ten mg of stock chemicals which were then dissolved in 1ml of methanol. Exactly 40 µl of the calibration sample were placed in an autosampler vial and dried with a nitrogen flow. When the sample was dry 300 µl pyridine and 300 µl BTSFA derivatizing solution were added. The calibration vial was capped using a crimping tool. The calibration sample was vortexed and placed in a 70 °C oven overnight. The next day the calibration vial was opened and half of its contents, 300 µl, were transferred to a new autosampler vial that contained 300 µl DCM. Again half of its contents, 300 µl, were transferred to a new autosampler vial that contained 300 µl DCM. This was done seven times creating eight serial dilution calibration samples where each new vial was half the concentration of the previous. 300 µl of the last dilution was discarded leaving eight samples all with 300 ml

of calibration standards. One ml of dilute internal standard solution was added to all the calibration vials and the vials were sealed.

All sample vials and calibration vials were placed in the Agilent 6890GC-MS autosampler tray. The run order was started with a neat DCM vial to ensure a flat baseline was observed and the instrument was not contaminated. Three runs of a test mix, provided by Dr. Kubatova's group, was then analyzed to ensure the detector's measurements were accurate and repeatable. Another neat DCM blank was injected to flush the column and check again for possible carryover of analytes. The eight calibration runs, starting with the most dilute were injected with another DCM blank after the first four. Then the reactor samples were injected with a DCM blank after every three or four injections. After all the reactor samples were injected the eight calibration runs were injected again with another DCM blank after the first four. The sequence was ended with another triplicate of the test mix and DCM blank. If the sequence lasted more than a day, intermediate calibrations were inserted to ensure everything was working correctly. Table 10 shows an example of the GC-MS analysis used on a multiday sequence used for during the DOE study.

Table 10: Example of GC-MS analysis sequence

13-0813_EI_CK					
DB-5ms 28m Column, Splitless w/o Glass Wool, 50 mL/min split					
Type	Vial	Sample	Method	Data File	Notes
Blank	1	DCM blank	TM01_EI	001_Blank	
Sample	2	Testmix_low	TM01_EI	002_MC59-2D	Test Mix
Sample	2	Testmix_low	TM01_EI	003_MC59-2D	Test Mix
Sample	2	Testmix_low	TM01_EI	004_MC59-2D	Test Mix
Blank	1	DCM blank	CK_TEST03_EI	005_Blank	
Sample	3	CK23_01	CK_TEST03_EI	006_CK23_01	Underivatized Calibration
Sample	4	CK23_02	CK_TEST03_EI	007_CK23_02	Underivatized Calibration
Sample	5	CK23_03	CK_TEST03_EI	008_CK23_03	Underivatized Calibration
Sample	6	CK23_04	CK_TEST03_EI	009_CK23_04	Underivatized Calibration
Blank	1	DCM blank	TM01_EI	010_Blank	
Sample	7	CK23_05	CK_TEST03_EI	011_CK23_05	Underivatized Calibration
Sample	8	CK23_06	CK_TEST03_EI	012_CK23_06	Underivatized Calibration
Sample	9	CK23_07	CK_TEST03_EI	013_CK23_07	Underivatized Calibration
Sample	10	CK23_08	CK_TEST03_EI	014_CK23_08	Underivatized Calibration
Blank	1	DCM blank	TM01_EI	015_Blank	
Sample	11	CK23_098	CK_TEST03_EI	016_CK23_098	Underivatized Sample
Sample	12	CK23_099	CK_TEST03_EI	017_CK23_099	Underivatized Sample
Sample	13	CK23_100	CK_TEST03_EI	018_CK23_100	Underivatized Sample
Blank	1	DCM blank	TM01_EI	019_Blank	
Sample	14	CK23_101	CK_TEST03_EI	020_CK23_101	Underivatized Sample
Sample	15	CK23_102	CK_TEST03_EI	021_CK23_102	Underivatized Sample
Sample	16	CK23_103	CK_TEST03_EI	022_CK23_103	Underivatized Sample
Blank	1	DCM blank	TM01_EI	023_Blank	

Table 10 Continued					
Sample	17	CK23_106	CK_TEST03_EI	024_CK23_106	Underivatized Sample
Sample	18	CK23_107	CK_TEST03_EI	025_CK23_107	Underivatized Sample
Sample	19	CK23_108	CK_TEST03_EI	026_CK23_108	Underivatized Sample
Blank	1	DCM blank	TM01_EI	027_Blank	
Sample	20	CK23_109	CK_TEST03_EI	028_CK23_109	Underivatized Sample
Sample	21	CK23_110	CK_TEST03_EI	029_CK23_110	Underivatized Sample
Sample	22	CK23_111	CK_TEST03_EI	030_CK23_111	Underivatized Sample
Blank	1	DCM blank	TM01_EI	031_Blank	
Sample	7	CK23_05	CK_TEST03_EI	032_CK23_05	Underivatized Check
Blank	1	DCM blank	TM01_EI	033_Blank	
Sample	23	CK23_114	CK_TEST03_EI	034_CK23_114	Underivatized Sample
Sample	24	CK23_115	CK_TEST03_EI	035_CK23_115	Underivatized Sample
Sample	25	CK23_116	CK_TEST03_EI	036_CK23_116	Underivatized Sample
Blank	1	DCM blank	TM01_EI	037_Blank	
Sample	26	CK23_117	CK_TEST03_EI	038_CK23_117	Underivatized Sample
Sample	27	CK23_118	CK_TEST03_EI	039_CK23_118	Underivatized Sample
Sample	28	CK23_119	CK_TEST03_EI	040_CK23_119	Underivatized Sample
Blank	1	DCM blank	TM01_EI	041_Blank	
Sample	29	CK23_122	CK_TEST03_EI	042_CK23_122	Underivatized Sample
Sample	30	CK23_123	CK_TEST03_EI	043_CK23_123	Underivatized Sample
Sample	31	CK23_124	CK_TEST03_EI	044_CK23_124	Underivatized Sample
Blank	1	DCM blank	TM01_EI	045_Blank	
Sample	32	CK23_125	CK_TEST03_EI	046_CK23_125	Underivatized Sample
Sample	33	CK23_126	CK_TEST03_EI	047_CK23_126	Underivatized Sample

Table 10 Continued					
Sample	34	CK23_127	CK_TEST03_EI	048_CK23_127	Underivatized Sample
Blank	1	DCM blank	TM01_EI	049_Blank	
Sample	7	CK23_05	CK_TEST03_EI	050_CK23_05	Underivatized Check
Blank	1	DCM blank	TM01_EI	051_Blank	
Sample	35	CK23_130	CK_TEST03_EI	052_CK23_130	Underivatized Sample
Sample	36	CK23_131	CK_TEST03_EI	053_CK23_131	Underivatized Sample
Sample	37	CK23_132	CK_TEST03_EI	054_CK23_132	Underivatized Sample
Blank	1	DCM blank	TM01_EI	055_Blank	
Sample	38	CK23_133	CK_TEST03_EI	056_CK23_133	Underivatized Sample
Sample	39	CK23_134	CK_TEST03_EI	057_CK23_134	Underivatized Sample
Sample	40	CK23_135	CK_TEST03_EI	058_CK23_135	Underivatized Sample
Blank	1	DCM blank	TM01_EI	059_Blank	
Sample	41	CK23_138	CK_TEST03_EI	060_CK23_138	Underivatized Sample
Sample	42	CK23_139	CK_TEST03_EI	061_CK23_139	Underivatized Sample
Sample	43	CK23_140	CK_TEST03_EI	062_CK23_140	Underivatized Sample
Blank	1	DCM blank	TM01_EI	063_Blank	
Sample	44	CK23_141	CK_TEST03_EI	064_CK23_141	Underivatized Sample
Sample	45	CK23_142	CK_TEST03_EI	065_CK23_142	Underivatized Sample
Sample	46	CK23_143	CK_TEST03_EI	066_CK23_143	Underivatized Sample
Blank	1	DCM blank	TM01_EI	067_Blank	
Sample	3	CK23_01	CK_TEST03_EI	068_CK23_01	Underivatized Calibration
Sample	4	CK23_02	CK_TEST03_EI	069_CK23_02	Underivatized Calibration
Sample	5	CK23_03	CK_TEST03_EI	070_CK23_03	Underivatized Calibration
Sample	6	CK23_04	CK_TEST03_EI	071_CK23_04	Underivatized Calibration

Table 10 Continued					
Blank	1	DCM blank	TM01_EI	072_Blank	
Sample	7	CK23_05	CK_TEST03_EI	073_CK23_05	Underivatized Calibration
Sample	8	CK23_06	CK_TEST03_EI	074_CK23_06	Underivatized Calibration
Sample	9	CK23_07	CK_TEST03_EI	075_CK23_07	Underivatized Calibration
Sample	10	CK23_08	CK_TEST03_EI	076_CK23_08	Underivatized Calibration
Blank	1	DCM blank	TM01_EI	077_Blank	
Sample	47	CK23_146	CK_TEST03_EI	078_CK23_146	Underivatized Sample
Sample	48	CK23_147	CK_TEST03_EI	079_CK23_147	Underivatized Sample
Sample	49	CK23_148	CK_TEST03_EI	080_CK23_148	Underivatized Sample
Blank	1	DCM blank	TM01_EI	081_Blank	
Sample	50	CK23_149	CK_TEST03_EI	082_CK23_149	Underivatized Sample
Sample	51	CK23_150	CK_TEST03_EI	083_CK23_150	Underivatized Sample
Sample	52	CK23_151	CK_TEST03_EI	084_CK23_151	Underivatized Sample
Blank	1	DCM blank	TM01_EI	085_Blank	
Sample	53	CK23_154	CK_TEST03_EI	086_CK23_154	Underivatized Sample
Sample	54	CK23_155	CK_TEST03_EI	087_CK23_155	Underivatized Sample
Sample	55	CK23_156	CK_TEST03_EI	088_CK23_156	Underivatized Sample
Blank	1	DCM blank	TM01_EI	089_Blank	
Sample	56	CK23_157	CK_TEST03_EI	090_CK23_157	Underivatized Sample
Sample	57	CK23_158	CK_TEST03_EI	091_CK23_158	Underivatized Sample
Sample	58	CK23_159	CK_TEST03_EI	092_CK23_159	Underivatized Sample
Blank	1	DCM blank	TM01_EI	093_Blank	
Sample	7	CK23_05	CK_TEST03_EI	094_CK23_05	Underivatized Check
Blank	1	DCM blank	TM01_EI	095_Blank	

Table 10 Continued					
Sample	59	CK23_162	CK_TEST03_EI	096_CK23_162	Underivatized Sample
Sample	60	CK23_163	CK_TEST03_EI	097_CK23_163	Underivatized Sample
Sample	61	CK23_164	CK_TEST03_EI	098_CK23_164	Underivatized Sample
Blank	1	DCM blank	TM01_EI	099_Blank	
Sample	62	CK23_165	CK_TEST03_EI	100_CK23_165	Underivatized Sample
Sample	63	CK23_166	CK_TEST03_EI	101_CK23_166	Underivatized Sample
Sample	64	CK23_167	CK_TEST03_EI	102_CK23_167	Underivatized Sample
Blank	1	DCM blank	TM01_EI	103_Blank	
Sample	65	CK23_170	CK_TEST03_EI	104_CK23_170	Underivatized Sample
Sample	66	CK23_171	CK_TEST03_EI	105_CK23_171	Underivatized Sample
Sample	67	CK23_172	CK_TEST03_EI	106_CK23_172	Underivatized Sample
Blank	1	DCM blank	TM01_EI	107_Blank	
Sample	68	CK23_173	CK_TEST03_EI	108_CK23_173	Underivatized Sample
Sample	69	CK23_174	CK_TEST03_EI	109_CK23_174	Underivatized Sample
Sample	70	CK23_175	CK_TEST03_EI	110_CK23_175	Underivatized Sample
Blank	1	DCM blank	TM01_EI	111_Blank	
Sample	7	CK23_05	CK_TEST03_EI	112_CK23_05	Underivatized Check
Blank	1	DCM blank	TM01_EI	113_Blank	
Sample	71	CK23_178	CK_TEST03_EI	114_CK23_178	Underivatized Sample
Sample	72	CK23_179	CK_TEST03_EI	115_CK23_179	Underivatized Sample
Sample	73	CK23_180	CK_TEST03_EI	116_CK23_180	Underivatized Sample
Blank	1	DCM blank	TM01_EI	117_Blank	
Sample	74	CK23_181	CK_TEST03_EI	118_CK23_181	Underivatized Sample
Sample	75	CK23_182	CK_TEST03_EI	119_CK23_182	Underivatized Sample

Table 10 Continued					
Sample	76	CK23_183	CK_TEST03_EI	120_CK23_183	Underivatized Sample
Blank	1	DCM blank	TM01_EI	121_Blank	
Sample	77	CK23_186	CK_TEST03_EI	122_CK23_186	Underivatized Sample
Sample	78	CK23_187	CK_TEST03_EI	123_CK23_187	Underivatized Sample
Sample	79	CK23_188	CK_TEST03_EI	124_CK23_188	Underivatized Sample
Blank	1	DCM blank	TM01_EI	125_Blank	
Sample	80	CK23_189	CK_TEST03_EI	126_CK23_189	Underivatized Sample
Sample	81	CK23_190	CK_TEST03_EI	127_CK23_190	Underivatized Sample
Sample	82	CK23_191	CK_TEST03_EI	128_CK23_191	Underivatized Sample
Blank	1	DCM blank	TM01_EI	129_Blank	
Sample	3	CK23_01	CK_TEST03_EI	130_CK23_01	Underivatized Calibration
Sample	4	CK23_02	CK_TEST03_EI	131_CK23_02	Underivatized Calibration
Sample	5	CK23_03	CK_TEST03_EI	132_CK23_03	Underivatized Calibration
Sample	6	CK23_04	CK_TEST03_EI	133_CK23_04	Underivatized Calibration
Blank	1	DCM blank	TM01_EI	134_Blank	
Sample	7	CK23_05	CK_TEST03_EI	135_CK23_05	Underivatized Calibration
Sample	8	CK23_06	CK_TEST03_EI	136_CK23_06	Underivatized Calibration
Sample	9	CK23_07	CK_TEST03_EI	137_CK23_07	Underivatized Calibration
Sample	10	CK23_08	CK_TEST03_EI	138_CK23_08	Underivatized Calibration
Blank	1	DCM blank	TM01_EI	139_Blank	
Sample	2	Testmix_low	TM01_EI	140_MC59-2D	Test Mix
Sample	2	Testmix_low	TM01_EI	141_MC59-2D	Test Mix
Sample	2	Testmix_low	TM01_EI	142_MC59-2D	Test Mix
Blank	1	DCM blank	TM01_EI	143_Blank	
Sample	11	CK19_09d	JR_BSTFA_06_EI	144_CK19-09d	Derivatized Calibration

Table 10 Continued					
Sample	12	CK19_10d	JR_BSTFA_06_EI	145_CK19-10d	Derivatized Calibration
Sample	13	CK19_11d	JR_BSTFA_06_EI	146_CK19-11d	Derivatized Calibration
Sample	14	CK19_12d	JR_BSTFA_06_EI	147_CK19-12d	Derivatized Calibration
Blank	1	DCM blank	TM01_EI	148_Blank	
Sample	15	CK19_13d	JR_BSTFA_06_EI	149_CK19-13d	Derivatized Calibration
Sample	16	CK19_14d	JR_BSTFA_06_EI	150_CK19-14d	Derivatized Calibration
Sample	17	CK19_15d	JR_BSTFA_06_EI	151_CK19-15d	Derivatized Calibration
Sample	18	CK19_16d	JR_BSTFA_06_EI	152_CK19-16d	Derivatized Calibration
Blank	1	DCM blank	TM01_EI	153_Blank	
Sample	19	CK19_96d	JR_BSTFA_06_EI	154_CK19-96d	Derivatized Sample
Sample	20	CK19_97d	JR_BSTFA_06_EI	155_CK19-97d	Derivatized Sample
Sample	21	CK19_98d	JR_BSTFA_06_EI	156_CK19-98d	Derivatized Sample
Sample	22	CK19_99d	JR_BSTFA_06_EI	157_CK19-99d	Derivatized Sample
Blank	1	DCM blank	TM01_EI	158_Blank	
Sample	15	CK19_13d	JR_BSTFA_06_EI	159_CK19-13d	Derivatized Check
Blank	1	DCM blank	TM01_EI	160_Blank	
Sample	23	CK20_02d	JR_BSTFA_06_EI	161_CK20-02d	Derivatized Sample
Sample	24	CK20_03d	JR_BSTFA_06_EI	162_CK20-03d	Derivatized Sample
Sample	25	CK20_04d	JR_BSTFA_06_EI	163_CK20-04d	Derivatized Sample
Blank	1	DCM blank	TM01_EI	164_Blank	
Sample	26	CK20_05d	JR_BSTFA_06_EI	165_CK20-05d	Derivatized Sample
Sample	27	CK20_06d	JR_BSTFA_06_EI	166_CK20-06d	Derivatized Sample
Sample	28	CK20_07d	JR_BSTFA_06_EI	167_CK20-07d	Derivatized Sample
Blank	1	DCM blank	TM01_EI	168_Blank	

Table 10 Continued					
Sample	29	CK20_10d	JR_BSTFA_06_EI	169_CK20-10d	Derivatized Sample
Sample	30	CK20_11d	JR_BSTFA_06_EI	170_CK20-11d	Derivatized Sample
Sample	31	CK20_12d	JR_BSTFA_06_EI	171_CK20-12d	Derivatized Sample
Blank	1	DCM blank	TM01_EI	172_Blank	
Sample	32	CK20_13d	JR_BSTFA_06_EI	173_CK20-13d	Derivatized Sample
Sample	33	CK20_14d	JR_BSTFA_06_EI	174_CK20-14d	Derivatized Sample
Sample	34	CK20_15d	JR_BSTFA_06_EI	175_CK20-15d	Derivatized Sample
Blank	1	DCM blank	TM01_EI	176_Blank	
Sample	15	CK19_13d	JR_BSTFA_06_EI	177_CK19-13d	Derivatized Check
Blank	1	DCM blank	TM01_EI	178_Blank	
Sample	35	CK20_18d	JR_BSTFA_06_EI	179_CK20-18d	Derivatized Sample
Sample	36	CK20_19d	JR_BSTFA_06_EI	180_CK20-19d	Derivatized Sample
Sample	37	CK20_20d	JR_BSTFA_06_EI	181_CK20-20d	Derivatized Sample
Blank	1	DCM blank	TM01_EI	182_Blank	
Sample	38	CK20_21d	JR_BSTFA_06_EI	183_CK20-21d	Derivatized Sample
Sample	39	CK20_22d	JR_BSTFA_06_EI	184_CK20-22d	Derivatized Sample
Sample	40	CK20_23d	JR_BSTFA_06_EI	185_CK20-23d	Derivatized Sample
Blank	1	DCM blank	TM01_EI	186_Blank	
Sample	41	CK20_26d	JR_BSTFA_06_EI	187_CK20-26d	Derivatized Sample
Sample	42	CK20_27d	JR_BSTFA_06_EI	188_CK20-27d	Derivatized Sample
Sample	43	CK20_28d	JR_BSTFA_06_EI	189_CK20-28d	Derivatized Sample
Blank	1	DCM blank	TM01_EI	190_Blank	
Sample	44	CK20_29d	JR_BSTFA_06_EI	191_CK20-29d	Derivatized Sample
Sample	45	CK20_30d	JR_BSTFA_06_EI	192_CK20-30d	Derivatized Sample

Table 10 Continued					
Sample	46	CK20_31d	JR_BSTFA_06_EI	193_CK20-31d	Derivatized Sample
Blank	1	DCM blank	TM01_EI	194_Blank	
Sample	15	CK19_13d	JR_BSTFA_06_EI	195_CK19-13d	Derivatized Check
Blank	1	DCM blank	TM01_EI	196_Blank	
Sample	47	CK20_34d	JR_BSTFA_06_EI	167_CK20-34d	Derivatized Sample
Sample	48	CK20_35d	JR_BSTFA_06_EI	198_CK20-35d	Derivatized Sample
Sample	49	CK20_36d	JR_BSTFA_06_EI	199_CK20-36d	Derivatized Sample
Blank	1	DCM blank	TM01_EI	200_Blank	
Sample	50	CK20_37d	JR_BSTFA_06_EI	201_CK20-37d	Derivatized Sample
Sample	51	CK20_38d	JR_BSTFA_06_EI	202_CK20-38d	Derivatized Sample
Sample	52	CK20_39d	JR_BSTFA_06_EI	203_CK20-39d	Derivatized Sample
Blank	1	DCM blank	TM01_EI	204_Blank	
Sample	53	CK20_42d	JR_BSTFA_06_EI	205_CK20-42d	Derivatized Sample
Sample	54	CK20_43d	JR_BSTFA_06_EI	206_CK20-43d	Derivatized Sample
Sample	55	CK20_44d	JR_BSTFA_06_EI	207_CK20-44d	Derivatized Sample
Blank	1	DCM blank	TM01_EI	208_Blank	
Sample	56	CK20_45d	JR_BSTFA_06_EI	209_CK20-45d	Derivatized Sample
Sample	57	CK20_46d	JR_BSTFA_06_EI	210_CK20-46d	Derivatized Sample
Sample	58	CK20_47d	JR_BSTFA_06_EI	211_CK20-47d	Derivatized Sample
Blank	98	DCM blank	TM01_EI	212_Blank	
Sample	11	CK19_09d	JR_BSTFA_06_EI	213_CK19-09d	Derivatized Calibration
Sample	12	CK19_10d	JR_BSTFA_06_EI	214_CK19-10d	Derivatized Calibration
Sample	13	CK19_11d	JR_BSTFA_06_EI	215_CK19-11d	Derivatized Calibration
Sample	14	CK19_12d	JR_BSTFA_06_EI	216_CK19-12d	Derivatized Calibration

Table 10 Continued					
Blank	98	DCM blank	TM01_EI	217_Blank	
Sample	15	CK19_13d	JR_BSTFA_06_EI	218_CK19-13d	Derivatized Calibration
Sample	16	CK19_14d	JR_BSTFA_06_EI	219_CK19-14d	Derivatized Calibration
Sample	17	CK19_15d	JR_BSTFA_06_EI	220_CK19-15d	Derivatized Calibration
Sample	18	CK19_16d	JR_BSTFA_06_EI	221_CK19-16d	Derivatized Calibration
Blank	98	DCM blank	TM01_EI	222_Blank	
Sample	59	CK20_50d	JR_BSTFA_06_EI	223_CK20-50d	Derivatized Sample
Sample	60	CK20_51d	JR_BSTFA_06_EI	224_CK20-51d	Derivatized Sample
Sample	61	CK20_52d	JR_BSTFA_06_EI	225_CK20-52d	Derivatized Sample
Blank	98	DCM blank	TM01_EI	226_Blank	
Sample	62	CK20_53d	JR_BSTFA_06_EI	227_CK20-53d	Derivatized Sample
Sample	63	CK20_54d	JR_BSTFA_06_EI	228_CK20-54d	Derivatized Sample
Sample	64	CK20_55d	JR_BSTFA_06_EI	229_CK20-55d	Derivatized Sample
Blank	98	DCM blank	TM01_EI	230_Blank	
Sample	65	CK20_58d	JR_BSTFA_06_EI	231_CK20-58d	Derivatized Sample
Sample	66	CK20_59d	JR_BSTFA_06_EI	232_CK20-59d	Derivatized Sample
Sample	67	CK20_60d	JR_BSTFA_06_EI	233_CK20-60d	Derivatized Sample
Blank	98	DCM blank	TM01_EI	234_Blank	
Sample	68	CK20_61d	JR_BSTFA_06_EI	235_CK20-61d	Derivatized Sample
Sample	69	CK20_62d	JR_BSTFA_06_EI	236_CK20-62d	Derivatized Sample
Sample	70	CK20_63d	JR_BSTFA_06_EI	237_CK20-63d	Derivatized Sample
Blank	98	DCM blank	TM01_EI	238_Blank	
Sample	15	CK19_13d	JR_BSTFA_06_EI	239_CK19-13d	Underivatized Check
Blank	98	DCM blank	TM01_EI	240_Blank	

Table 10 Continued					
Sample	71	CK20_66d	JR_BSTFA_06_EI	241_CK20-66d	Derivatized Sample
Sample	72	CK20_67d	JR_BSTFA_06_EI	242_CK20-67d	Derivatized Sample
Sample	73	CK20_68d	JR_BSTFA_06_EI	243_CK20-68d	Derivatized Sample
Blank	98	DCM blank	TM01_EI	244_Blank	
Sample	74	CK20_69d	JR_BSTFA_06_EI	245_CK20-69d	Derivatized Sample
Sample	75	CK20_70d	JR_BSTFA_06_EI	246_CK20-70d	Derivatized Sample
Sample	76	CK20_71d	JR_BSTFA_06_EI	247_CK20-71d	Derivatized Sample
Blank	98	DCM blank	TM01_EI	248_Blank	
Sample	77	CK20_74d	JR_BSTFA_06_EI	249_CK20-74d	Derivatized Sample
Sample	78	CK20_75d	JR_BSTFA_06_EI	250_CK20-75d	Derivatized Sample
Sample	79	CK20_76d	JR_BSTFA_06_EI	251_CK20-76d	Derivatized Sample
Blank	98	DCM blank	TM01_EI	252_Blank	
Sample	80	CK20_77d	JR_BSTFA_06_EI	253_CK20-77d	Derivatized Sample
Sample	81	CK20_78d	JR_BSTFA_06_EI	254_CK20-78d	Derivatized Sample
Sample	82	CK20_79d	JR_BSTFA_06_EI	255_CK20-79d	Derivatized Sample
Blank	98	DCM blank	TM01_EI	256_Blank	
Sample	15	CK19_13d	JR_BSTFA_06_EI	257_CK19-13d	Derivatized Check
Blank	98	DCM blank	TM01_EI	258_Blank	
Sample	83	CK20_82d	JR_BSTFA_06_EI	259_CK20-82d	Derivatized Sample
Sample	84	CK20_83d	JR_BSTFA_06_EI	260_CK20-83d	Derivatized Sample
Sample	85	CK20_84d	JR_BSTFA_06_EI	261_CK20-84d	Derivatized Sample
Blank	98	DCM blank	TM01_EI	262_Blank	
Sample	86	CK20_85d	JR_BSTFA_06_EI	263_CK20-85d	Derivatized Sample
Sample	87	CK20_86d	JR_BSTFA_06_EI	264_CK20-86d	Derivatized Sample

Table 10 Continued					
Sample	88	CK20_87d	JR_BSTFA_06_EI	265_CK20-87d	Derivatized Sample
Blank	98	DCM blank	TM01_EI	266_Blank	
Sample	89	CK20_90d	JR_BSTFA_06_EI	267_CK20-90d	Derivatized Sample
Sample	90	CK20_91d	JR_BSTFA_06_EI	268_CK20-91d	Derivatized Sample
Sample	91	CK20_92d	JR_BSTFA_06_EI	269_CK20-92d	Derivatized Sample
Blank	98	DCM blank	TM01_EI	270_Blank	
Sample	92	CK20_93d	JR_BSTFA_06_EI	271_CK20-93d	Derivatized Sample
Sample	93	CK20_94d	JR_BSTFA_06_EI	272_CK20-94d	Derivatized Sample
Sample	94	CK20_95d	JR_BSTFA_06_EI	273_CK20-95d	Derivatized Sample
Blank	98	DCM blank	TM01_EI	274_Blank	
Sample	11	CK19_09d	JR_BSTFA_06_EI	275_CK19-09d	Derivatized Calibration
Sample	12	CK19_10d	JR_BSTFA_06_EI	276_CK19-10d	Derivatized Calibration
Sample	13	CK19_11d	JR_BSTFA_06_EI	277_CK19-11d	Derivatized Calibration
Sample	14	CK19_12d	JR_BSTFA_06_EI	278_CK19-12d	Derivatized Calibration
Blank	98	DCM blank	TM01_EI	279_Blank	
Sample	15	CK19_13d	JR_BSTFA_06_EI	280_CK19-13d	Derivatized Calibration
Sample	16	CK19_14d	JR_BSTFA_06_EI	281_CK19-14d	Derivatized Calibration
Sample	17	CK19_15d	JR_BSTFA_06_EI	282_CK19-15d	Derivatized Calibration
Sample	18	CK19_16d	JR_BSTFA_06_EI	283_CK19-16d	Derivatized Calibration
Blank	98	DCM blank	TM01_EI	284_Blank	
Sample	2	Testmix_low	TM01_EI	285_MC59-2D	Test Mix
Sample	2	Testmix_low	TM01_EI	286_MC59-2D	Test Mix
Sample	2	Testmix_low	TM01_EI	287_MC59-2D	Test Mix
Blank	98	DCM blank	TM01_EI	288_Blank	
Sample	19	CK19_96d	JR_BSTFA_06_EI	289_CK19-96d	Derivatized Calibration

Table 10 Continued					
Sample	20	CK19_97d	JR_BSTFA_06_EI	290_CK19-97d	Derivatized Calibration
Sample	21	CK19_98d	JR_BSTFA_06_EI	291_CK19-98d	Derivatized Calibration
Sample	22	CK19_99d	JR_BSTFA_06_EI	292_CK19-99d	Derivatized Calibration
Blank	1	DCM blank	TM01_EI	293_Blank	
Sample	11	CK19_09d	JR_BSTFA_06_EI	294_CK19-09d	Derivatized Calibration
Sample	12	CK19_10d	JR_BSTFA_06_EI	295_CK19-10d	Derivatized Calibration
Sample	13	CK19_11d	JR_BSTFA_06_EI	296_CK19-11d	Derivatized Calibration
Sample	14	CK19_12d	JR_BSTFA_06_EI	297_CK19-12d	Derivatized Calibration
Blank	1	DCM blank	TM01_EI	298_Blank	
Sample	15	CK19_13d	JR_BSTFA_06_EI	299_CK19-13d	Derivatized Calibration
Sample	16	CK19_14d	JR_BSTFA_06_EI	300_CK19-14d	Derivatized Calibration
Sample	17	CK19_15d	JR_BSTFA_06_EI	301_CK19-15d	Derivatized Calibration
Sample	18	CK19_16d	JR_BSTFA_06_EI	302_CK19-16d	Derivatized Calibration
Blank	1	DCM blank	TM01_EI	303_Blank	
Sample	3	CK23_01d	JR_BSTFA_06_EI	304_CK23_01d	Derivatized Calibration
Sample	4	CK23_02d	JR_BSTFA_06_EI	305_CK23_02d	Derivatized Calibration
Sample	5	CK23_03d	JR_BSTFA_06_EI	306_CK23_03d	Derivatized Calibration
Sample	6	CK23_04d	JR_BSTFA_06_EI	307_CK23_04d	Derivatized Calibration
Blank	1	DCM blank	TM01_EI	308_Blank	
Sample	7	CK23_05d	JR_BSTFA_06_EI	309_CK23_05d	Derivatized Calibration
Sample	8	CK23_06d	JR_BSTFA_06_EI	310_CK23_06d	Derivatized Calibration
Sample	9	CK23_07d	JR_BSTFA_06_EI	311_CK23_07d	Derivatized Calibration
Sample	10	CK23_08d	JR_BSTFA_06_EI	312_CK23_08d	Derivatized Calibration

Table 10 Continued					
Blank	1	DCM blank	TM01_EI	312a_Blank	
Sample	11	CK23_098d	JR_BSTFA_06_EI	313_CK23_098d	Derivatized Sample
Sample	12	CK23_099d	JR_BSTFA_06_EI	314_CK23_099d	Derivatized Sample
Sample	13	CK23_100d	JR_BSTFA_06_EI	315_CK23_100d	Derivatized Sample
Blank	1	DCM blank	TM01_EI	316_Blank	
Sample	14	CK23_101d	JR_BSTFA_06_EI	317_CK23_101d	Derivatized Sample
Sample	15	CK23_102d	JR_BSTFA_06_EI	318_CK23_102d	Derivatized Sample
Sample	16	CK23_103d	JR_BSTFA_06_EI	319_CK23_103d	Derivatized Sample
Blank	1	DCM blank	TM01_EI	320_Blank	
Sample	17	CK23_106d	JR_BSTFA_06_EI	321_CK23_106d	Derivatized Sample
Sample	18	CK23_107d	JR_BSTFA_06_EI	322_CK23_107d	Derivatized Sample
Sample	19	CK23_108d	JR_BSTFA_06_EI	323_CK23_108d	Derivatized Sample
Blank	1	DCM blank	TM01_EI	324_Blank	
Sample	20	CK23_109d	JR_BSTFA_06_EI	325_CK23_109d	Derivatized Sample
Sample	21	CK23_110d	JR_BSTFA_06_EI	326_CK23_110d	Derivatized Sample
Sample	22	CK23_111d	JR_BSTFA_06_EI	327_CK23_111d	Derivatized Sample
Blank	1	DCM blank	TM01_EI	328_Blank	
Sample	87	CK19_13d	JR_BSTFA_06_EI	329_CK19-13d	Derivatized Check
Blank	1	DCM blank	TM01_EI	330_Blank	
Sample	23	CK23_114d	JR_BSTFA_06_EI	331_CK23_114d	Derivatized Sample
Sample	24	CK23_115d	JR_BSTFA_06_EI	332_CK23_115d	Derivatized Sample
Sample	25	CK23_116d	JR_BSTFA_06_EI	333_CK23_116d	Derivatized Sample
Blank	1	DCM blank	TM01_EI	334_Blank	
Sample	26	CK23_117d	JR_BSTFA_06_EI	335_CK23_117d	Derivatized Sample

Table 10 Continued					
Sample	27	CK23_118d	JR_BSTFA_06_EI	336_CK23_118d	Derivatized Sample
Sample	28	CK23_119d	JR_BSTFA_06_EI	337_CK23_119d	Derivatized Sample
Blank	1	DCM blank	TM01_EI	338_Blank	
Sample	29	CK23_122d	JR_BSTFA_06_EI	339_CK23_122d	Derivatized Sample
Sample	30	CK23_123d	JR_BSTFA_06_EI	340_CK23_123d	Derivatized Sample
Sample	31	CK23_124d	JR_BSTFA_06_EI	341_CK23_124d	Derivatized Sample
Blank	1	DCM blank	TM01_EI	342_Blank	
Sample	32	CK23_125d	JR_BSTFA_06_EI	343_CK23_125d	Derivatized Sample
Sample	33	CK23_126d	JR_BSTFA_06_EI	344_CK23_126d	Derivatized Sample
Sample	34	CK23_127d	JR_BSTFA_06_EI	345_CK23_127d	Derivatized Sample
Blank	1	DCM blank	TM01_EI	346_Blank	
Sample	87	CK19_13d	JR_BSTFA_06_EI	347_CK19-13d	Derivatized Check
Blank	1	DCM blank	TM01_EI	348_Blank	
Sample	35	CK23_130d	JR_BSTFA_06_EI	349_CK23_130d	Derivatized Sample
Sample	36	CK23_131d	JR_BSTFA_06_EI	350_CK23_131d	Derivatized Sample
Sample	37	CK23_132d	JR_BSTFA_06_EI	351_CK23_132d	Derivatized Sample
Blank	1	DCM blank	TM01_EI	352_Blank	
Sample	38	CK23_133d	JR_BSTFA_06_EI	353_CK23_133d	Derivatized Sample
Sample	39	CK23_134d	JR_BSTFA_06_EI	354_CK23_134d	Derivatized Sample
Sample	40	CK23_135d	JR_BSTFA_06_EI	355_CK23_135d	Derivatized Sample
Blank	1	DCM blank	TM01_EI	356_Blank	
Sample	41	CK23_138d	JR_BSTFA_06_EI	357_CK23_138d	Derivatized Sample
Sample	42	CK23_139d	JR_BSTFA_06_EI	358_CK23_139d	Derivatized Sample
Sample	43	CK23_140d	JR_BSTFA_06_EI	359_CK23_140d	Derivatized Sample

Table 10 Continued					
Blank	1	DCM blank	TM01_EI	360_Blank	
Sample	44	CK23_141d	JR_BSTFA_06_EI	361_CK23_141d	Derivatized Sample
Sample	45	CK23_142d	JR_BSTFA_06_EI	362_CK23_142d	Derivatized Sample
Sample	46	CK23_143d	JR_BSTFA_06_EI	363_CK23_143d	Derivatized Sample
Blank	1	DCM blank	TM01_EI	364_Blank	
Sample	83	CK19_09d	JR_BSTFA_06_EI	365_CK19-09d	Derivatized Calibration
Sample	84	CK19_10d	JR_BSTFA_06_EI	366_CK19-10d	Derivatized Calibration
Sample	85	CK19_11d	JR_BSTFA_06_EI	367_CK19-11d	Derivatized Calibration
Sample	86	CK19_12d	JR_BSTFA_06_EI	368_CK19-12d	Derivatized Calibration
Blank	1	DCM blank	TM01_EI	369_Blank	
Sample	87	CK19_13d	JR_BSTFA_06_EI	370_CK19-13d	Derivatized Calibration
Sample	88	CK19_14d	JR_BSTFA_06_EI	371_CK19-14d	Derivatized Calibration
Sample	89	CK19_15d	JR_BSTFA_06_EI	372_CK19-15d	Derivatized Calibration
Sample	90	CK19_16d	JR_BSTFA_06_EI	373_CK19-16d	Derivatized Calibration
Blank	1	DCM blank	TM01_EI	374_Blank	
Sample	47	CK23_146d	JR_BSTFA_06_EI	375_CK23_146d	Derivatized Sample
Sample	48	CK23_147d	JR_BSTFA_06_EI	376_CK23_147d	Derivatized Sample
Sample	49	CK23_148d	JR_BSTFA_06_EI	377_CK23_148d	Derivatized Sample
Blank	1	DCM blank	TM01_EI	378_Blank	
Sample	50	CK23_149d	JR_BSTFA_06_EI	379_CK23_149d	Derivatized Sample
Sample	51	CK23_150d	JR_BSTFA_06_EI	380_CK23_150d	Derivatized Sample
Sample	52	CK23_151d	JR_BSTFA_06_EI	381_CK23_151d	Derivatized Sample
Blank	1	DCM blank	TM01_EI	382_Blank	
Sample	53	CK23_154d	JR_BSTFA_06_EI	383_CK23_154d	Derivatized Sample

Table 10 Continued					
Sample	54	CK23_155d	JR_BSTFA_06_EI	384_CK23_155d	Derivatized Sample
Sample	55	CK23_156d	JR_BSTFA_06_EI	385_CK23_156d	Derivatized Sample
Blank	1	DCM blank	TM01_EI	386_Blank	
Sample	56	CK23_157d	JR_BSTFA_06_EI	387_CK23_157d	Derivatized Sample
Sample	57	CK23_158d	JR_BSTFA_06_EI	388_CK23_158d	Derivatized Sample
Sample	58	CK23_159d	JR_BSTFA_06_EI	389_CK23_159d	Derivatized Sample
Blank	1	DCM blank	TM01_EI	390_Blank	
Sample	87	CK23_05d	JR_BSTFA_06_EI	391_CK23_05d	Derivatized Check
Blank	1	DCM blank	TM01_EI	392_Blank	
Sample	59	CK23_162d	JR_BSTFA_06_EI	393_CK23_162d	Derivatized Sample
Sample	60	CK23_163d	JR_BSTFA_06_EI	394_CK23_163d	Derivatized Sample
Sample	61	CK23_164d	JR_BSTFA_06_EI	395_CK23_164d	Derivatized Sample
Blank	1	DCM blank	TM01_EI	396_Blank	
Sample	62	CK23_165d	JR_BSTFA_06_EI	397_CK23_165d	Derivatized Sample
Sample	63	CK23_166d	JR_BSTFA_06_EI	398_CK23_166d	Derivatized Sample
Sample	64	CK23_167d	JR_BSTFA_06_EI	399_CK23_167d	Derivatized Sample
Blank	1	DCM blank	TM01_EI	400_Blank	
Sample	65	CK23_170d	JR_BSTFA_06_EI	401_CK23_170d	Derivatized Sample
Sample	66	CK23_171d	JR_BSTFA_06_EI	402_CK23_171d	Derivatized Sample
Sample	67	CK23_172d	JR_BSTFA_06_EI	403_CK23_172d	Derivatized Sample
Blank	1	DCM blank	TM01_EI	404_Blank	
Sample	68	CK23_173d	JR_BSTFA_06_EI	405_CK23_173d	Derivatized Sample
Sample	69	CK23_174d	JR_BSTFA_06_EI	406_CK23_174d	Derivatized Sample
Sample	70	CK23_175d	JR_BSTFA_06_EI	407_CK23_175d	Derivatized Sample

Table 10 Continued					
Blank	1	DCM blank	TM01_EI	408_Blank	
Sample	87	CK19_13d	JR_BSTFA_06_EI	409_CK19-13d	Derivatized Check
Blank	1	DCM blank	TM01_EI	410_Blank	
Sample	71	CK23_178d	JR_BSTFA_06_EI	411_CK23_178d	Derivatized Sample
Sample	72	CK23_179d	JR_BSTFA_06_EI	412_CK23_179d	Derivatized Sample
Sample	73	CK23_180d	JR_BSTFA_06_EI	413_CK23_180d	Derivatized Sample
Blank	1	DCM blank	TM01_EI	414_Blank	
Sample	74	CK23_181d	JR_BSTFA_06_EI	415_CK23_181d	Derivatized Sample
Sample	75	CK23_182d	JR_BSTFA_06_EI	416_CK23_182d	Derivatized Sample
Sample	76	CK23_183d	JR_BSTFA_06_EI	417_CK23_183d	Derivatized Sample
Blank	1	DCM blank	TM01_EI	418_Blank	
Sample	77	CK23_186d	JR_BSTFA_06_EI	419_CK23_186d	Derivatized Sample
Sample	78	CK23_187d	JR_BSTFA_06_EI	420_CK23_187d	Derivatized Sample
Sample	79	CK23_188d	JR_BSTFA_06_EI	421_CK23_188d	Derivatized Sample
Blank	1	DCM blank	TM01_EI	422_Blank	
Sample	80	CK23_189d	JR_BSTFA_06_EI	423_CK23_189d	Derivatized Sample
Sample	81	CK23_190d	JR_BSTFA_06_EI	424_CK23_190d	Derivatized Sample
Sample	82	CK23_191d	JR_BSTFA_06_EI	425_CK23_191d	Derivatized Sample
Blank	1	DCM blank	TM01_EI	426_Blank	
Sample	83	CK19_09d	JR_BSTFA_06_EI	427_CK19-09d	Derivatized Calibration
Sample	84	CK19_10d	JR_BSTFA_06_EI	428_CK19-10d	Derivatized Calibration
Sample	85	CK19_11d	JR_BSTFA_06_EI	429_CK19-11d	Derivatized Calibration
Sample	86	CK19_12d	JR_BSTFA_06_EI	430_CK19-12d	Derivatized Calibration
Blank	1	DCM blank	TM01_EI	431_Blank	

Table 10 Continued					
Sample	87	CK19_13d	JR_BSTFA_06_EI	432_CK19-13d	Derivatized Calibration
Sample	88	CK19_14d	JR_BSTFA_06_EI	433_CK19-14d	Derivatized Calibration
Sample	89	CK19_15d	JR_BSTFA_06_EI	434_CK19-15d	Derivatized Calibration
Sample	90	CK19_16d	JR_BSTFA_06_EI	435_CK19-16d	Derivatized Calibration
Blank	1	DCM blank	TM01_EI	436_Blank	
Sample	2	Testmix_low	TM01_EI	437_MC59-2D	Test Mix
Sample	2	Testmix_low	TM01_EI	438_MC59-2D	Test Mix
Sample	2	Testmix_low	TM01_EI	439_MC59-2D	Test Mix
Blank	1	DCM blank	TM01_EI	440_Blank	

APPENDIX D
GC-MS DATA PROCESSING

The areas of analyte peaks were calculated using Agilent ChemStation software based on target ions unique for each analyte. Table 11 shows each analyte with its respective retention times and target ions. Figure 22 shows the chromatogram form a derivatized sample, the large peak at the beginning is end of the DCM solvent peak, the large peak at four minutes is from the derivatizing agent and the large peak near 8 minutes is pyridine. Each analyte peak area was divided by the internal standard peak area to remove any error from varying injection volume amounts. The calibration standards responses were paired with its known concentration to construct a calibration curve. Figure 24 shows an example of the constructed calibration curve. The least squared curve is shown for the fructose analyte to show the equation used to calculate the concentrations in reactor samples. During data processing this equation was calculated with the LINEST function in MS Excel so the cell could be linked for further calculations.

Table 11: Analyte target ions and retention time

Analyte	Retention Time	Target Ion 1	Target Ion 2	Target Ion 3	Target Ion 4	Target Ion 5
Methyl Lactate	4.0 Minutes	45 (100%)	61 (10%)	89 (10%)	-	-
Methyl Vinyl Glycolate	6.7 Minutes	57 (100%)	84 (30%)	29 (20%)	-	-
Methyl Levulinate	10.5 Minutes	43 (100%)	55 (20%)	99 (20%)	115 (20%)	-
Derivatized Lactic Acid	11.9 Minutes	73 (100%)	147 (100%)	117 (80%)	191 (25%)	45 (25%)
Derivatized Levulinic Acid	13.2 Minutes	75 (100%)	43 (35%)	145 (35%)	145 (35%)	-
Derivatized Fructose	21.8 Minutes	73 (100%)	217 (90%)	147 (25%)	437 (25%)	-
Derivatized Mannose	22.7 Minutes	204 (100%)	73 (60%)	147 (20%)	-	-
Derivatized Glucose	23.5 Minutes	204 (100%)	73 (60%)	147 (20%)	-	-
o-Terphenyl	22.8 Minutes	230 (100%)	215 (30%)	101 (10%)	114 (10%)	202 (10%)

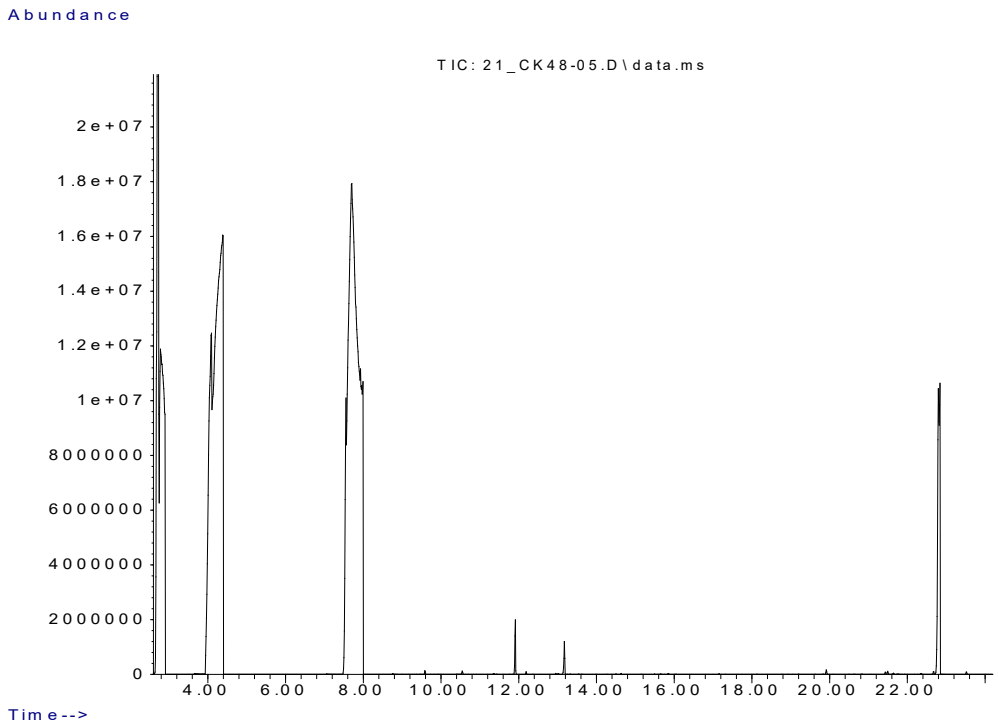

Figure 22: Chromatogram example from derivatized samples

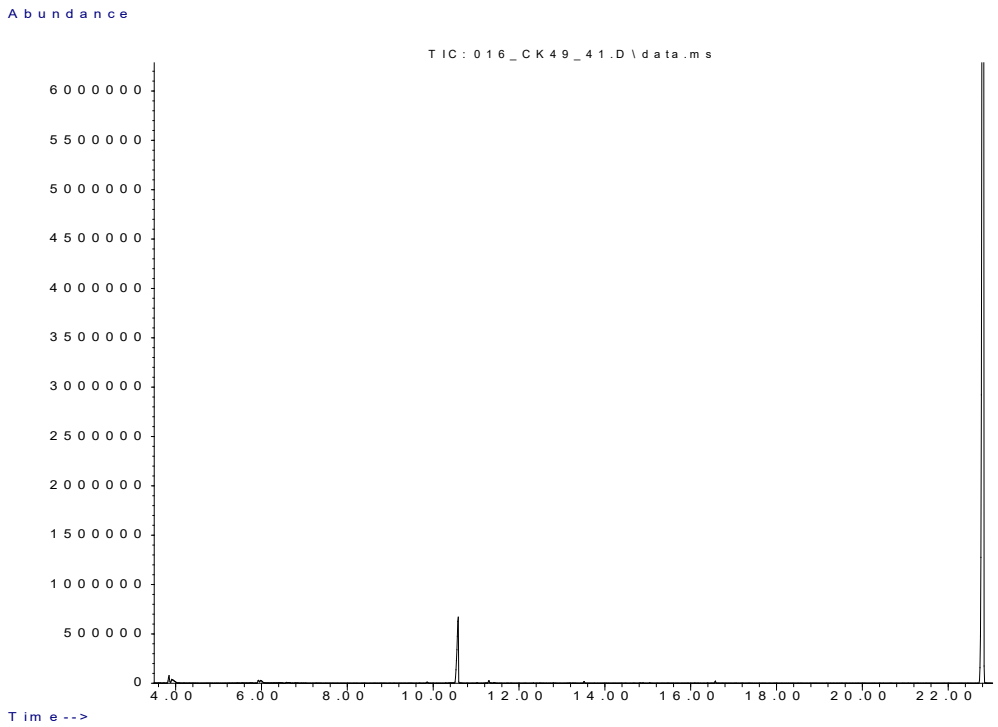

Figure 23: Chromatogram example from underivatized samples

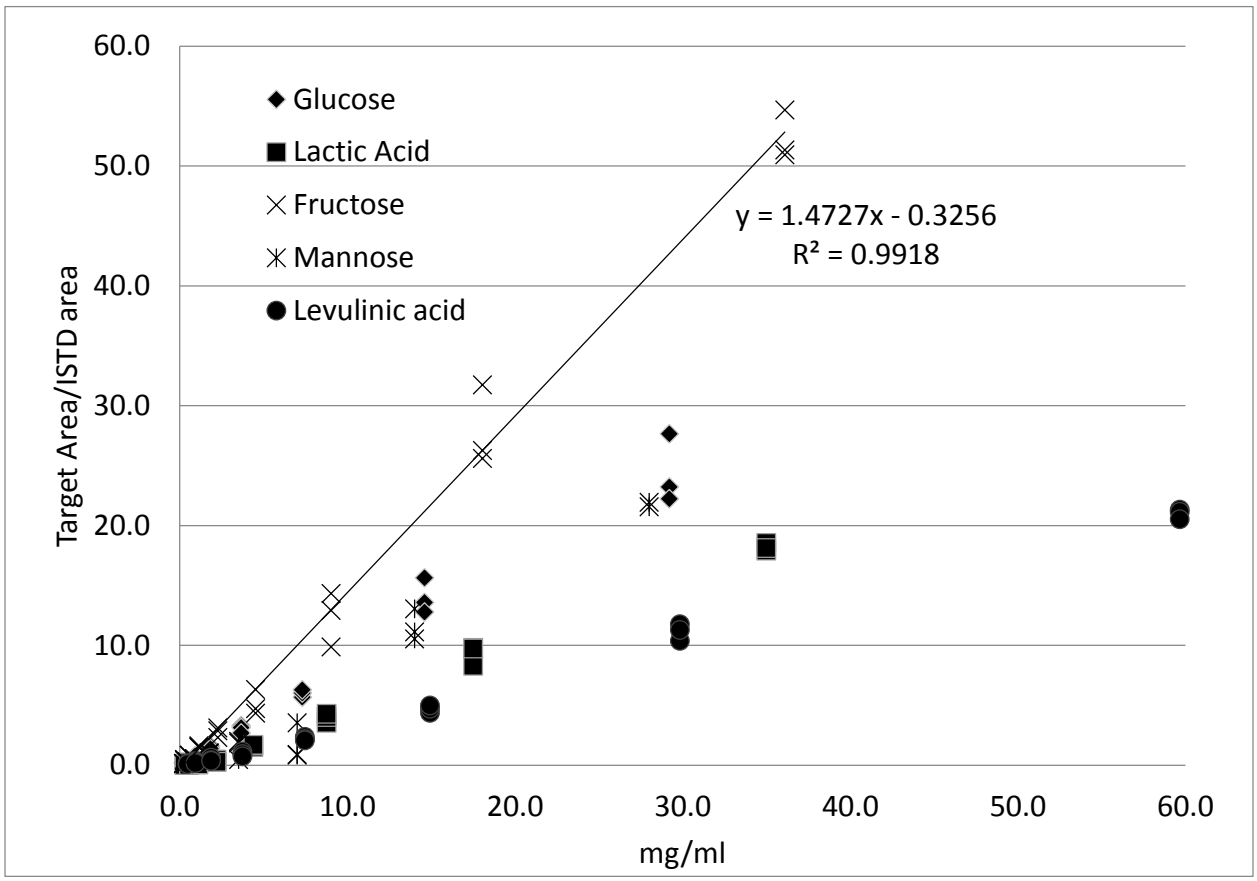

Figure 24: Calibration curve example showing relationship with known concentrations of analytes with GC-MS response

The Y=mX + b equation created from the calibration samples can be transformed into Equation 1.

$$X=(Y-b)/m \qquad \text{Equation 1}$$

Where:

X = Sample concentration (mg/ml)

Y = Analyte area/internal standard area response

b = Intercept from calibration experiments

m = Slope from calibration experiments

Since both 20 µl of reactor sample and 20 µl of calibration solution were used in the highest calibration sample, a direct one-to-one comparison can be used to determine unknown concentrations. Once the concentration of the analyte is known it is divided by the known concentration of glucose in the starting reactor solution. This provides the weight percent of recovered products.

APPENDIX E
ALL DATA

Table 12: GC-MS triplicate results from 20140325

Notes	Lactic Acid	Levulinic acid	Fructose	Mannose	Glucose
	Target/ISTD	Target/ISTD	Target/ISTD	Target/ISTD	Target/ISTD
Acid Calibration 1	0.000991	0.000535	0.000182	0.000286	0.000305
Acid Calibration 2	0.001305	0.000756	0.000465	0.00044	0.000482
Acid Calibration 3	0.00289	0.002141	0.001106	0.00103	0.001177
Acid Calibration 4	0.006409	0.003791	0.002402	0.001826	0.002597
Acid Calibration 5	0.019611	0.01168	0.007108	0.001102	0.006583
Acid Calibration 6	0.045028	0.021992	0.012852	0.003101	0.013157
MeOH SnCl4 5g glucose	0.001091	0.000893	0.003873	0.001365	0.000134
MeOH SnCl4 5g glucose	0.001747	0.001321	0.007118	0.002167	0.000236
MeOH SnCl4 5g glucose	0.001581	0.001297	0.006154	0.002021	0.000152
H2O SnCl4 5g glucose	0.072635	0.058761	0.012975	0.003681	0.012006
H2O SnCl4 5g glucose	0.081991	0.060984	0.00535	0.003054	0.004521
H2O SnCl4 5g glucose	0.07625	0.055052	0.003414	0.004907	0.003258
H2O SnCl2 5g glucose	0.009466	0.087913	0.00069	0.0008	0.000739
H2O SnCl2 5g glucose	0.009375	0.08522	0.001088	0.000617	0.001061
H2O SnCl2 5g glucose	0.01058	0.076696	0	0.001061	0.000667

Table 12 Continued					
H2O SnCl4 2g glucose	0.08019	0.000104	0.000489	0.000927	0
H2O SnCl4 2g glucose	0.086577	0.000154	0.000339	0.001162	0
H2O SnCl4 2g glucose	0.081934	0.000125	0.00018	0.001127	0
Acid Calibration 1	0.000313	0.000304	0.000298	0	0.000214
Acid Calibration 2	0.000461	0.000479	0.000659	0.000418	0.000487
Acid Calibration 3	0.000803	0.001312	0.001103	0.000691	0.00111
Acid Calibration 4	0.006995	0.003938	0.002841	0.000918	0.002749
Acid Calibration 5	0.016216	0.009723	0.006389	0.000996	0.006104
Acid Calibration 6	0.049005	0.023686	0.015672	0.003843	0.014597

Table 13: GC-MS results from 20140324

Notes	Methyl Lactate	Methyl Vinylglycolate	Furfural	Methyl Levulinate	5-HMF
	Target/ISTD	Target/ISTD	Target/ISTD	Target/ISTD	Target/ISTD
NonAcid Calibration 1	0.000592	0.000328	0.000549	0.000455	0
NonAcid Calibration 2	0	0.000607	0.001351	0.001199	0
NonAcid Calibration 3	0	0	0.001522	0.002236	0
NonAcid Calibration 4	0.001154	0.000795	0.003759	0.004383	0
NonAcid Calibration 5	0.001866	0.004929	0.008754	0.00933	0
NonAcid Calibration 6	0.010972	0.004584	0.00831	0.017186	0.001611
NonAcid Calibration 7	0.030567	0.012688	0.052457	0.058777	0.005983
NonAcid Calibration 8	0.036011	0.015344	0.059992	0.071805	0.007732
47-01 undiv	0.020103	0.00104	0.000468	0.101324	0
47-02 undiv	0.018444	0.001467	0	0.094026	0
47-03 undiv	0.018385	0.001406	0	0.09534	0
NonAcid Calibration 1	0	0	0.000607	0.000412	0
NonAcid Calibration 2	0	0.001332	0.002312	0.002484	0
NonAcid Calibration 3	0	0.000582	0.00127	0.001864	0
NonAcid Calibration 4	0.000591	0.001291	0.003447	0.00435	0
NonAcid Calibration 5	0.006605	0.003043	0.0056	0.009331	0.000404
NonAcid Calibration 6	0.010787	0.004006	0.007954	0.016324	0.001746
NonAcid Calibration 7	0.018934	0.008212	0.013969	0.031288	0.003671
NonAcid Calibration 8	0.034295	0.013977	0.05801	0.06779	0.008351

Table 14: GC-MS results from 20140213

Notes	Formic Acid	Lactic Acid	Levulinic acid	Fructose	Mannose	Glucose
	Target/ ISTD	Target/ ISTD	Target/ ISTD	Target/ ISTD	Target/ ISTD	Target/ ISTD
Acid Calibration 1	0	0.012478	0.009222	0.004978	0.002481	0.004988
Acid Calibration 2	0	0.021046	0.017108	0.010232	0.005581	0.010827
Acid Calibration 3	0	0.040215	0.035991	0.023128	0.012206	0.022925
Acid Calibration 4	0	0.10183	0.075728	0.058621	0.030401	0.062139
Acid Calibration 5	0	0.213013	0.159867	0.11815	0.059791	0.122108
Acid Calibration 6	0	0.487855	0.356841	0.254223	0.134204	0.279449
Acid Calibration 7	0	0.955609	0.708677	0.537354	0.264059	0.580581
Acid Calibration 8	0.232373	2.060935	1.537002	1.166882	0.589341	1.191026
Ba(OH)2	0.265351	0.032991	0	0.025334	0.007542	0.008658
HCl 300 SnCl4 300psi	0	1.031071	0.005206	0.037032	0.013291	0
HCl 300 SnCl4 0psi 2day	0	0.429769	0.026459	0.046894	0.016559	0
HCl 300 SnCl4 0psi 4day	0	0.460401	0.063365	0.039026	0.023269	0
HCl 300 SnCl4 1000psi H2	0	0.486609	0.042425	0.026845	0.016109	0.003298
DCM Wash of 03&04	0	0	0.004225	0.001404	0	0
Top aqueous phase of 07	0	0.012478	0.009222	0.004978	0.002481	0.004988
Acid Calibration 1	0	0.004666	0.005174	0.003863	0.002544	0.002794
Acid Calibration 2	0	0.006959	0.010563	0.007189	0.006332	0.009824
Acid Calibration 3	0	0.018655	0.024066	0.01716	0.006115	0.022619
Acid Calibration 4	0	0.094904	0.072616	0.049009	0.025703	0.052025
Acid Calibration 5	0	0.213674	0.163048	0.1168	0.053224	0.125358

Table 14 Continued						
Acid Calibration 6	0	0.484907	0.367243	0.273651	0.132304	0.306185
Acid Calibration 7	0	0.98076	0.722401	0.555163	0.267959	0.596823
Acid Calibration 8	0.313403	2.024146	1.473488	1.208262	0.59091	1.23336

Table 15: GC-MS results from 20140128

Notes	Formic Acid	Lactic Acid	Levulinic acid	Fructose	Mannose	Glucose
	Target/ ISTD	Target/ ISTD	Target/ ISTD	Target/ ISTD	Target/ ISTD	Target/ ISTD
Acid Calibration 1	0	0.012478	0.009222	0.004978	0.002481	0.004988
Acid Calibration 2	0	0.021046	0.017108	0.010232	0.005581	0.010827
Acid Calibration 3	0	0.040215	0.035991	0.023128	0.012206	0.022925
Acid Calibration 4	0	0.10183	0.075728	0.058621	0.030401	0.062139
Acid Calibration 5	0	0.213013	0.159867	0.11815	0.059791	0.122108
Acid Calibration 6	0	0.487855	0.356841	0.254223	0.134204	0.279449
Acid Calibration 7	0	0.955609	0.708677	0.537354	0.264059	0.580581
Acid Calibration 8	0.232373	2.060935	1.537002	1.166882	0.589341	1.191026
Ba(OH)2	0.265351	0.032991	0	0.025334	0.007542	0.008658
HCl 300 SnCl4 300psi	0	1.031071	0.005206	0.037032	0.013291	0
HCl 300 SnCl4 0psi 2day	0	0.429769	0.026459	0.046894	0.016559	0
HCl 300 SnCl4 0psi 4day	0	0.460401	0.063365	0.039026	0.023269	0
HCl 300 SnCl4 1000psi H2	0	0.486609	0.042425	0.026845	0.016109	0.003298
DCM Wash of 03&04	0	0	0.004225	0.001404	0	0
Top aqueous phase of 07	0	0.012478	0.009222	0.004978	0.002481	0.004988
Acid Calibration 1	0	0.004666	0.005174	0.003863	0.002544	0.002794
Acid Calibration 2	0	0.006959	0.010563	0.007189	0.006332	0.009824
Acid Calibration 3	0	0.018655	0.024066	0.01716	0.006115	0.022619
Acid Calibration 4	0	0.094904	0.072616	0.049009	0.025703	0.052025
Acid Calibration 5	0	0.213674	0.163048	0.1168	0.053224	0.125358

Table 10 Continued						
Acid Calibration 6	0	0.484907	0.367243	0.273651	0.132304	0.306185
Acid Calibration 7	0	0.98076	0.722401	0.555163	0.267959	0.596823
Acid Calibration 8	0.313403	2.024146	1.473488	1.208262	0.59091	1.23336

Table 16: GC-MS results from 20140103

Notes	Lactic Acid	Levulinic acid	Unreacted Sugars 1	Unreacted Sugars 2	Glucose
	Target/ISTD	Target/ISTD	Target/ISTD	Target/ISTD	Target/ISTD
Acid Calibration 1	0.0146	0.010134	0.015546	0.014281	0.014541
Acid Calibration 2	0.031931	0.023505	0.030535	0.031323	0.030455
Acid Calibration 3	0.07263	0.049576	0.064944	0.062607	0.063156
Acid Calibration 4	0.142427	0.104608	0.115071	0.125975	0.142376
Acid Calibration 5	0.282561	0.204008	0.252393	0.255577	0.272297
Acid Calibration 6	0.548419	0.381271	0.478429	0.499263	0.538728
Acid Calibration 7	1.123932	0.841129	1.019469	1.047437	1.128403
Acid Calibration 8	1.991749	1.422855	2.00897	3.964635	1.943376
CK41-01	0.097026	0.453242	0.217753	0.013722	0.227754
CK41-04	0.158357	0.452555	0.14772	0.012765	0.137816
CK41-06	0.14192	0.52753	0.188531	0.012922	0.187039
CK41-07	0.133552	0.511985	0.101794	0.01237	0.098559
CK41-10	0.344402	0.298047	0.058267	0.012866	0.048461
CK41-11	0.05063	0.529659	0.083951	0.012336	0.082058
CK41-29	0.004085	0.035879	0	0	0
CK41-41	0.8774	0.308508	0.029303	0.031179	0.022537
CK41-42	0.64697	0.358606	0.01057	0.015509	0.009104
CK41-43	0.593728	0.320634	0.003886	0.014581	0
Acid Calibration 1	0.007663	0.009657	0.016401	0.036845	0.014867
Acid Calibration 2	0.019931	0.021887	0.027212	0.028238	0.032944
Acid Calibration 3	0.073525	0.047712	0.064245	0.05991	0.069903
Acid Calibration 4	0.141698	0.102087	0.130005	0.120811	0.141384
Acid Calibration 6	0.545022	0.389952	0.48461	0.501099	0.554546
Acid Calibration 7	1.143611	0.799187	1.05654	1.092728	1.169289
Calibration 8	1.856318	1.359764	2.009369	4.070064	1.924087

Table 17: GC-MS results from 20131220

Notes	Lactic Acid	Levulinic acid	Unreacted Sugars 1	Unreacted Sugars 2	Glucose
	Target/ISTD	Target/ISTD	Target/ISTD	Target/ISTD	Target/ISTD
Acid Calibration 1	0.013689	0.011166	0.010762	0.012152	0.01093
Acid Calibration 2	0.032264	0.026218	0.025319	0.023897	0.023777
Acid Calibration 3	0.067983	0.047834	0.060244	0.048914	0.057124
Acid Calibration 4	0.129971	0.103084	0.129197	0.103113	0.128236
Acid Calibration 5	0.271929	0.210785	0.258822	0.220733	0.258728
Acid Calibration 6	0.517688	0.414624	0.51993	0.444505	0.538199
Acid Calibration 7	1.017919	0.794573	0.976952	0.837399	1.008295
Acid Calibration 8	1.891923	1.541524	2.049504	1.666692	1.803176
CK40-02	0.122365	0.442852	0.282128	0.019896	0.279994
CK40-03	0.146744	0.447529	0.457974	0.041258	0.523869
CK40-05	0.131305	0.548367	0.131786	0.00778	0.12527
CK40-07	0.148508	0.541588	0.121206	0.0057	0.109586
CK40-08	0.165999	0.478381	0.183714	0.012599	0.189711
CK40-10	0.009043	0.084374	1.232091	0.016772	2.01026
CK40-11	0.00645	0.024991	1.686143	0.041549	2.782208
CK40-30	0.031943	0.434073	0.003504	0.005702	0.003858
CK40-31	0.032998	0.762342	0	0.008951	0
CK40-32	0.436953	0.485392	0.002601	0.008161	0.004358
Acid Calibration 1	0.005586	0.008756	0.010906	0.02665	0.012797
Acid Calibration 2	0.021655	0.022994	0.031169	0.024046	0.027074
Acid Calibration 3	0.064768	0.049648	0.064053	0.056589	0.06361
Acid Calibration 4	0.135101	0.102096	0.125847	0.106058	0.135456
Acid Calibration 5	0.265104	0.209296	0.257318	0.217373	0.258842
Calibration 6	0.527023	0.40542	0.499039	0.439003	0.511528
Calibration 7	1.040352	0.810884	1.048385	0.91312	1.049434
Calibration 8	1.872402	1.535779	2.101289	1.67606	1.806155

Table 18: GC-MS results from 20131210

Notes	Furfural	Lactic Acid	Levulinic acid	Glucose
	Target/ISTD	Target/ISTD	Target/ISTD	Target/ISTD
Acid Calibration 1	0	0.015696	0.011509	0.017926
Acid Calibration 2	0	0.035636	0.023186	0.04124
Acid Calibration 3	0	0.07673	0.049917	0.083674
Acid Calibration 4	0	0.1562	0.096109	0.177954
Acid Calibration 5	0	0.286265	0.179015	0.332275
Acid Calibration 6	0	0.593193	0.360603	0.690587
Acid Calibration 7	0	1.1955	0.725267	1.367044
Acid Calibration 8	0	2.183391	1.311895	2.620571
300/4 210	0	0.056592	0.560813	0.70135
300/4 210	0	0.059064	0.531048	0.49984
300/4 210	0	0.059046	0.527816	0.617933
300/4 200	0	0.059531	0.397788	1.663826
300/4 200	0	0.061124	0.447175	1.254806
300/4 200	0	0.066639	0.50301	0.483594
Lactic Acid std	0	5.427643	0	0.004916
Acid Calibration 1	0	0.012581	0.010604	0.018213
Acid Calibration 2	0	0.037909	0.023154	0.040894
Acid Calibration 3	0	0.080116	0.048581	0.086405
Acid Calibration 4	0	0.158019	0.101999	0.185586
Acid Calibration 5	0	0.280873	0.179599	0.335314
Acid Calibration 6	0	0.593358	0.366586	0.720971
Acid Calibration 7	0	1.156434	0.72898	1.356952

Table 19: GC-MS results from 20131203

Notes	Furfural	Lactic Acid	Levulinic acid	All Unreacted Sugars	Glucose
	Target/ ISTD	Target/ ISTD	Target/ ISTD	Target/ ISTD	Target/ ISTD
Acid Calibration 1	0	0.00858	0.003749	0.00784	0.006638
Acid Calibration 2	0	0.012006	0.009031	0.013024	0.017339
Acid Calibration 3	0	0.030803	0.022317	0.023565	0.038631
Acid Calibration 4	0	0.059089	0.039409	0.053225	0.067055
Acid Calibration 5	0	0.128467	0.076452	0.110036	0.149782
Acid Calibration 6	0	0.242724	0.151179	0.198376	0.302929
Acid Calibration 7	0	0.494428	0.315175	0.417088	0.618026
Acid Calibration 8	0	0.923362	0.60472	0.160421	1.181008
300/4 210	0	1.012751	0.299777	0.031874	0.035848
300/4 220	0	0.741202	0.339672	0.011908	0.014199
300/4 230	0	0.732378	0.333545	0	0
300/noSn-210	0	0.028341	0.538188	0.114559	0.171543
300/noSn-220	0	0.097408	0.280417	0.130593	0.17767
300/noSn-230	0	0.021941	0.504031	0	0.001779
300/Ba-230	0	0.095974	0.26268	0.021232	0
Acid Calibration 1	0	0.092913	0.069592	0.646542	0.012207
Acid Calibration 2	0	0.009833	0.00703	1.878264	6.6777
Acid Calibration 3	0	0.015135	1.017472	0	0.006579

Table 20: GC-MS results from 20131018

Notes	Furfural	Lactic Acid	Levulinic acid	Glucose
	Target/ISTD	Target/ISTD	Target/ISTD	Target/ISTD
Acid Calibration 1	0	0.057475	0.057526	0.10171
Acid Calibration 2	0	0.076801	0.11045	0.201355
Acid Calibration 3	0.000206	0.113151	0.191047	0.442603
Acid Calibration 4	0	0.343618	0.332254	0.867188
Acid Calibration 5	0	1.31608	0.510205	1.788912
Acid Calibration 6	0	3.034917	2.289052	4.088768
Acid Calibration 7	0	5.901867	4.440931	7.80007
Acid Calibration 8	0.148441	9.622384	7.470762	13.18508
E/2-170	0.018344	0.098444	0.070178	0.069264
300/4-170	0.007503	0.027706	0.023457	0.034948
300/2-170	0.008018	0.042534	0.052723	0.013071
E/4-170	0	0.03985	0.158105	0.050412
300/4-170	0	0.030559	0.039307	0.013443
300/4-180	0.002773	0.031491	0.029936	0.008858
300/4-170 sonicated	0	0.040981	0.044801	0.004681
300/4-190	0.449575	0.070838	0.055132	0.007666
300/4-200	0	0.092913	0.069592	0.012207
BaCl2 - 160	0	0.009833	0.00703	6.6777
Me-Levulinate	0	0.015135	1.017472	0.006579
300/Ba2 200 ME	0.318627	0.021315	0.012729	0.074483
300/Ba2 160 ME	0	0.010394	0	1.252712
300/Ba2 200 H20	0	0.617447	0.211977	1.777112
300/Sn2 25%Me H1	0	0.013292	0	11.51432
300/Sn2 25%Me H2	0	0.126898	0.003457	1.638662
300/Sn2 25%Me H3	0	0.047646	0.006253	0.006095
300/Sn2 25%Me H20	0	0.214955	0.047512	0.054557
300/Sn2 25%Me H21	0	0.151546	0.032567	0.064868
300/Sn2 25%Me H22	0	0.148161	0.031636	0.071278
300/Sn2 25%Me H1	0	0.007098	0	10.43621
300/Sn2 25%Me H2	0	0.096204	0.004896	1.859244
300/Sn2 25%Me H3	0	0.139883	0.012911	0.939722
300/Sn2 25%Me H20	0	0.150428	0.030919	0.093676
300/Sn2 25%Me H21	0	0.133917	0.026983	0.101752
300/Sn2 25%Me H22	0	0.140636	0.030382	0.080374
Acid Calibration 1	0	0.005069	0.036432	0.110506
Acid Calibration 2	0	0.017545	0.042706	0.206449
Acid Calibration 3	0	0.047469	0.079014	0.397019

Table 20 Continued				
Acid Calibration 4	0	0.342633	0.22774	0.791729
Acid Calibration 5	0	1.33356	0.613944	1.80244
Acid Calibration 6	0	3.084693	2.184201	4.225819
Acid Calibration 7	0	6.454687	4.546477	9.034488
Acid Calibration 8	0	10.4089	7.083893	15.26826
300/Sn2 25%Me H1	0	0.009347	0	12.58148
300/Sn2 25%Me H2	0	0.093565	0	1.693166
300/Sn2 25%Me H3	0	0.112959	0.008254	1.178087
300/Sn2 25%Me H20	0	0.145797	0.032873	0.09918
300/Sn2 25%Me H21	0	0.172363	0.046994	0.091477
300/Sn2 25%Me H22	0	0.173853	0.059971	0.077173
Acid Calibration 1	0	0	0.023031	0.109635
Acid Calibration 2	0	0.011852	0.040174	0.206256
Acid Calibration 3	0	0.034186	0.067561	0.375562
Acid Calibration 4	0	0.181065	0.079779	0.715075
Acid Calibration 5	0	1.349133	0.580912	1.861241
Acid Calibration 6	0	3.189958	2.355852	4.323448
Acid Calibration 7	0	6.845747	4.623579	9.028281
Acid Calibration 8	0	11.15889	6.868133	15.71194

Table 21: GC-MS results from 20131014

Notes	Methyl Lactate	Methyl Vinyl-glycolate	Furfural	Methyl Levulinate	Levulinic acid	5-HMF
	Target/ ISTD	Target/ ISTD	Target/ ISTD	Target/ ISTD	Target/ ISTD	Target/ ISTD
Nonacid Calibration 1	0.048907	0.037575	0	0.0807	0	0
Nonacid Calibration 2	0.01991	0.010032	0	0.055491	0	0
Nonacid Calibration 3	0.040601	0.031386	0	0.132831	0	0.011364
Nonacid Calibration 4	0.083234	0.087542	0.002042	0.202936	0	0.029472
Nonacid Calibration 5	0.339236	0.149669	0.014783	0.503218	0	0.081137
Nonacid Calibration 6	1.326224	0.555471	0.032279	1.186908	0	0.255594
Nonacid Calibration 7	2.722615	1.165431	0.063073	2.375809	0	0.436131
Nonacid Calibration 8	4.568039	1.998771	0.107124	3.962035	0	0.44525
300/4-170	0.180758	0	0	1.909649	0	0
300/4-180	0.357786	0.026691	0	1.646245	0	0
300/4-170 sonicated	0.392566	0.053681	0	1.560882	0	0
300/4-190	0.565828	0.040171	0	2.025746	0	0
300/4-200	0.505777	0.047951	0	1.894392	0	0
BaCl2 - 160	0.009978	0	0	0.011896	0	0.020951
Me-Levulinate	0.010647	0	0	6.300652	0	0
300/Ba2 200 ME	0.368746	0	0	0.126518	0.006659	0.010119
300/Ba2 160 ME	0.125274	0	0	0.011929	0.003745	0.020805
E/2-170	0.473787	0.02235	0	1.342034	0	0
300/4-170	0.242687	0.046684	0	1.05442	0	0
300/2-170	0.392687	0.08625	0	1.778793	0	0
E/4-170	0.171268	0.009528	0	2.771811	0	0
Nonacid Calibration 1	0.06349	0.043861	0	0.083723	0	0.012063
Nonacid Calibration 2	0.024681	0.025193	0	0.060263	0	0

Table 21 Continued						
Nonacid Calibration 3	0.087519	0.071345	0	0.140104	0	0.021556
Nonacid Calibration 4	0.093612	0.094067	0	0.204763	0	0.044256
Nonacid Calibration 5	0.631798	0.253832	0.013605	0.517659	0	0.117067
Nonacid Calibration 6	1.153986	0.497239	0.027748	1.033839	0	0.292779
Nonacid Calibration 7	2.569537	1.110072	0.052433	2.217216	0	0.621752
Nonacid Calibration 8	3.951054	1.717075	0.077461	3.432621	0.002764	0.890238
300/Sn2 25%Me H1	0.016345	0	0	0	0	0
300/Sn2 25%Me H2	0.143396	0.01624	0	0.00958	0	0.030729
300/Sn2 25%Me H3	0.191384	0.022978	0	0.022856	0	0.032463
300/Sn2 25%Me H20	0.261253	0.014619	0	0.243436	0	0
300/Sn2 25%Me H21	0.243285	0.030169	0	0.26309	0	0.002151
300/Sn2 25%Me H22	0.214703	0.032931	0.002191	0.249127	0	0
300/Sn2 25%Me H1	0.013552	0	0	0	0	0
300/Sn2 25%Me H2	0.132459	0.01406	0	0.009188	0	0.038179
300/Sn2 25%Me H3	0.166671	0	0	0.022343	0	0.035441
300/Sn2 25%Me H20	0.212904	0.01091	0	0.241845	0	0.00384
300/Sn2 25%Me H21	0.222087	0.030932	0	0.241029	0	0
300/Sn2 25%Me H22	0.211598	0.027131	0	0.259485	0	0
300/Sn2 25%Me H1	0.004121	0	0	0	0	0
300/Sn2 25%Me H2	0.121588	0.012025	0	0.008912	0	0.031
300/Sn2 25%Me H3	0.150374	0.002881	0	0.018946	0	0.032926

Table 21 Continued						
300/Sn2 25%Me H20	0.220669	0.019513	0	0.232509	0	0
300/Sn2 25%Me H21	0.198703	0.017306	0	0.237501	0	0.004068
300/Sn2 25%Me H22	0.208964	0.023617	0.002594	0.259282	0	0.003138
Nonacid Calibration 1	0.042261	0.024181	0.002539	0.081534	0	0.007683
Nonacid Calibration 2	0.013047	0.024517	0	0.05104	0	0
Nonacid Calibration 3	0.081248	0.061704	0	0.120063	0	0.016814
Nonacid Calibration 4	0.089632	0.053634	0	0.199959	7.09E-05	0.038941
Nonacid Calibration 5	0.311581	0.230984	0.01444	0.47245	0	0.104144
Nonacid Calibration 6	1.295601	0.545691	0.030784	1.061783	0	0.302139
Nonacid Calibration 7	2.532195	1.088787	0.053411	2.168497	0	0.437348
Nonacid Calibration 8	1.6816	1.212069	0.091763	3.496525	0	0.390462

Table 22: GC-MS results for 20131001

Notes	Furfural	Lactic Acid	Levulinic acid	Unreacted Sugars 1	Unreacted Sugars 2	Glucose
	Target/ ISTD	Target/ ISTD	Target/ ISTD	Target/ ISTD	Target/ ISTD	Target/ ISTD
Acid Calibration 1	0.000000	0.135331	0.164853	0.396895	0.135700	0.183524
Acid Calibration 2	0.000000	0.221286	0.333753	0.810194	0.257273	0.363882
Acid Calibration 3	0.000000	0.328547	0.630366	1.622480	0.520359	0.757105
Acid Calibration 4	0.000000	0.466102	1.146228	3.123866	1.012499	1.493907
Acid Calibration 5	0.000000	1.506334	2.359491	6.331570	0.467588	3.297574
Acid Calibration 6	0.000000	3.540066	4.375137	9.880320	3.539065	5.692264
Acid Calibration 7	0.000000	9.787221	11.774231	26.276337	11.129242	13.578914
Acid Calibration 8	0.000000	17.917948	21.314031	51.346460	21.560331	27.666477
Lactic Acid Std	0.000000	45.855836	0.010238	0.000000	0.011859	0.014336
Levulinic Acid Std	0.000000	0.037491	47.559793	0.000000	0.000000	0.000000
Glucose Std	0.000000	0.005345	0.028085	0.003958	21.086690	22.219406
Fructose Std	0.000000	0.011461	0.017505	16.605824	15.284923	0.105506
Mannose Std	0.000000	0.006580	0.009648	59.236142	29.835708	0.012637
300-Sn4 200C	0.000000	2.286629	1.887496	0.274016	0.156307	0.258998
300-Sn4 190C	0.000000	1.198152	2.237449	0.185831	0.547124	0.829278
300-Sn4 180C	0.000000	1.049028	2.084620	0.151417	1.624270	2.510328
300-Sn4 170C	0.000000	0.304913	1.555725	1.271615	5.852159	9.344453
E-Sn2 180 Initial	0.000000	0.006665	0.008950	0.015034	14.864735	41.123474
E-Sn2 180 T-60min	0.000000	0.438048	2.049815	0.155378	3.149134	5.216391
E-Sn2 180 T-30min	0.000000	0.482755	2.366509	0.149369	3.452206	5.051621
E-Sn2 180 T	0.000000	0.436911	1.684635	0.144051	3.217476	4.586432

Table 22 Continued						
Acid Calibration 1	0.000000	0.050887	0.140962	0.469838	0.142155	0.216665
Acid Calibration 2	0.000000	0.047129	0.247871	0.859409	0.310088	0.390176
Acid Calibration 3	0.000000	0.071592	0.415922	1.531925	0.510337	0.770638
Acid Calibration 4	0.000000	0.297535	0.933747	2.875099	1.035876	1.588455
Acid Calibration 5	0.000000	1.639541	2.173226	4.726713	1.989481	3.136829
Acid Calibration 6	0.000000	4.035709	4.709213	12.922811	0.904983	6.038466
Acid Calibration 7	0.000000	8.310515	10.381399	25.596771	10.535928	12.785988
Acid Calibration 8	0.000000	18.537616	21.129909	54.678058	21.944666	23.231511
E-Sn2 170 Initial	0.000000	0.007408	0.024769	0.000000	16.837800	47.333991
E-Sn2 170 T-60min	0.000000	0.768709	1.470370	0.222424	2.995838	4.962434
E-Sn2 170 T-30min	0.000000	0.326351	1.725646	1.171568	5.841825	9.928565
E-Sn2 170 T	0.000000	0.292646	1.305522	1.422766	0.377635	10.210958
E-Sn2 200 Initial	0.000000	0.028497	0.029690	0.006140	15.907831	41.314262
E-Sn2 200 T-60min	0.000000	0.611727	3.001523	0.099298	0.190049	0.236332
E-Sn2 200 T-30min	0.000000	0.647232	3.334877	0.103711	0.196477	0.231022
E-Sn2 200 T	0.000000	0.567013	1.658246	0.078491	0.066978	0.093415
E-Sn2 190 Initial	0.000000	0.000000	0.000000	0.000000	16.198174	42.428434
E-Sn2 190 T-60min	0.000000	0.564877	2.516659	0.111744	1.103058	1.440116
E-Sn2 190 T-30min	0.000000	0.602809	2.696248	0.117351	1.086687	1.573984
E-Sn2 190 T	0.000000	0.555585	2.113852	0.105399	1.050278	1.519126
Acid Calibration 1	0.000000	0.026776	0.113025	0.467117	0.158662	0.209064
Acid Calibration 2	0.000000	0.018863	0.180052	0.826156	0.291897	0.371526
Acid Calibration 3	0.000000	0.063879	0.359881	1.481962	0.558284	0.780351

Table 22 Continued						
Acid Calibration 4	0.000000	0.285101	0.731929	2.317099	0.990088	1.384147
Acid Calibration 5	0.000000	1.689606	2.082672	4.354575	1.859182	2.695995
Acid Calibration 6	0.000000	4.283538	4.979893	14.333925	0.855542	6.302699
Acid Calibration 7	0.000000	9.730209	11.299224	31.748818	13.046900	15.633702
Acid Calibration 8	0.000000	18.128993	20.526618	50.949701	1.903746	22.227810

Table 23: GC-MS derivatized results from DOE block 2

Notes	Lactic Acid	Levulinic acid	Unreacted Sugar 1	Unreacted Sugar 2	Glucose
	Target/ ISTD	Target/ ISTD	Target/ ISTD	Target/ ISTD	Target/ ISTD
Acid Calibration 1	0.23538	0.01104	2.07366	1.68554	0.13715
Acid Calibration 2	0.16873	0.00798	0.44197	0.60610	0.04979
Acid Calibration 3	0.37147	0.01496	0.56400	0.28377	0.01680
Acid Calibration 4	0.78195	0.02533	0.55402	0.21294	0.13513
Acid Calibration 5	0.88570	0.02412	0.34931	0.10962	0.06907
Acid Calibration 6	2.11661	0.19311	0.57959	0.17976	0.03148
Acid Calibration 7	2.71001	1.38001	0.61542	0.13708	0.02534
Acid Calibration 8	5.14858	4.13219	0.62654	0.16292	0.02713
06CK23-178	0.00703	0.00380	1.03581	33.44809	27.43508
06CK23-179	0.09183	0.01589	0.96188	11.07574	5.54053
06CK23-180	0.16085	0.04384	1.17645	9.57031	7.40402
06CK23-181	0.33062	0.47778	1.08272	2.39260	7.48070
06CK23-182	0.36034	0.48408	1.22788	2.44142	7.88916
06CK23-183	0.31595	0.47717	0.97837	2.34580	7.13644
10CK23-106	0.00648	0.00481	0.85243	14.91209	12.56474
10CK23-107	0.01441	0.00337	1.03253	14.99423	12.97064
10CK23-108	0.02089	0.00146	1.02865	14.49084	12.66357
10CK23-109	0.05782	0.01363	2.33507	25.11793	21.82001
10CK23-110	0.06925	0.01279	2.38104	25.73026	26.71188
10CK23-111	0.06077	0.01623	2.39444	25.12178	26.28376
17CK23-130	0.00782	0.00456	1.05484	17.09665	14.34981
17CK23-131	0.01097	0.00649	1.11261	13.03527	4.16202
17CK23-132	0.00923	0.01061	1.02543	11.07591	5.47676
17CK23-133	0.05107	0.10791	1.09151	2.12962	9.54717
17CK23-134	0.05279	0.10979	1.07446	1.92341	9.33575
17CK23-135	0.05098	0.11923	1.02478	2.11430	9.27452
12CK23-186	0.01030	0.00482	1.32519	21.30966	18.03465
12CK23-187	0.02808	0.00893	1.35972	13.20873	4.20587
12CK23-188	0.04901	0.01587	1.34972	9.80803	5.61589

Table 23 Continued					
12CK23-189	0.23423	0.21634	1.18385	2.12830	8.49916
12CK23-190	0.20570	0.21837	1.02331	1.13617	7.76344
12CK23-191	0.23490	0.22665	1.20368	1.77211	8.33066
14CK23-170	0.00647	0.00382	1.16956	36.29476	32.49632
14CK23-171	0.00589	0.00703	1.16571	33.77056	27.31027
14CK23-172	0.00704	0.00735	1.18904	33.29003	30.48313
14CK23-173	0.02054	0.01997	4.60846	57.07528	58.53312
14CK23-174	0.01724	0.01864	4.69950	56.39351	57.72237
14CK23-175	0.01923	0.02236	4.34205	55.74944	59.01393
11CK23-122	0.02111	0.00430	1.21210	15.64482	13.50474
11CK23-123	0.30929	0.01339	0.97127	6.60791	6.07294
11CK23-124	0.42297	0.02854	1.06360	5.94769	5.79660
11CK23-125	0.77079	0.02435	1.21380	3.14301	0.99563
11CK23-126	0.79900	0.02088	1.25256	2.78307	1.06882
11CK23-127	0.87708	0.01963	0.86866	3.05792	1.14042
Acid Calibration 1	0.09568	0.00482	0.85913	0.67669	0.05203
Acid Calibration 2	0.13658	0.00720	0.38705	0.50134	0.03800
Acid Calibration 3	0.23168	0.00935	0.35561	0.17469	0.00721
Acid Calibration 4	0.59135	0.01763	0.40585	0.14676	0.12566
Acid Calibration 5	1.07901	0.03501	0.44956	0.14436	0.14196
Acid Calibration 6	1.93591	0.17511	0.53200	0.16193	0.15626
Acid Calibration 7	2.09475	1.08639	0.51592	0.11228	0.01960
Acid Calibration 8	3.51640	2.96646	0.42939	0.10936	0.06643
07CK23-98	0.00844	0.00000	0.77052	28.50119	24.90054
07CK23-99	0.01678	0.00629	0.73488	24.41682	21.04625
07CK23-100	0.02242	0.00702	0.70975	24.56052	20.80657
07CK23-101	0.11752	0.20068	0.84493	17.64594	14.96514
07CK23-102	0.11493	0.21704	0.81662	16.85916	14.25431
07CK23-103	0.15064	0.21313	0.94058	18.52434	22.47854
13CK23-154	0.00734	0.00456	1.14004	34.80031	28.67670
13CK23-155	0.00947	0.00862	1.32832	39.71755	35.23982
13CK23-156	0.01223	0.01350	1.35082	34.01746	32.94546
13CK23-157	0.10419	0.39605	1.17087	20.26935	16.32198

Table 21 Continued					
13CK23-158	0.11807	0.38083	1.34145	22.47219	16.67692
13CK23-159	0.12415	0.40069	1.43722	21.93287	15.81677
15CK23-114	0.01446	0.00458	0.73036	28.35463	23.43163
15CK23-115	0.06914	0.00640	0.74821	20.97459	19.90827
15CK23-116	0.11813	0.01036	0.84734	21.62013	21.15703
15CK23-117	0.27916	0.10019	2.07735	39.42962	37.10871
15CK23-118	0.28194	0.09800	2.04348	39.30373	38.56429
15CK23-119	0.29745	0.12227	2.20181	48.01720	48.30913
08CK23-162	0.00633	0.00815	1.17831	23.94311	20.37833
08CK23-163	0.00630	0.00000	1.17136	19.85630	17.31439
08CK23-164	0.00712	0.00403	1.43917	22.70924	20.57608
08CK23-165	0.02674	0.00627	2.30202	33.95901	30.54060
08CK23-166	0.03047	0.00737	2.14958	31.40738	29.78543
08CK23-167	0.02627	0.00633	2.26712	33.38395	31.38673
09CK23-138	0.01214	0.00934	1.04456	35.62421	33.72376
09CK23-139	0.01393	0.00600	0.90686	28.72881	23.61827
09CK23-140	0.01729	0.00749	0.91713	26.67682	24.10229
09CK23-141	0.04921	0.02200	4.42414	61.04932	63.10822
09CK23-142	0.04894	0.01983	4.53419	58.94932	64.79646
09CK23-143	0.05592	0.02559	4.44389	61.13744	63.54302
16CK23-146	0.00578	0.00515	1.24750	19.16332	15.38849
16CK23-147	0.00734	0.00379	1.29559	19.02134	15.17702
16CK23-148	0.00794	0.00574	1.39699	18.63822	15.12035
16CK23-149	0.01140	0.00729	3.76100	37.22213	39.08304
16CK23-150	0.00766	0.00645	3.76585	35.96807	38.11844
16CK23-151	0.00965	0.00889	3.85022	31.65500	38.24551
Acid Calibration 1	0.20057	0.00821	1.84248	1.41863	1.41730
Acid Calibration 2	0.26444	0.01573	0.74127	0.98507	0.07042
Acid Calibration 3	0.40621	0.01779	0.63343	0.30974	0.29689
Acid Calibration 4	0.94124	0.03308	0.70632	0.24904	0.25043
Acid Calibration 5	1.13121	0.02508	0.55730	0.17134	0.11668
Acid Calibration 6	2.66245	0.26710	0.75632	0.23703	0.20527
Calibration 7	2.94811	1.63163	0.79733	0.18546	0.18206
Calibration 8	7.18969	6.21404	0.99403	0.25894	0.25164

Table 24: GC-MS underivatized results from DOE block 2

Notes	Methyl Lactate	Methyl Vinylglycolate	Furfural	Methyl Levulinate
	Target/ISTD	Target/ISTD	Target/ISTD	Target/ISTD
Nonacid Calibrations 1	0.028093	0.012586	0.01092	0.012444
Nonacid Calibrations 2	0.051825	0.018703	0.041112	0.057158
Nonacid Calibrations 3	0.117263	0.051474	0.073191	0.166415
Nonacid Calibrations 4	0.241221	0.108169	0.138764	0.341251
Nonacid Calibrations 5	0.495311	0.209812	0.277569	0.708927
Nonacid Calibrations 6	0.936436	0.407366	0.498848	1.414353
Nonacid Calibrations 7	1.810831	0.752086	1.593894	2.71374
Nonacid Calibrations 8	2.443509	1.298727	2.940571	4.958656
06CK23-178	0	0	0	0
06CK23-179	0.056133	0.008514	0.010189	0.007541
06CK23-180	0.079579	0.008495	0.02558	0.046626
06CK23-181	0.164433	0.023848	0.066631	1.196924
06CK23-182	0.180271	0.02689	0.051188	1.273011
06CK23-183	0.194852	0.020102	0.084308	1.452822
10CK23-106	0	0	0	0
10CK23-107	0	0	0	0
10CK23-108	0	0	0	0
10CK23-109	0.002692	0	0	0
10CK23-110	0.002603	0	0	0
10CK23-111	0.002304	0	0.001615	0.001551
17CK23-130	0	0	0	0
17CK23-131	0	0	0	0
17CK23-132	0.002286	0	0	0.002971
17CK23-133	0.014963	0	0.018573	0.399548
17CK23-134	0.022391	0	0.020144	0.424206
17CK23-135	0.03187	0	0.019951	0.419376
12CK23-186	0	0	0	0
12CK23-187	0	0	0.003672	0.002667
12CK23-188	0.006177	0	0.000801	0.007454
12CK23-189	0.126343	0	0.030051	0.646198

Table 24 Continued				
12CK23-190	0.128292	0	0.034876	0.628897
12CK23-191	0.129965	0	0.035766	0.6312
Nonacid Calibrations 1	0.023719	0.012403	0.015947	0.026065
Nonacid Calibrations 2	0.045939	0.027713	0.036025	0.057499
Nonacid Calibrations 3	0.094007	0.043147	0.081959	0.139717
Nonacid Calibrations 4	0.209185	0.101458	0.183398	0.302292
Nonacid Calibrations 5	0.445429	0.200711	0.390711	0.646086
Nonacid Calibrations 6	0.881789	0.395303	0.785735	1.310856
Nonacid Calibrations 7	1.487957	0.596307	1.450261	2.52536
Nonacid Calibrations 8	2.190925	1.169625	2.730268	4.497917
14CK23-170	0	0	0	0
14CK23-171	0	0	0	0
14CK23-172	0	0	0	0
14CK23-173	0.00207	0	0.00249	0.020884
14CK23-174	0.006904	0	0.001435	0.02209
14CK23-175	0.00262	0	0.001651	0.024918
11CK23-122	0	0	0	0
11CK23-123	0.039948	0.006991	0.00372	0
11CK23-124	0.04345	0.006929	0.007097	0.001409
11CK23-125	0.075828	0.011075	0.019614	0.169651
11CK23-126	0.065138	0.01367	0.023612	0.170765
11CK23-127	0.073514	0.008773	0.009043	0.182964
07CK23-98	0	0	0	0
07CK23-99	0.002308	0	0	0
07CK23-100	0	0	0	0
07CK23-101	0.016445	0	0.028175	0.149762
07CK23-102	0.012922	0	0.029572	0.156007
07CK23-103	0.012364	0	0.019102	0.153093
13CK23-154	0	0	0	0
13CK23-155	0	0	0	0
13CK23-156	0	0	0	0
13CK23-157	0.003062	0	0.021505	0.16054
13CK23-158	0.00343	0	0.023839	0.16836

Table 24 Continued				
13CK23-159	0.002818	0	0.025699	0.181691
15CK23-114	0	0	0	0
15CK23-115	0.003507	0	0	0
15CK23-116	0.010897	0	0.002906	0
15CK23-117	0.010085	0.00337	0.009475	0.034664
15CK23-118	0.029672	0.002144	0.012411	0.047769
15CK23-119	0.032872	0.003006	0.013144	0.057157
08CK23-162	0	0	0	0
08CK23-163	0	0	0	0
08CK23-164	0	0	0.00047	0
08CK23-165	0.003876	0	0	0
08CK23-166	0.006529	0	0	0
08CK23-167	0.010345	0	0	0
09CK23-138	0	0	0.000336	0
09CK23-139	0	0	0	0
09CK23-140	0.002848	0	0	0
09CK23-141	0.024482	0.003009	0.005446	0.030562
09CK23-142	0.025105	0.002915	0.004882	0.032651
09CK23-143	0.027014	0.003017	0.013008	0.037275
16CK23-146	0	0	0	0
16CK23-147	0	0	0	0
16CK23-148	0	0	0	0
16CK23-149	0	0	0	0
16CK23-150	0	0	0.000392	0
16CK23-151	0	0	0	0
Nonacid Calibrations 1	0.019796	0.010579	0.015324	0.012233
Nonacid Calibrations 2	0.042811	0.02181	0.029128	0.041103
Nonacid Calibrations 3	0.093181	0.04287	0.073067	0.120509
Nonacid Calibrations 4	0.176885	0.074876	0.106961	0.2763
Nonacid Calibrations 5	0.408943	0.189667	0.262736	0.595575
Nonacid Calibrations 6	0.7468	0.302527	0.782002	1.195661
Nonacid Calibrations 7	1.358089	0.542797	1.406961	2.237869
Nonacid Calibrations 8	2.865705	1.156127	2.77114	4.448039

Table 25: GC-MS derivatized results for DOE block 1

Notes	Lactic Acid	Levulinic acid	Unreacted sugars 1	Unreacted sugars 2	Glucose
	Target/ ISTD	Target/ ISTD	Target/ ISTD	Target/ ISTD	Target/ ISTD
Acid Calibration 1	0.12320	0.00423	0.82971	0.79828	0.03558
Acid Calibration 2	0.42900	0.01915	1.38545	0.80715	0.01799
Acid Calibration 3	0.78686	0.02298	0.48662	0.27924	0.00552
Acid Calibration 4	1.68445	0.02831	0.36014	0.21833	0.00353
Acid Calibration 5	3.09850	0.08445	0.30628	0.19260	0.00000
Acid Calibration 6	4.72629	0.40591	0.29776	0.17801	0.00117
Acid Calibration 7	5.42697	2.83530	0.21283	0.12256	0.00000
154_CK19-96d	0.58406	0.10141	68.76024	68.72304	5.04276
155_CK19-97d	0.44562	0.18300	134.57069	138.33248	22.21780
156_CK19-98d	0.16215	0.05056	50.98503	43.18957	7.57866
157_CK19-99d	0.05132	0.07948	70.09910	67.61275	8.93521
159_CK19-13d	3.22526	0.10018	0.32804	0.05846	0.00475
161_CK20-02d	0.12410	0.15953	106.11056	101.65269	20.07271
162_CK20-03d	0.13027	0.13396	35.63399	34.21762	2.86226
163_CK20-04d	0.40964	0.35194	46.58788	12.94535	3.69481
165_CK20-05d	0.62473	0.79998	9.13582	10.92431	0.57867
166_CK20-06d	0.70178	0.78699	8.28857	1.64642	0.79613
167_CK20-07d	0.75125	0.87153	8.23945	2.96172	0.57258
169_CK20-10d	0.23733	0.05984	37.42560	33.29309	4.55103
170_CK20-11d	0.13600	0.09215	42.90373	36.73458	2.13408
171_CK20-12d	0.11920	0.05411	35.48301	31.65155	2.89861
173_CK20-13d	0.17056	0.03461	27.10860	24.89062	2.40477
174_CK20-14d	0.16858	0.03518	27.94786	25.38578	2.99837
175_CK20-15d	0.16679	0.04703	26.30720	23.42179	2.40255
179_CK20-18d	0.19139	0.13259	75.32223	73.91316	10.59005
180_CK20-19d	0.13992	0.04777	0.99671	0.84618	0.07176
181_CK20-20d	0.50445	0.35045	62.65600	55.11722	6.96734
183_CK20-21d	0.41444	0.26708	6.77076	36.70116	0.65065
184_CK20-22d	0.42058	0.27424	7.83997	28.28020	0.59025
185_CK20-23d	0.41348	0.28894	8.52291	31.88120	0.84701

Table 25 Continued					
187_CK20-26d	0.09596	0.05747	52.25443	48.81962	6.69383
188_CK20-27d	0.07212	0.08805	47.55347	52.59076	6.36402
189_CK20-28d	0.11157	0.09805	38.72102	16.85310	3.61240
191_CK20-29d	0.38366	0.36288	3.19724	17.62298	0.42236
192_CK20-30d	0.46233	0.34402	2.85848	20.54487	0.44142
193_CK20-31d	0.55895	0.32753	5.02473	25.65502	0.47015
197_CK20-34d	0.14045	0.09385	64.91434	76.86721	22.26055
198_CK20-35d	0.09776	0.07544	56.82565	51.97228	14.52474
199_CK20-36d	0.12246	0.11013	80.71905	75.59070	12.09488
201_CK20-37d	0.13810	0.14412	66.32299	81.05262	10.90795
202_CK20-38d	0.14992	0.17434	65.35696	84.02227	10.32847
203_CK20-39d	0.13077	0.14894	81.49917	61.11110	13.44067
205_CK20-42d	0.06379	0.03214	29.06343	22.75756	4.50796
206_CK20-43d	0.88628	0.03980	23.20079	21.15995	1.73430
207_CK20-44d	0.79654	0.03136	10.64731	10.20848	0.65008
209_CK20-45d	1.07908	0.05405	5.19988	3.24253	0.24756
210_CK20-46d	1.15814	0.05729	4.44811	2.68069	0.22575
211_CK20-47d	1.01497	0.06032	4.66380	2.82680	0.42655
Acid Calibration 1	0.11736	0.00535	0.80848	0.46018	0.01409
Acid Calibration 2	0.38553	0.01994	1.40130	0.31549	0.02252
Acid Calibration 3	0.74476	0.02607	0.51790	0.09308	0.00922
Acid Calibration 4	1.52995	0.04459	0.36252	0.06340	0.00516
Acid Calibration 5	2.69586	0.08895	0.33513	0.05821	0.00454
Acid Calibration 6	4.05952	0.37732	0.29522	0.05503	0.00443
Acid Calibration 7	4.57750	2.34440	0.21681	0.03988	0.00343
Acid Calibration 8	9.08904	7.66220	0.24955	0.04446	0.00373
223_CK20-50d	0.07569	0.04538	69.23368	60.13851	9.01765
224_CK20-51d	0.07510	0.05269	58.83650	53.70908	9.57592
225_CK20-52d	0.11656	0.04957	59.87388	56.69016	10.05151
227_CK20-53d	0.50376	0.15141	22.72517	24.92201	1.70647
228_CK20-54d	0.45920	0.13888	18.07640	19.51425	1.68417
229_CK20-55d	0.47006	0.19159	19.83161	22.43297	2.33966
231_CK20-58d	0.06273	0.04915	62.66787	54.78389	9.49832

Table 25 Continued					
232_CK20-59d	0.04953	0.08437	64.46727	61.87620	11.27294
233_CK20-60d	0.05578	0.05769	63.51344	59.58644	9.25039
235_CK20-61d	0.24145	0.85773	16.31986	11.74089	1.31643
236_CK20-62d	0.26853	0.80098	22.01048	11.77455	1.30596
237_CK20-63d	0.28366	0.78558	18.06270	11.11695	1.55547
241_CK20-66d	0.02285	0.03385	54.61886	53.06561	9.01141
242_CK20-67d	0.12015	0.03593	65.94870	47.16794	11.79284
243_CK20-68d	0.15392	0.04590	44.35531	40.81406	6.37732
245_CK20-69d	0.42846	0.10148	43.44536	40.99882	4.26627
246_CK20-70d	0.40388	0.12846	41.04013	33.04751	6.06348
247_CK20-71d	0.44332	0.09886	40.76607	38.88255	4.96582
249_CK20-74d	0.03377	0.02347	73.30025	65.90272	10.87990
250_CK20-75d	0.02439	0.02531	42.65838	44.02688	7.28777
251_CK20-76d	0.03174	0.04556	62.93925	62.04842	9.85548
253_CK20-77d	0.10714	0.03007	27.39794	32.19882	4.86813
254_CK20-78d	0.20805	0.04074	23.84363	34.66054	5.04566
255_CK20-79d	0.22018	0.04537	24.90101	30.73589	4.36294
259_CK20-82d	0.02999	0.04443	121.50569	120.84976	29.70852
260_CK20-83d	0.03140	0.04942	110.79805	103.27652	19.23918
261_CK20-84d	0.05993	0.05442	135.85663	114.32420	19.28740
263_CK20-85d	0.19352	0.10738	79.48780	87.25007	8.47654
264_CK20-86d	0.18957	0.09993	76.26285	81.86977	7.58653
265_CK20-87d	0.23578	0.11043	79.71203	88.33358	7.72947
267_CK20-90d	0.01132	0.02416	37.06121	32.14164	5.82717
268_CK20-91d	0.01231	0.01813	40.38426	35.94652	4.54028
269_CK20-92d	0.01297	0.01886	37.15254	33.42876	5.51886
271_CK20-93d	0.02441	0.04023	42.01154	39.40282	5.76396
272_CK20-94d	0.02205	0.01875	41.95146	38.68350	5.74677
273_CK20-95d	0.02082	0.02250	40.67284	39.19649	6.32934
Acid Calibration 1	0.11302	0.00537	0.81984	0.07110	0.01473
Acid Calibration 2	0.38051	0.02321	1.43267	0.31886	0.02865
Acid Calibration 3	0.68175	0.02614	0.51532	0.08563	0.00861
Acid Calibration 4	1.39253	0.04485	0.37953	0.06680	0.00712
Acid Calibration 5	2.59219	0.07209	0.31586	0.21649	0.00282

Table 25 Continued					
Acid Calibration 6	3.88773	0.35395	0.32620	0.05875	0.00678
Acid Calibration 7	4.27242	2.21194	0.23472	0.03909	0.00463
Acid Calibration 8	8.37149	6.52080	0.25557	0.04533	0.00517

Table 26: GC-MS underivatized results for DOE block 1

Notes	Methyl Lactate	Methyl Vinylglycolate	Furfural	Methyl Levulinate
	Target/ISTD	Target/ISTD	Target/ISTD	Target/ISTD
Nonacid Calibration 1	0.029302658	0.016185504	0.023896838	0.037268564
Nonacid Calibration 2	0.054778355	0.033524006	0.047624462	0.083232354
Nonacid Calibration 3	0.117399301	0.07331718	0.107245176	0.177723738
Nonacid Calibration 4	0.238905354	0.166233291	0.227408996	0.377780119
Nonacid Calibration 5	0.512296304	0.377028221	0.505305199	0.812175456
Nonacid Calibration 6	1.033348808	0.766279317	0.989007608	1.606467691
Nonacid Calibration 7	1.682819079	1.624330043	2.019021986	3.187954261
Nonacid Calibration 8	4.681943004	2.203292784	3.824256469	5.986609622
Cat. CK13-06 Hour 0	0	0	0	0.002449039
Cat. CK13-06 Hour 1	0.005874104	0	0.004462076	0.016196937
Cat. CK13-06 Hour 2	0.040113185	0	0.019459266	0.140673398
Cat. CK13-06 Hour 20	0.190857913	0.003397065	0.059984298	1.513821098
Cat. CK13-06 Hour 21	0.204831799	0.003559977	0.064548733	1.588227452
Cat. CK13-06 Hour 22	0.202534625	0.003649852	0.067554899	1.622581203
Calibration Check	1.11661314	0.409759469	1.034095224	1.633898122
Cat. CK13-10 Hour 0	0	0	0	0
Cat. CK13-10 Hour 1	0	0	0	0
Cat. CK13-10 Hour 2	0	0	0	0
Cat. CK13-10 Hour 20	0.005724687	0	0.003337321	0.007641485

Table 26 Continued				
Cat. CK13-10 Hour 21	0.004592707	0	0.004678018	0.008789056
Cat. CK13-10 Hour 22	0.004122196	0	0.002237992	0.010332316
Calibration Check	1.112721784	0.441677207	0.969342037	1.538318991
Cat. CK13-17 Hour 0	0	0	0	0
Cat. CK13-17 Hour 1	0	0	0.001657012	0.003118633
Cat. CK13-17 Hour 2	0	0	0.001657012	0.003118633
Cat. CK13-17 Hour 20	0.049310098	0	0.026759505	0.367563633
Cat. CK13-17 Hour 21	0.048791983	0	0.024072331	0.379082313
Cat. CK13-17 Hour 22	0.058316484	0	0.027701335	0.402089322
Cat. CK13-12 Hour 0	0	0	0	0
Cat. CK13-12 Hour 1	0	0	0.003803122	0.0074867
Cat. CK13-12 Hour 2	0.005534658	0	0.008307284	0.046083792
Cat. CK13-12 Hour 20	0.123257979	0	0.045177338	0.785830323
Cat. CK13-12 Hour 21	0.126742319	0	0.048786052	0.809809484
Cat. CK13-12 Hour 22	0.132505031	0	0.054204834	0.869037475
Nonacid Calibration 1	0.025538581	0.015488859	0.024431373	0.038934651
Nonacid Calibration 2	0.053614422	0.020609656	0.052080281	0.082067012
Nonacid Calibration 3	0.115703218	0.044856085	0.07176257	0.179585625
Nonacid Calibration 4	0.245514573	0.094867595	0.239902809	0.380112163
Nonacid Calibration 5	0.482197295	0.363757354	0.514842237	0.799031218
Nonacid Calibration 6	0.969994256	0.752922218	1.026943239	1.555933503

Table 26 Continued				
Nonacid Calibration 7	1.625451742	1.570377088	2.049506796	3.097384978
Nonacid Calibration 8	7.102612336	3.097630769	3.964003972	5.601243124
Cat. CK13-14 Hour 0	0	0	0	0.00239999
Cat. CK13-14 Hour 1	0	0	0	0.001663443
Cat. CK13-14 Hour 2	0	0	0	0.003380545
Cat. CK13-14 Hour 20	0.005309065	0	0.009282133	0.048129815
Cat. CK13-14 Hour 21	0.008202352	0	0.019395026	0.119719417
Cat. CK13-14 Hour 22	0.003933857	0	0.01085318	0.060589251
Calibration Check	0.889517005	0.758525852	1.006565299	1.536112651
Cat. CK13-11 Hour 0	0.001444833	0	0	0
Cat. CK13-11 Hour 1	0.048615305	0.00973322	0.007391967	0.006208738
Cat. CK13-11 Hour 2	0.069010208	0.012188042	0.009723321	0.018938528
Cat. CK13-11 Hour 20	0.120468931	0.02078605	0.034281592	0.197393655
Cat. CK13-11 Hour 21	0.117338586	0.020170983	0.029432056	0.195340642
Cat. CK13-11 Hour 22	0.110932954	0.011335224	0.030138555	0.195806801
Calibration Check	0.943755082	0.751441401	1.024971209	1.529148465
Cat. CK13-07 Hour 0	0	0	0	0.003675723
Cat. CK13-07 Hour 1	0	0	0	0
Cat. CK13-07 Hour 2	0.001335967	0	0.003754381	0.007353356
Cat. CK13-07 Hour 20	0.034822853	0	0.021726657	0.112944696
Cat. CK13-07 Hour 21	0.030663983	0	0.031209705	0.105173165

Table 26 Continued				
Cat. CK13-07 Hour 22	0.033980849	0	0.017601845	0.111019084
Cat. CK13-13 Hour 0	0	0	0.002376321	0.008057427
Cat. CK13-13 Hour 1	0	0	0	0.001698301
Cat. CK13-13 Hour 2	0	0	0.003876198	0.008459091
Cat. CK13-13 Hour 20	0.005244057	0	0.030047067	0.22930378
Cat. CK13-13 Hour 21	0.007212778	0	0.038242492	0.265512643
Cat. CK13-13 Hour 22	0.005124895	0	0.033043977	0.262670761
Calibration Check	1.824601828	0.752705831	1.028417234	1.541159779
Cat. CK13-15 Hour 0	0	0	0	0.005529208
Cat. CK13-15 Hour 1	0.005059108	0	0	0
Cat. CK13-15 Hour 2	0.006029682	0	0.003965451	0.003866679
Cat. CK13-15 Hour 20	0.011643575	0.002157946	0.01650483	0.053028007
Cat. CK13-15 Hour 21	0.026234965	0	0.017532708	0.051475373
Cat. CK13-15 Hour 22	0.0109908	0.000917805	0.014556092	0.049447279
Cat. CK13-08 Hour 0	0	0	0	0
Cat. CK13-08 Hour 1	0	0	0	0
Cat. CK13-08 Hour 2	0	0	0	0
Cat. CK13-08 Hour 20	0.033427505	0	0.002316928	0.005847554
Cat. CK13-08 Hour 21	0.035890414	0	0.002695794	0.00765836
Cat. CK13-08 Hour 22	0.041996247	0	0.00325466	0.009136181
Cat. CK13-09 Hour 0	0	0	0	0

Table 26 Continued				
Cat. CK13-09 Hour 1	0	0	0	0
Cat. CK13-09 Hour 2	0	0	0	0
Cat. CK13-09 Hour 20	0.024557339	0	0.012491578	0.023301359
Cat. CK13-09 Hour 21	0.025966465	0	0.012860186	0.025771485
Cat. CK13-09 Hour 22	0.030872484	0	0.013743168	0.028242626
Cat. CK13-16 Hour 0	0	0	0	0
Cat. CK13-16 Hour 1	0	0	0	0
Cat. CK13-16 Hour 2	0	0	0	0
Cat. CK13-16 Hour 20	0	0	0	0.001763344
Cat. CK13-16 Hour 21	0	0	0	0
Cat. CK13-16 Hour 22	0	0	0	0.002490674
Nonacid Calibration 1	0.026187567	0.010957753	0.02336974	0.03524348
Nonacid Calibration 2	0.052926766	0.024849883	0.049672282	0.075546713
Nonacid Calibration 3	0.112870814	0.062670795	0.113295764	0.177075059
Nonacid Calibration 5	0.537991143	0.349253972	0.521348021	0.807855146
Nonacid Calibration 7	1.929088584	1.552249623	2.116165468	3.188027624
Nonacid Calibration 8	5.091292154	2.128117078	3.963437196	5.743984777

APPENDIX F:
MINITAB PLOTS

Versus fits, showing scatter, and normal probability plots, showing a roughly straight line, are used to verify no trends occurred as a result of the run order. Normal plots and half normal plots work similar to Pareto charts to determine which factors are significant. The following figures are individually labeled with chart title and respective target compound.

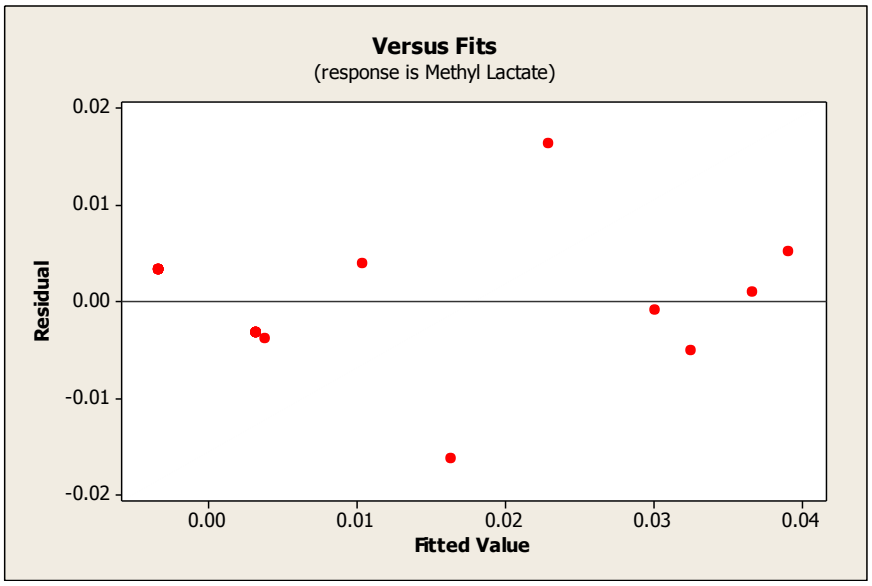
Versus Fits
(response is Methyl Lactate)
Residual
0.02
0.01
0.00
-0.01
-0.02
0.00
0.01
0.02
0.03
0.04
Fitted Value

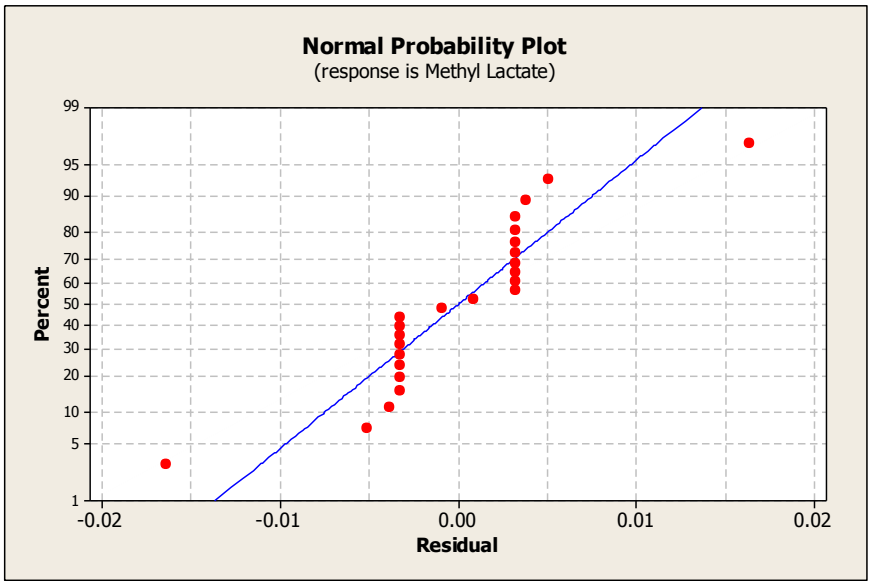
Normal Probability Plot
(response is Methyl Lactate)
Percent
99
95
90
80
70
60
50
40
30
20
10
5
1
-0.02
-0.01
0.00
0.01
0.02
Residual

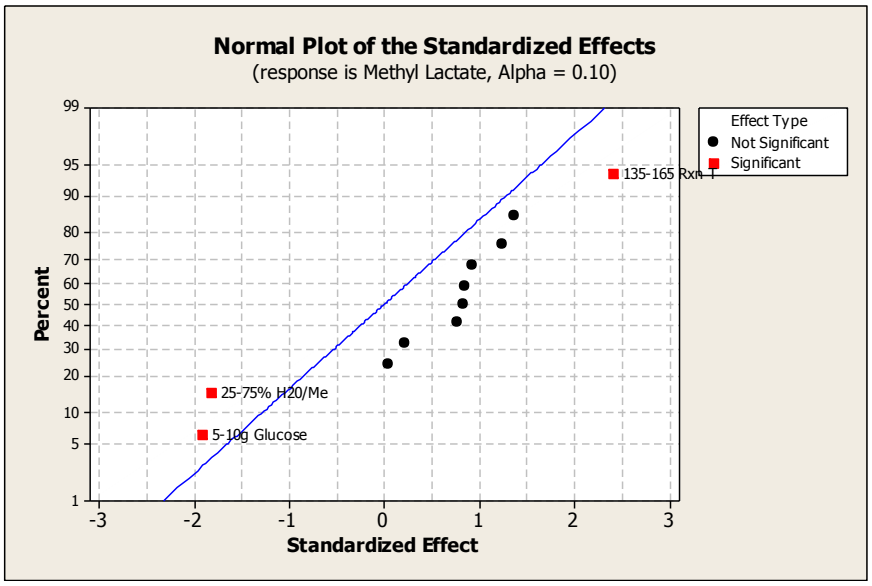
Normal Plot of the Standardized Effects
(response is Methyl Lactate, Alpha = 0.10)
Percent
Standardized Effect
Effect Type
Not Significant
Significant
135-165 Rxn T
25-75% H20/Me
5-10g Glucose

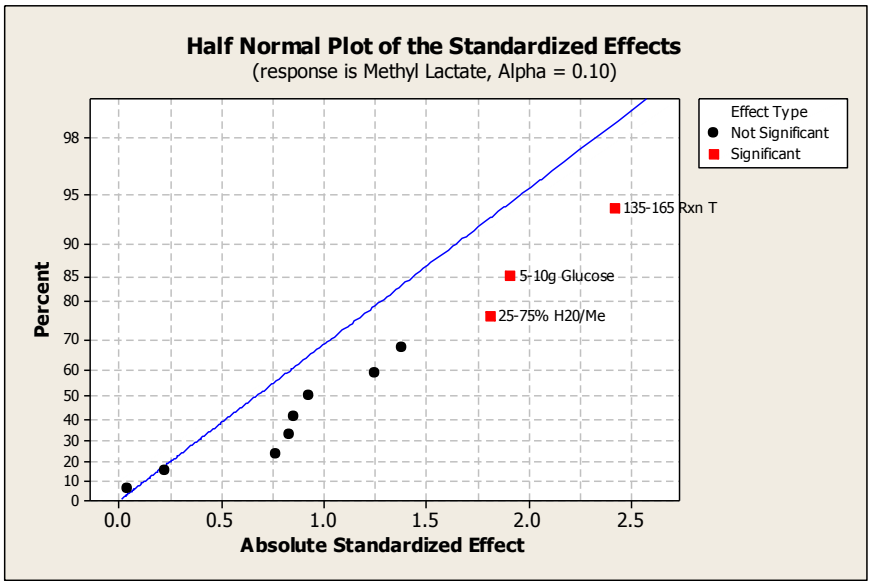
Half Normal Plot of the Standardized Effects
(response is Methyl Lactate, Alpha = 0.10)
Percent
Absolute Standardized Effect
Effect Type
Not Significant
Significant
135-165 Rxn T
5-10g Glucose
25-75% H20/Me

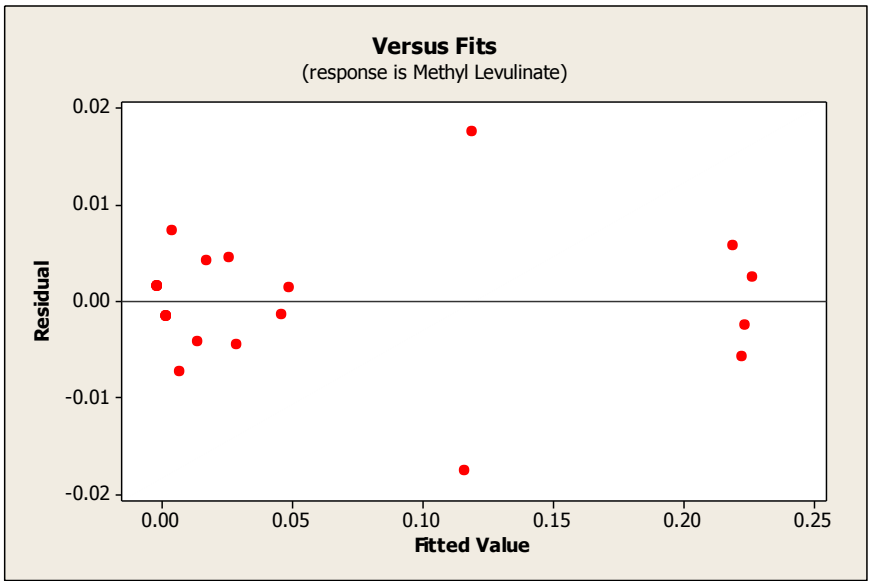
Versus Fits
(response is Methyl Levulinate)
Residual
0.02
0.01
0.00
-0.01
-0.02
0.00
0.05
0.10
0.15
0.20
0.25
Fitted Value

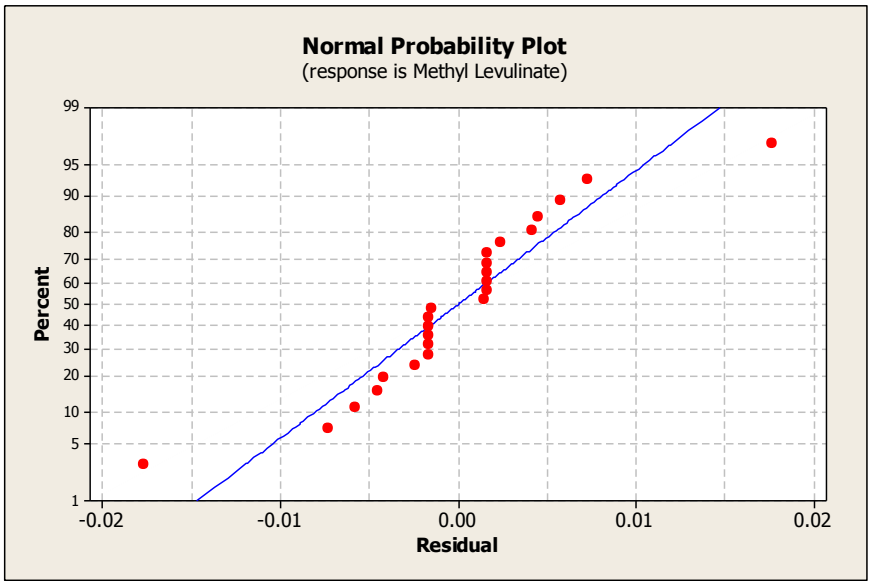
Normal Probability Plot
(response is Methyl Levulinate)
Percent
99
95
90
80
70
60
50
40
30
20
10
5
1
-0.02
-0.01
0.00
0.01
0.02
Residual

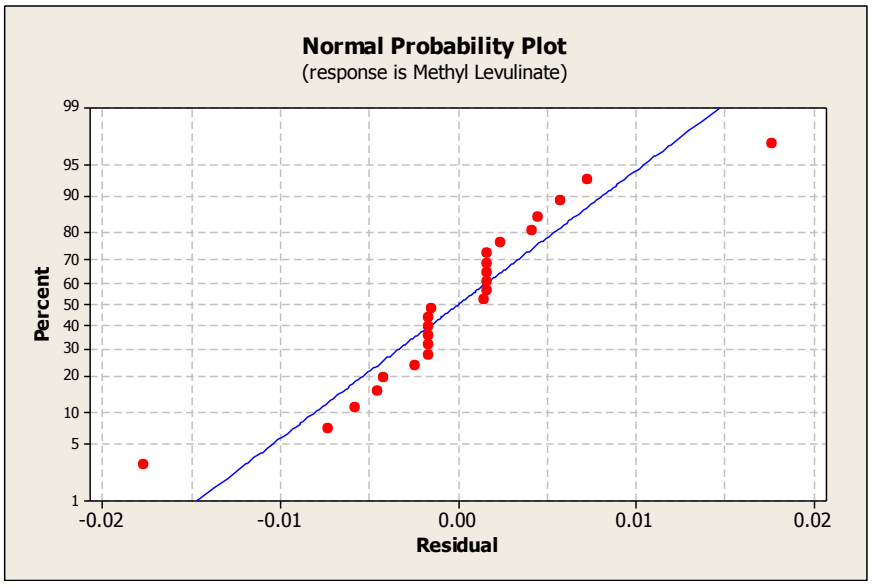
Normal Probability Plot
(response is Methyl Levulinate)
Percent
99
95
90
80
70
60
50
40
30
20
10
5
1
-0.02
-0.01
0.00
0.01
0.02
Residual

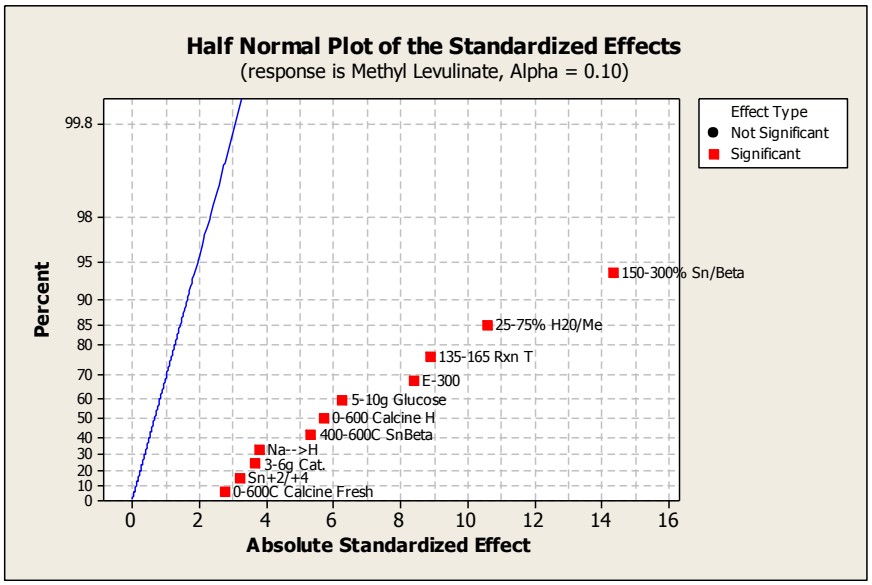
Half Normal Plot of the Standardized Effects
(response is Methyl Levulinate, Alpha = 0.10)
Effect Type
Not Significant
Significant
Percent
99.8
98
95
90
85
80
70
60
50
40
30
20
10
0
150-300% Sn/Beta
25-75% H20/Me
135-165 Rxn T
E-300
5-10g Glucose
0-600 Calcine H
400-600C SnBeta
Na-->H
3-6g Cat.
Sn+2/+4
0-600C Calcine Fresh
0
2
4
6
8
10
12
14
16
Absolute Standardized Effect

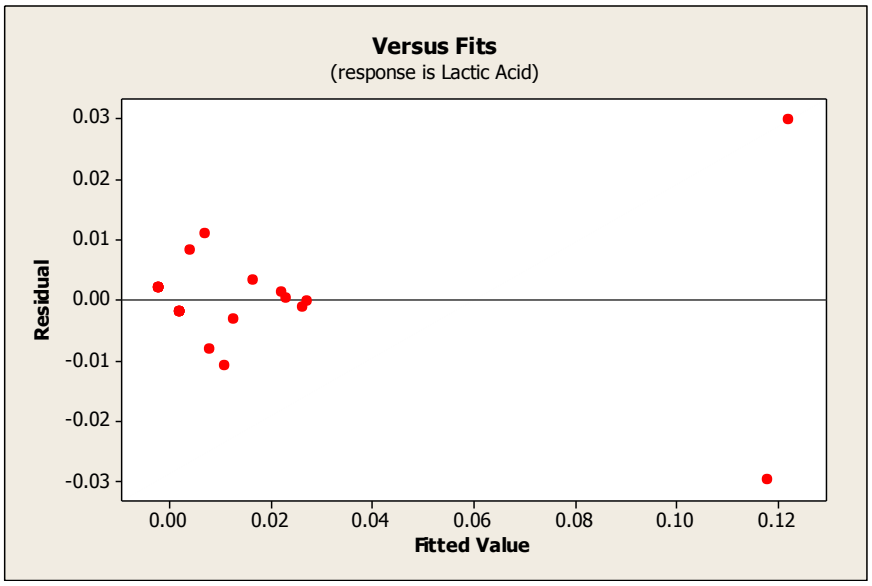
Versus Fits
(response is Lactic Acid)
Residual
0.03
0.02
0.01
0.00
-0.01
-0.02
-0.03
0.00
0.02
0.04
0.06
0.08
0.10
0.12
Fitted Value

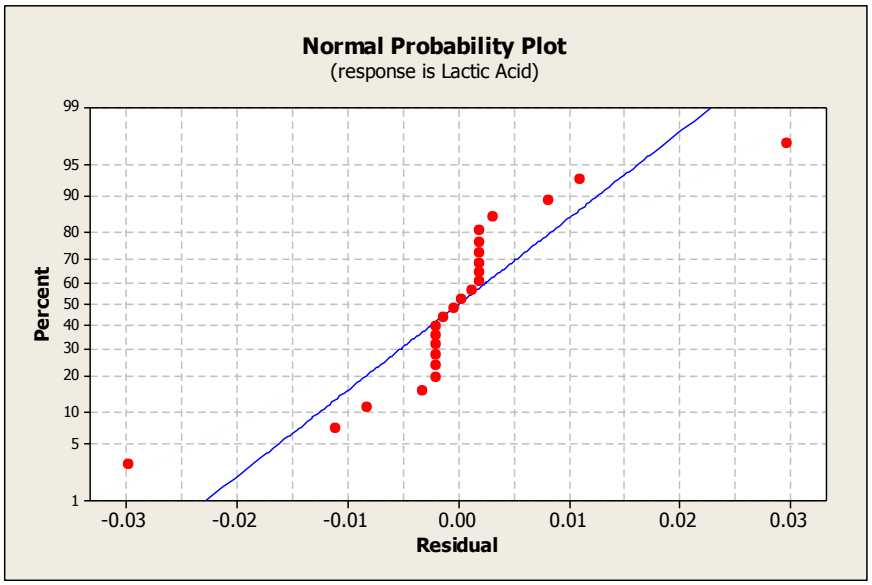
Normal Probability Plot
(response is Lactic Acid)
Percent
99
95
90
80
70
60
50
40
30
20
10
5
1
-0.03
-0.02
-0.01
0.00
0.01
0.02
0.03
Residual

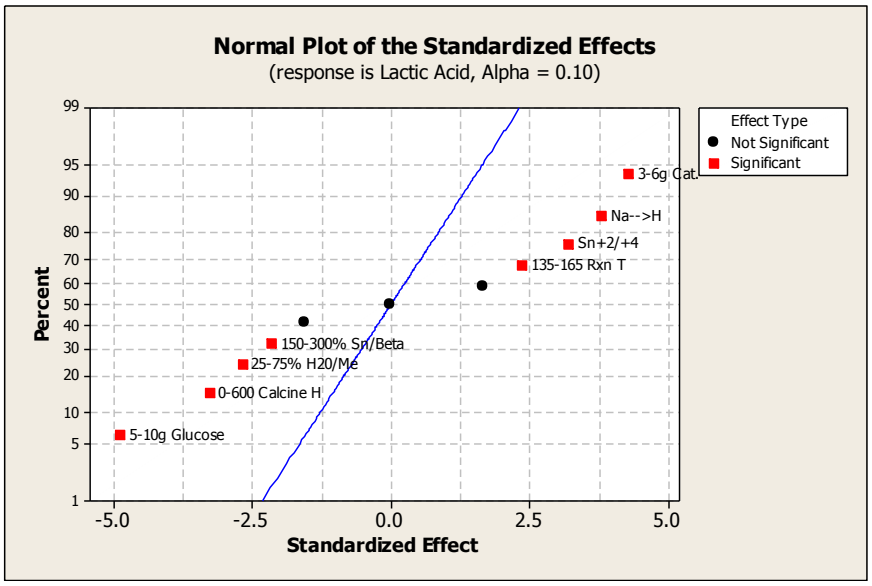
Normal Plot of the Standardized Effects
(response is Lactic Acid, Alpha = 0.10)
Percent
Standardized Effect
Effect Type
Not Significant
Significant
3-6g Cat.
Na-->H
Sn+2/+4
135-165 Rxn T
150-300% Sn/Beta
25-75% H20/Me
0-600 Calcine H
5-10g Glucose

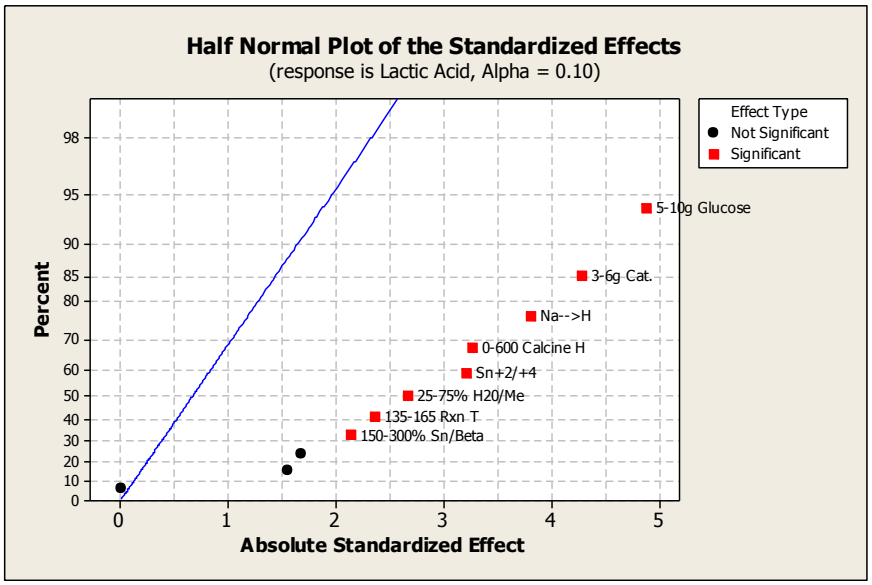
Half Normal Plot of the Standardized Effects
(response is Lactic Acid, Alpha = 0.10)
Percent
Absolute Standardized Effect
Effect Type
Not Significant
Significant
5-10g Glucose
3-6g Cat.
Na-->H
0-600 Calcine H
Sn+2/+4
25-75% H20/Me
135-165 Rxn T
150-300% Sn/Beta

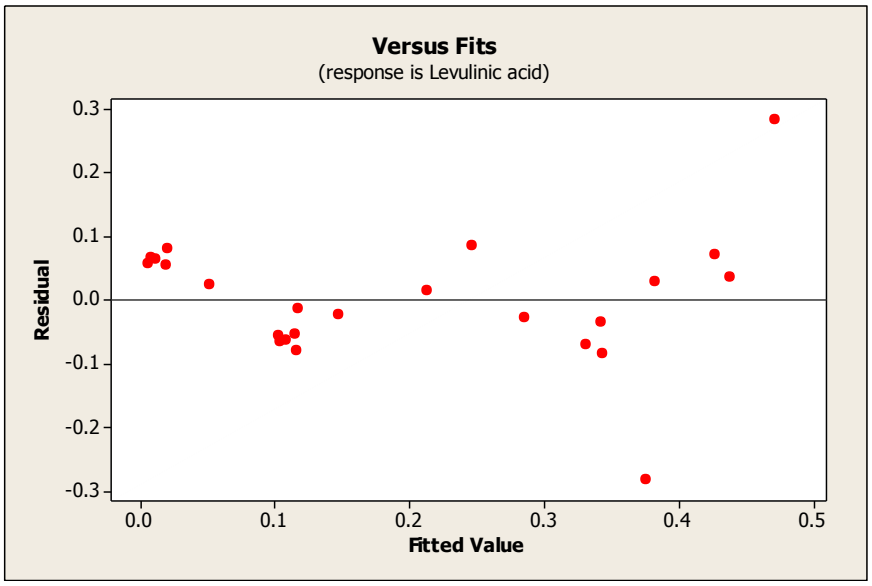
Versus Fits
(response is Levulinic acid)
Residual
Fitted Value
0.3
0.2
0.1
0.0
-0.1
-0.2
-0.3
0.0
0.1
0.2
0.3
0.4
0.5

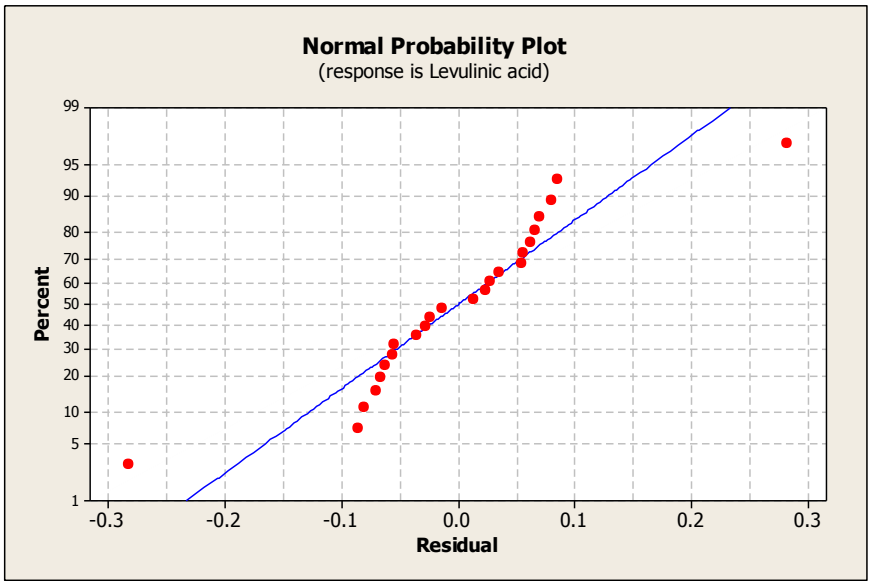
Normal Probability Plot
(response is Levulinic acid)
Percent
Residual
99
95
90
80
70
60
50
40
30
20
10
5
1
-0.3
-0.2
-0.1
0.0
0.1
0.2
0.3

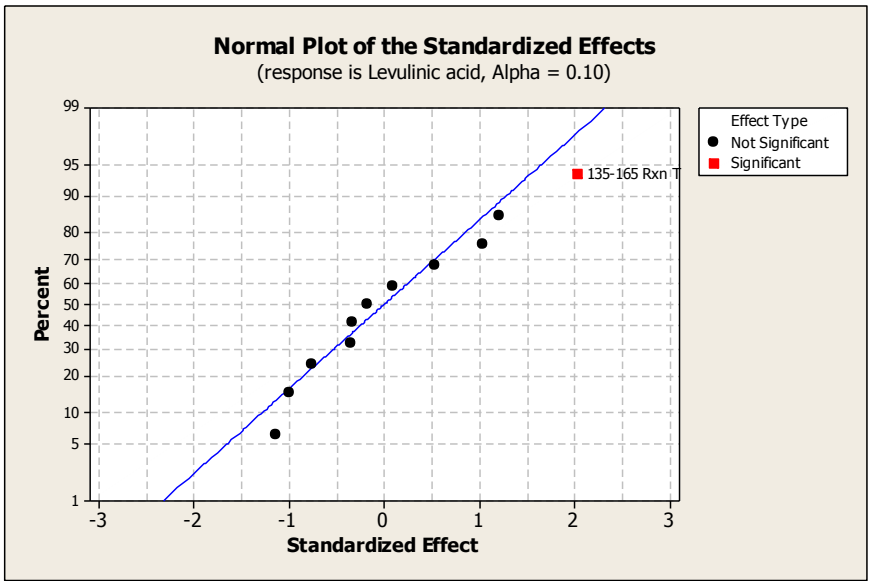
Normal Plot of the Standardized Effects
(response is Levulinic acid, Alpha = 0.10)
Percent
Standardized Effect
135-165 Rxn T
Effect Type
Not Significant
Significant

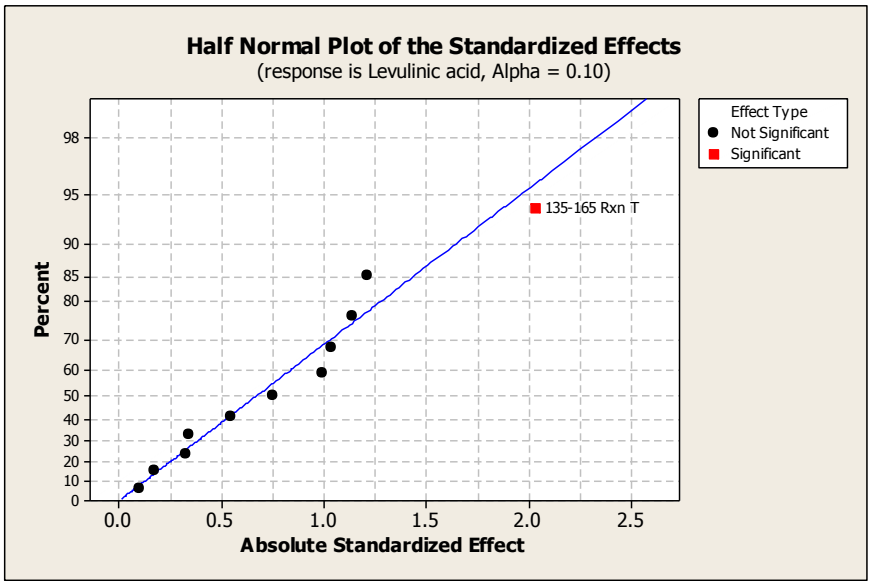
Half Normal Plot of the Standardized Effects
(response is Levulinic acid, Alpha = 0.10)
Percent
Absolute Standardized Effect
135-165 Rxn T
Effect Type
Not Significant
Significant

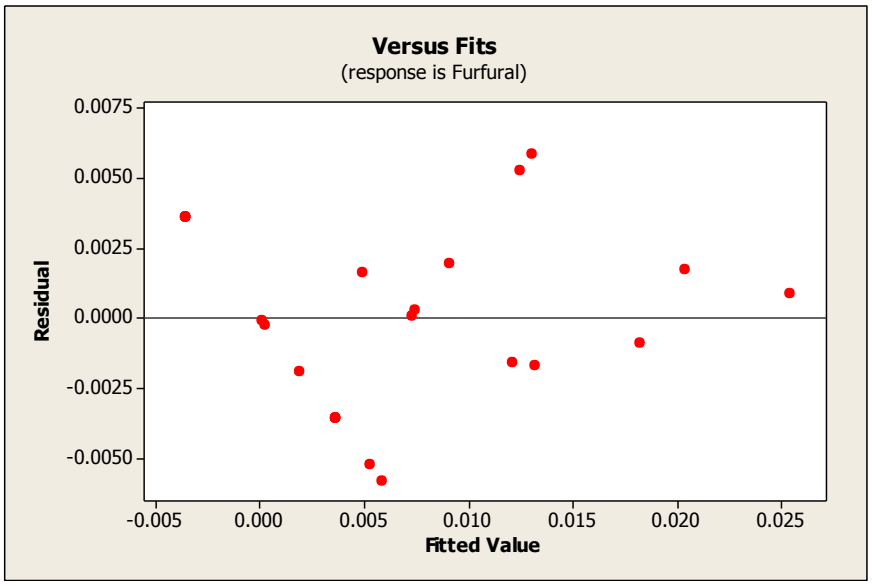
Versus Fits
(response is Furfural)
Residual
0.0075
0.0050
0.0025
0.0000
-0.0025
-0.0050
-0.005
0.000
0.005
0.010
0.015
0.020
0.025
Fitted Value

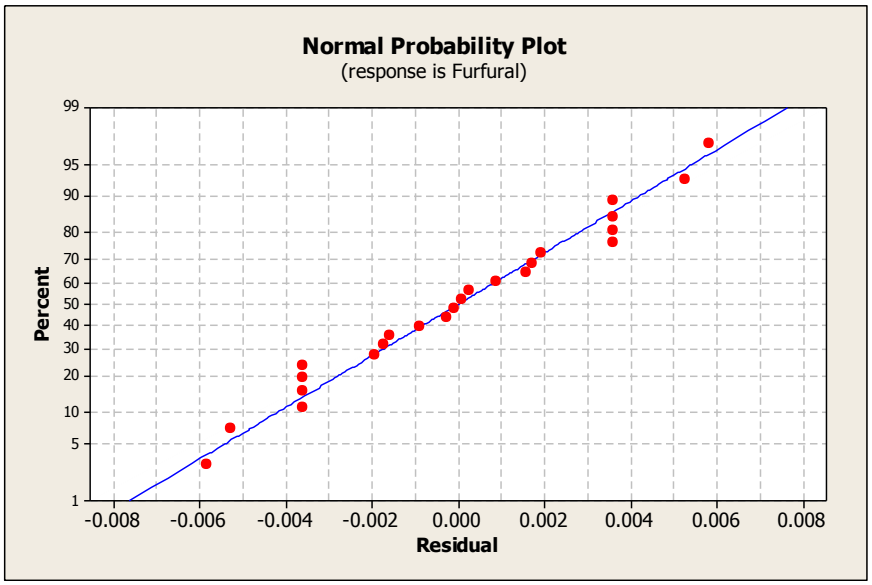
Normal Probability Plot
(response is Furfural)
Percent
99
95
90
80
70
60
50
40
30
20
10
5
1
-0.008
-0.006
-0.004
-0.002
0.000
0.002
0.004
0.006
0.008
Residual

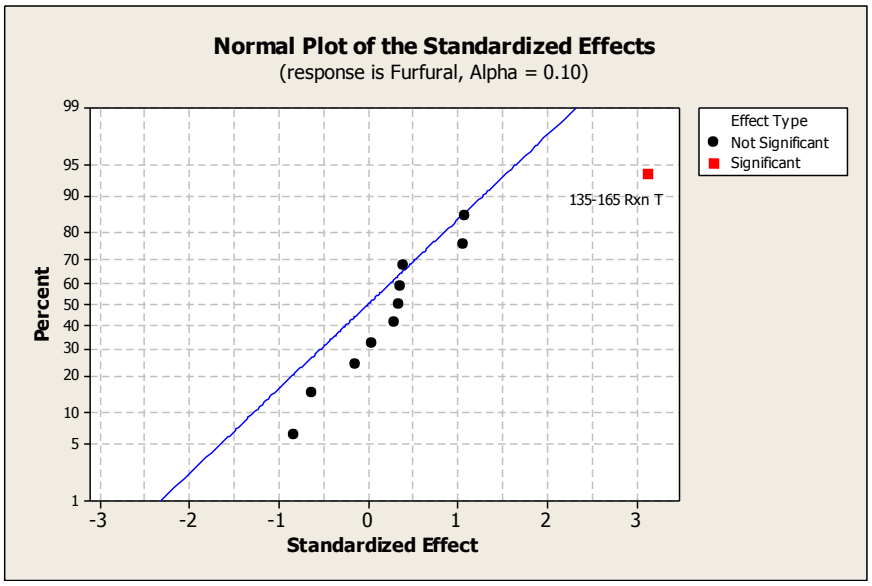
Normal Plot of the Standardized Effects
(response is Furfural, Alpha = 0.10)
Percent
Standardized Effect
135-165 Rxn T
Effect Type
Not Significant
Significant

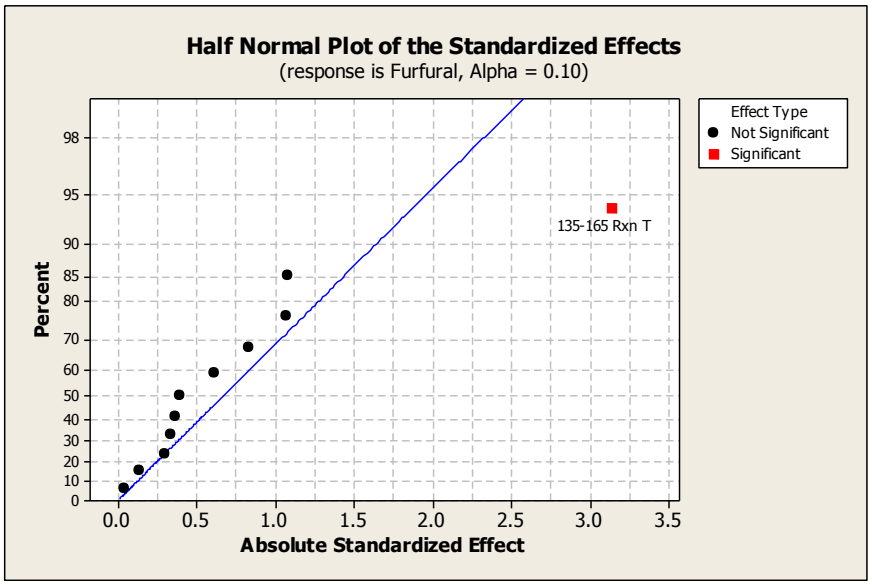
Half Normal Plot of the Standardized Effects
(response is Furfural, Alpha = 0.10)
Percent
Absolute Standardized Effect
135-165 Rxn T
Effect Type
Not Significant
Significant

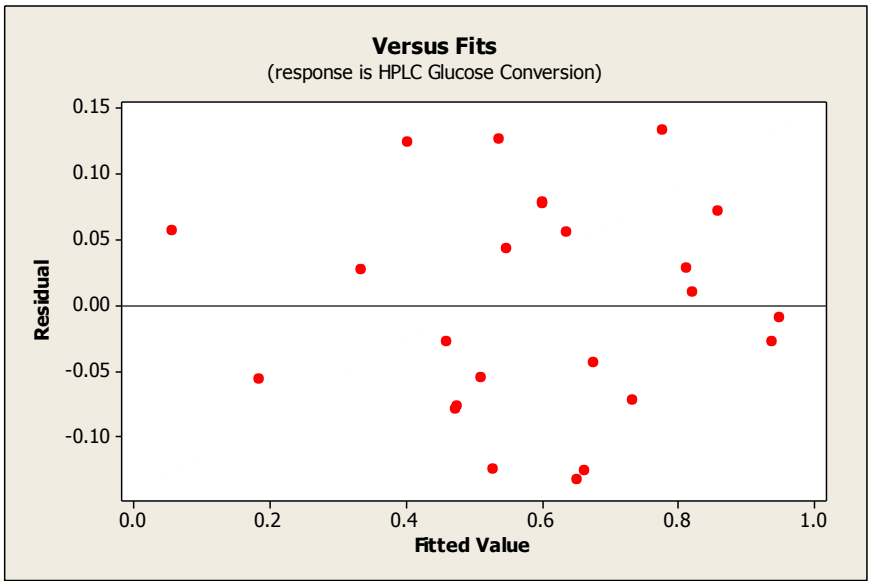
Versus Fits
(response is HPLC Glucose Conversion)
Residual
0.15
0.10
0.05
0.00
-0.05
-0.10
0.0
0.2
0.4
0.6
0.8
1.0
Fitted Value

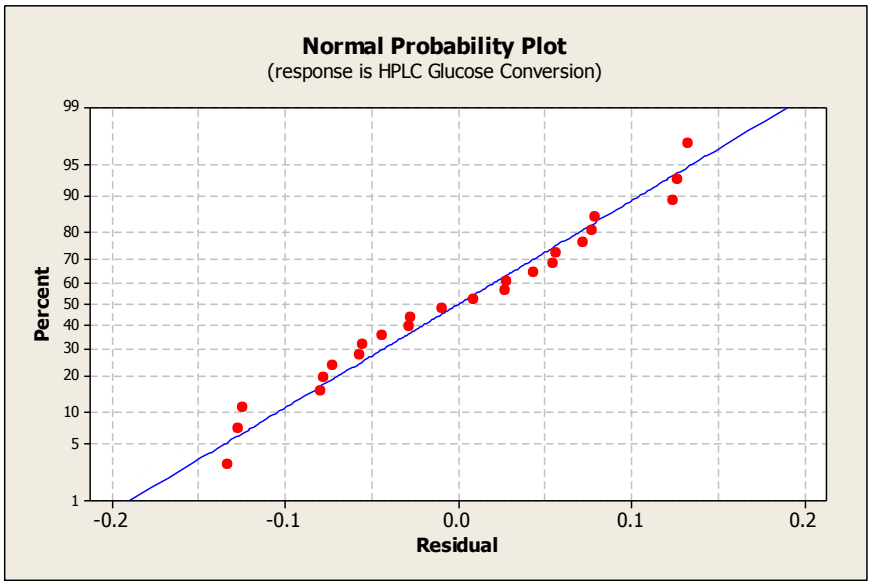
Normal Probability Plot
(response is HPLC Glucose Conversion)
Percent
99
95
90
80
70
60
50
40
30
20
10
5
1
-0.2
-0.1
0.0
0.1
0.2
Residual

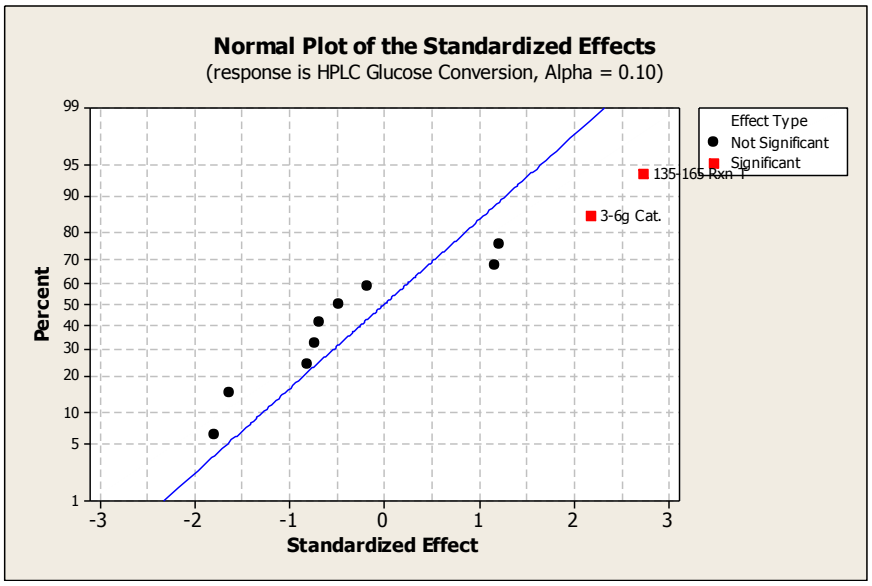
Normal Plot of the Standardized Effects
(response is HPLC Glucose Conversion, Alpha = 0.10)
Percent
Standardized Effect
Effect Type
Not Significant
Significant
135-165 Rxn T
3-6g Cat.

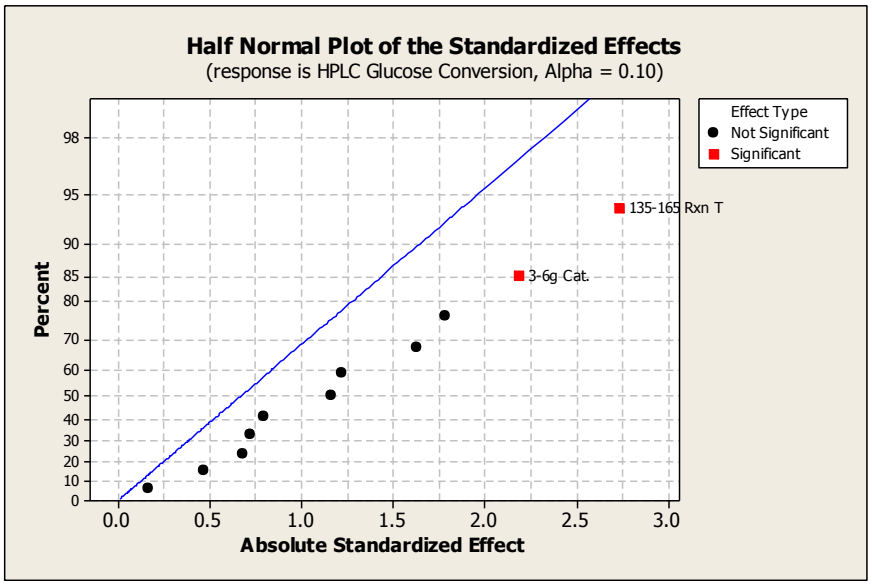
Half Normal Plot of the Standardized Effects
(response is HPLC Glucose Conversion, Alpha = 0.10)
Percent
Absolute Standardized Effect
Effect Type
Not Significant
Significant
135-165 Rxn T
3-6g Cat.

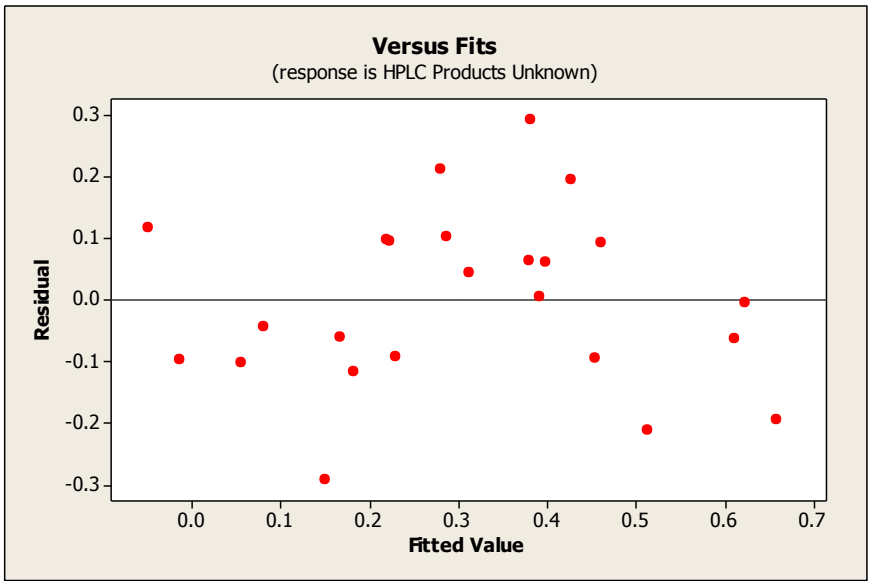
Versus Fits
(response is HPLC Products Unknown)
Residual
0.3
0.2
0.1
0.0
-0.1
-0.2
-0.3
0.0
0.1
0.2
0.3
0.4
0.5
0.6
0.7
Fitted Value

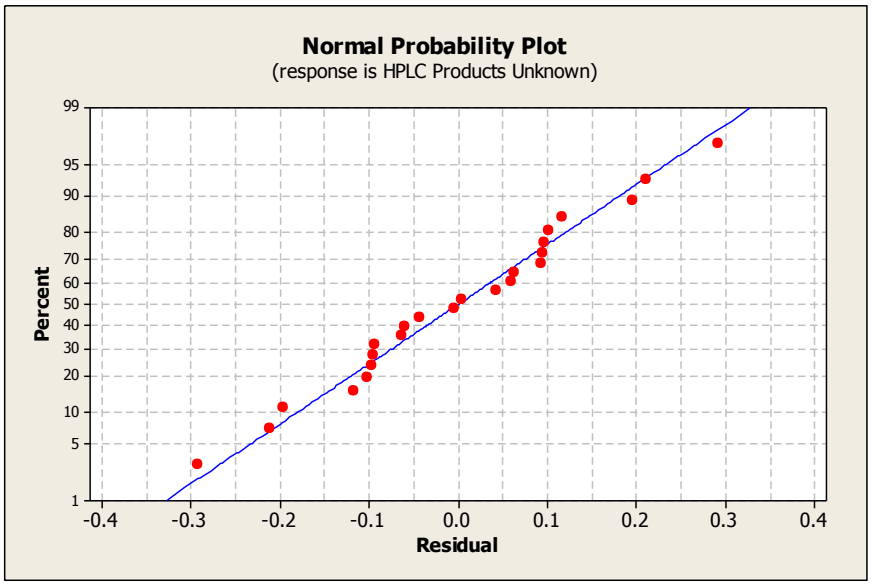
Normal Probability Plot
(response is HPLC Products Unknown)
Percent
99
95
90
80
70
60
50
40
30
20
10
5
1
-0.4
-0.3
-0.2
-0.1
0.0
0.1
0.2
0.3
0.4
Residual

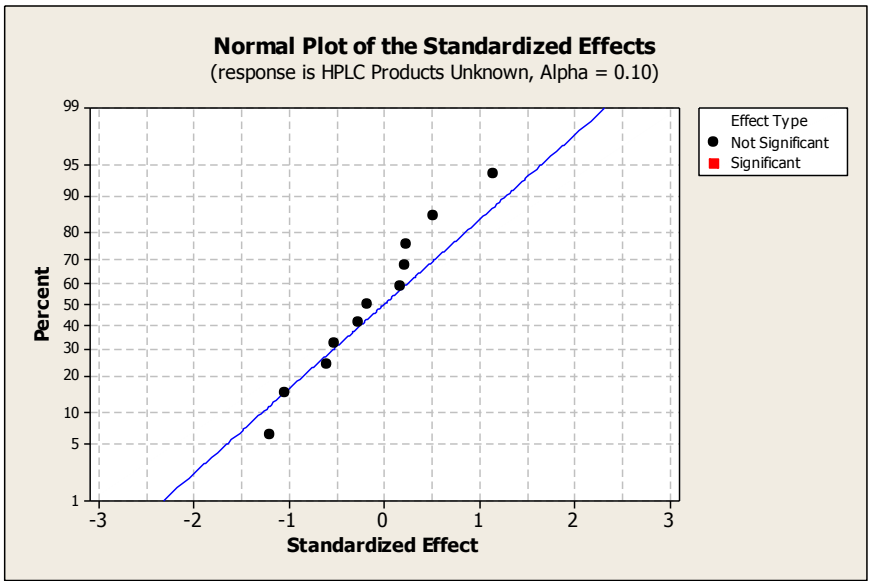
Normal Plot of the Standardized Effects
(response is HPLC Products Unknown, Alpha = 0.10)
Percent
99
95
90
80
70
60
50
40
30
20
10
5
1
-3
-2
-1
0
1
2
3
Standardized Effect
Effect Type
Not Significant
Significant

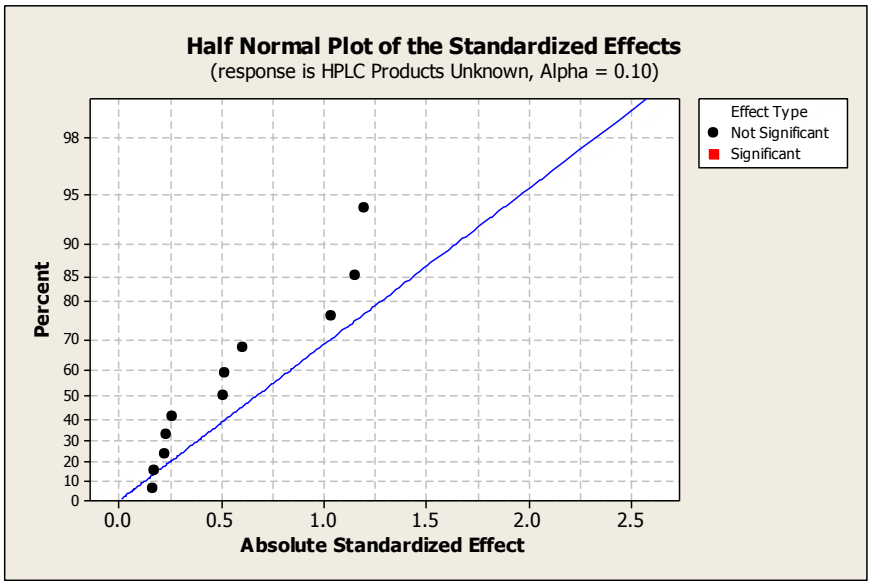
Half Normal Plot of the Standardized Effects
(response is HPLC Products Unknown, Alpha = 0.10)
Percent
98
95
90
85
80
70
60
50
40
30
20
10
0
0.0
0.5
1.0
1.5
2.0
2.5
Absolute Standardized Effect
Effect Type
Not Significant
Significant

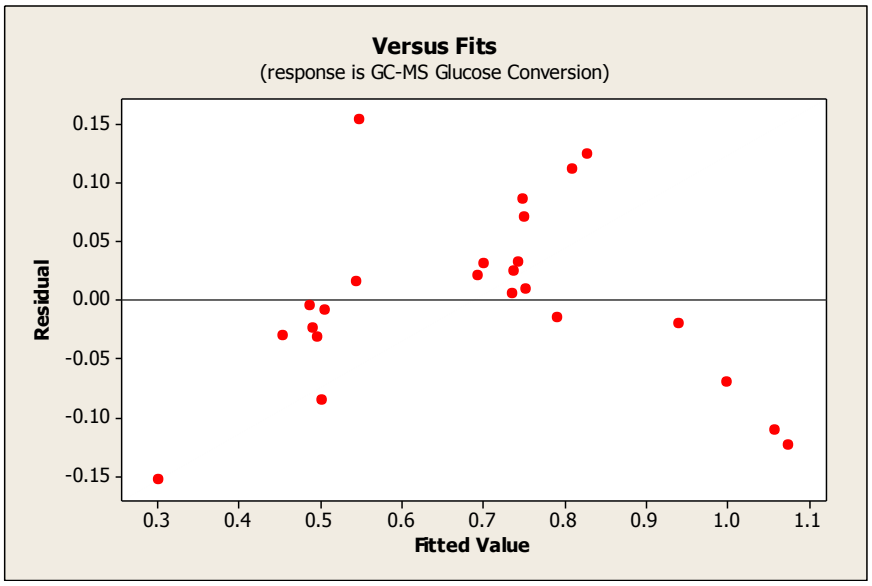
Versus Fits
(response is GC-MS Glucose Conversion)
Residual
0.15
0.10
0.05
0.00
-0.05
-0.10
-0.15
0.3
0.4
0.5
0.6
0.7
0.8
0.9
1.0
1.1
Fitted Value

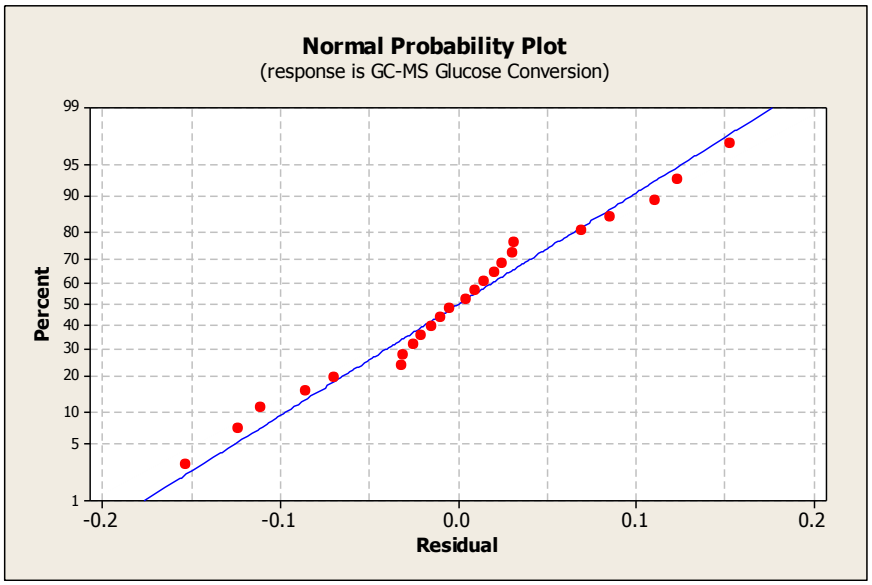
Normal Probability Plot
(response is GC-MS Glucose Conversion)
Percent
99
95
90
80
70
60
50
40
30
20
10
5
1
-0.2
-0.1
0.0
0.1
0.2
Residual

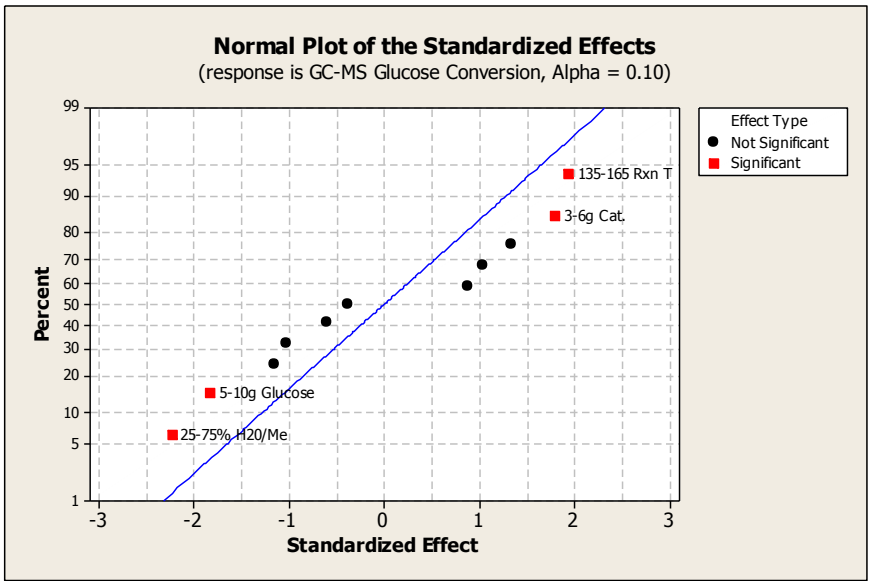
Normal Plot of the Standardized Effects
(response is GC-MS Glucose Conversion, Alpha = 0.10)
Percent
Standardized Effect
Effect Type
Not Significant
Significant
135-165 Rxn T
3-6g Cat.
5-10g Glucose
25-75% H20/Me

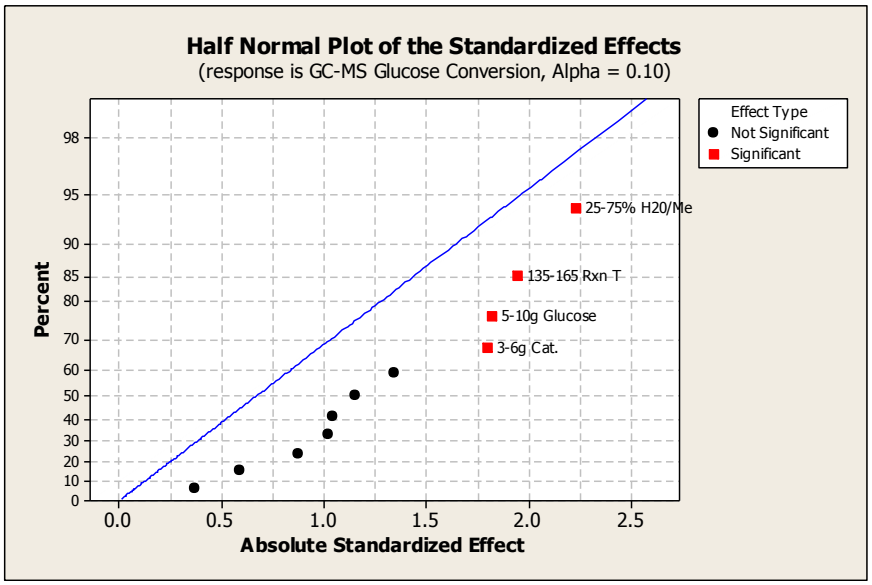
Half Normal Plot of the Standardized Effects
(response is GC-MS Glucose Conversion, Alpha = 0.10)
Percent
Absolute Standardized Effect
Effect Type
Not Significant
Significant
25-75% H20/Me
135-165 Rxn T
5-10g Glucose
3-6g Cat.

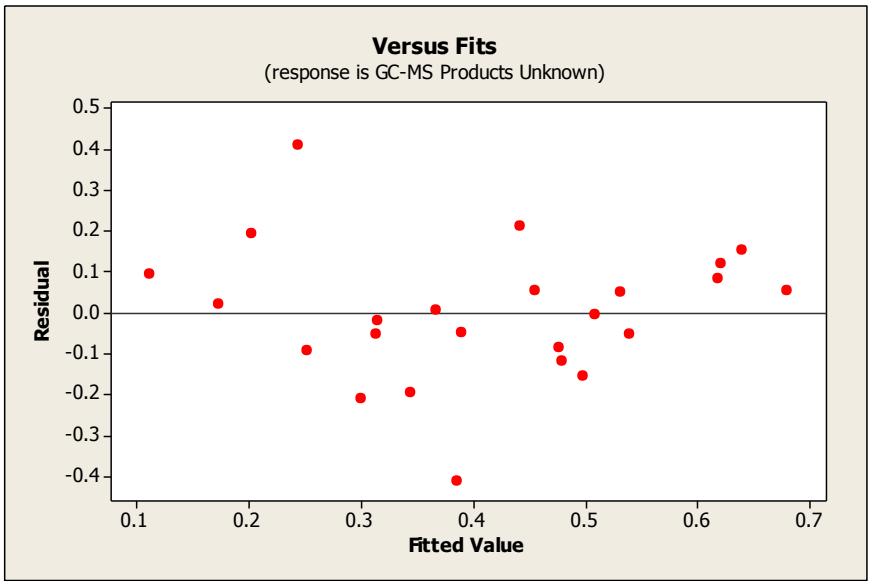
Versus Fits
(response is GC-MS Products Unknown)
Residual
Fitted Value
0.5
0.4
0.3
0.2
0.1
0.0
-0.1
-0.2
-0.3
-0.4
0.1
0.2
0.3
0.4
0.5
0.6
0.7

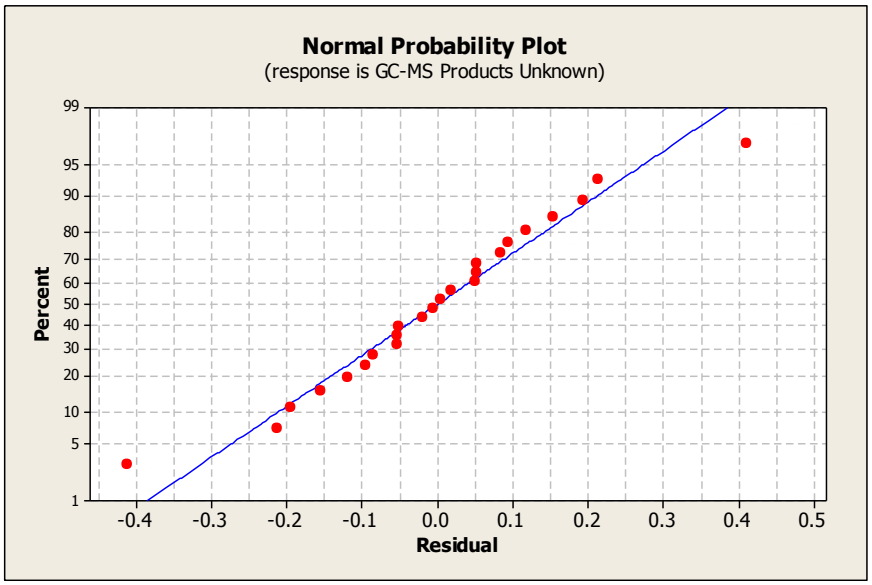
Normal Probability Plot
(response is GC-MS Products Unknown)
Percent
Residual
99
95
90
80
70
60
50
40
30
20
10
5
1
-0.4
-0.3
-0.2
-0.1
0.0
0.1
0.2
0.3
0.4
0.5

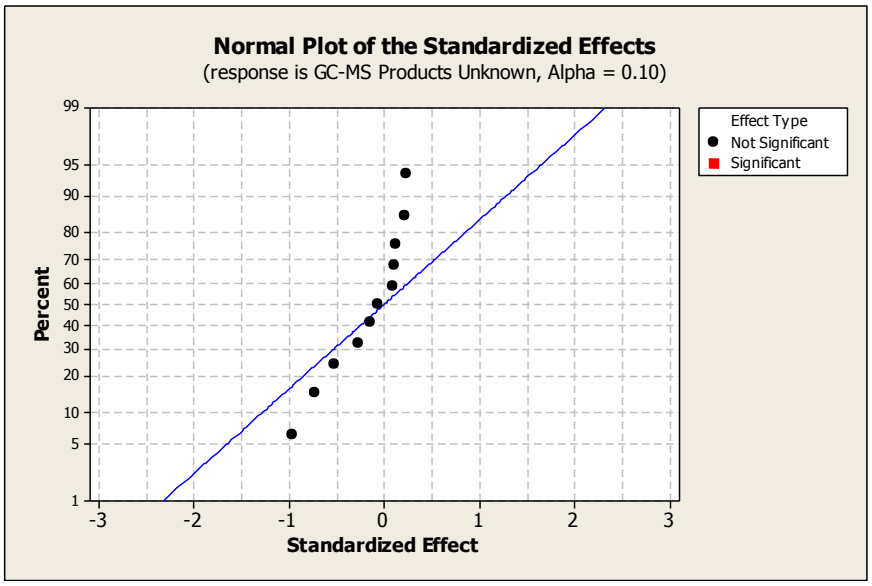
Normal Plot of the Standardized Effects
(response is GC-MS Products Unknown, Alpha = 0.10)
Percent
99
95
90
80
70
60
50
40
30
20
10
5
1
-3
-2
-1
0
1
2
3
Standardized Effect
Effect Type
Not Significant
Significant

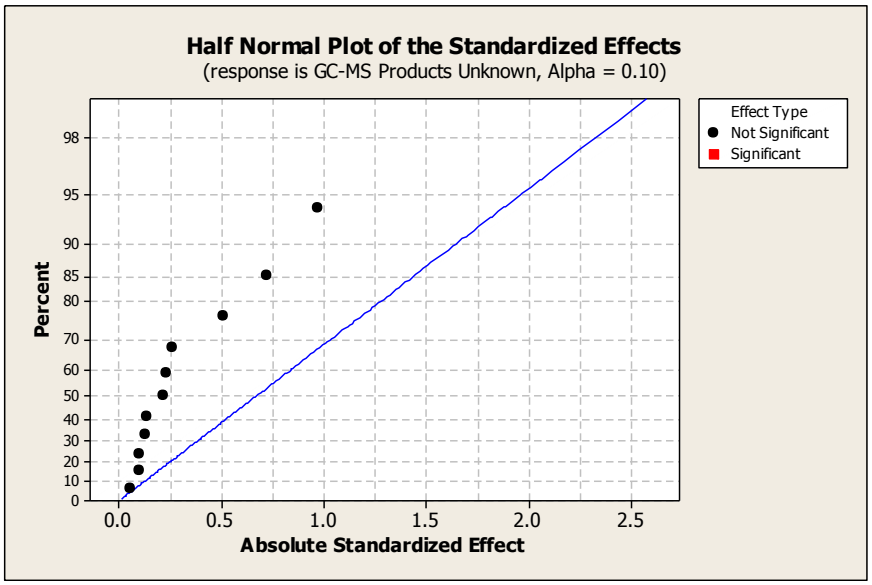
Half Normal Plot of the Standardized Effects
(response is GC-MS Products Unknown, Alpha = 0.10)
Percent
98
95
90
85
80
70
60
50
40
30
20
10
0
0.0
0.5
1.0
1.5
2.0
2.5
Absolute Standardized Effect
Effect Type
Not Significant
Significant

REFERENCES

[1] A. Muller, J. Schmidhuber, J. Hoogeveen and P. Steduto, "Some insights in the effect of growing bio-energy demand on global food security and natural resources," *Water Policy,* vol. 10, 2007.

[2] "Water Security: The Water-Energy-Food-Climate Nexus," World Economic Forum, Washington DC, 2011.

[3] O. Inderwildi and S. King, Energy, Transport, & the Environment, London: Spring-Verlag, 2012.

[4] "Bioenergy and Food Securit," Food and Agriculture Organization of the United Nations, Rome, 2010.

[5] P. Azadi, O. Inderwildi, R. Farnood and D. King, "Liquid fuels, hydrogen and chemicals from lignin: A critical review," *Renewable and Sustainable Energy Reviews,* vol. 21, pp. 506-523, 2013.

[6] R. Perlack, L. Wright, A. Turhollow, R. Graham, B. Strokes and D. Erbach, "Biomass as feedstock for a bioenergy and bioproducts industry: the technical feasibility of a billion-ton annual supply," OAK RIDGE NATIONAL LAB TN, 2005.

[7] R. Tol, T. Downing, O. Kuik and J. Smith, "Distributional aspects of climate change impacts," *Global Environmental Change Part A,* vol. 14, no. 3, pp. 259-272, 2004.

[8] N. Ravindranath and D. Hall, Biomass, energy, and environment: a developing country perspective from India., Oxford, United Kingdrom: Oxfor Universy Press, 1995.

[9] M. Tingem and M. Rivington, "Adaptation for crop agriculture to climate change," *Mitigation and Adaptation Strategies for Global Change,* vol. 14, pp. 153-168, 2009.

[10] A. Haines, R. Kovats, D. Campbell-Lendrum and C. Corvalan, "Climate change and human health: impacts, vulnerabiity and public heath," *Public Health,* vol. 120, pp. 585-596, 2006.

[11] I. Dincer, "Energy and environmental impacts: present and future perspectives," *Energy Sources, PartA: Recovery, Utilization, and Environmental Effects,* vol. 20, no. 4, pp. 427-453, 1998.

[12] N. Panwar, S. Kauski and S. Kothari, "Role of renewable energy sources in environmental protection: A review," *Renewable and Sustainable Energy Reviews,* vol. 15, pp. 1513-1524, 2011.

[13] B. Aebischer, B. Giovannini and D. Pain, "Scientific and technical arguments for the optimal use of energy," Internatinoal Energy Agency, Geneva, 19889.

[14] E. Worell, L. Bernstein, J. Roy, L. Price and J. Harnisch, "Industrial enery effieciency and climate change mitigration," *Energy Effieciency,* vol. 2, pp. 109-123, 2009.

[15] R. Sims, "Renewable energy: a response to climate change," *Solar Energy,* vol. 76, pp. 9-17, 2004.

[16] A. O'Sullivan and S. Sheffrin, Economics: Principles and Tools Second Edition, New Jersey: Prentice Hall, 2003.

[17] K. Alekkett, "Peak oil and the evolving strategies of oil importing and exporting countries: facing the hard truth about an import decline for the OECD countries," in *International Transport Forum, OECD/ITF*, 2007.

[18] C. Campbell and J. Laherrere, " Preventing the next oil crunch," *Scientific American,* vol. 278, pp. 77-83, 1998.

[19] J. Laherrere, "Oil peak or plateau?," in *St. Andrews Economy Forum.* , ASPO France, 2009.

[20] F. Robelius, "Giant Oil Fields-The Highway to Oil," in *Giant Oil Filds and their Importance for Future Oil Production*, Uppsala, 2007.

[21] D. Sperling, Two Billion Cars: Driving Towards Sustainability, New York: Oxford University Press, 2009.

[22] Energy Information Administration, World proved reserves of oil and natural gas, most recent estimates., Washington: EIA, 2009.

[23] U.S. Energy Information Administration, "Table 3a. International crude oil and liquid fuels supply, consumption and inventories," EIA, Washington, 2009.

[24] U.S. Energy Information Administration, "International Energy Outlook 2013," U.S. Energy Information Administration, Washignton, DC, 2013.

[25] N. Owen, O. Inderwildi and D. King, "The status of conventional world oil reserves - Hyper or cause for concern?," *Energy Policy,* vol. 38, no. 8, pp. 4743-4749, 2010.

[26] International Energy Agency, "Worl Energy Outlook 2008," IEA, Paris, France, 2008.

[27] United States Government Accountability Office, "Crude Oil: uncertainty about future oil supply makes it important to deveolp a strategy for addressing peak decline in oil production," USGAO, Washington DC, USA, 2007.

[28] G. Lafforgue, B. Magne and M. Mareaux, "Energy substitutions, climate change and carbon sinks," *Ecological Economics,* vol. 67, pp. 589-597, 2008.

[29] C. Christensen, J. Rass-Jansen, C. Marsden, E. Taarning and K. Egeblad, "The Renewable Chemicals Industry," *ChemSusChem,* vol. 1, pp. 283-289, 2008.

[30] D. Dodds and R. Gross, "Chemical from Biomass," *Science,* vol. 318, pp. 1250-1251, 2007.

[31] D. Klass, "Biomass for Renewable Energy, Fuels, and Chemicals," Academic Press, California, 1998.

[32] B. Palsson, S. Fathi-Afshar, F. Rudd and E. Lightfoot, "Biomass as a Source of Chemical Feedstocks: An Econmica Evaluation," *Science,* vol. 213, pp. 513-517, 1981.

[33] B. Kamm, "Production of Platform Chemicals and Synthesis Gas from Biomass," *Angewandte Chemie International,* vol. 46, no. 27, pp. 5056-5056, 2007.

[34] F. Lichtenthaler, Biorefineries-Industiral Processes and Products, Wiley-VCH: Weinheeim, 2006.

[35] H. Benninga, A History of Lactic Acid Making, Boston: Kluwer Academic Publishing, 1990.

[36] J. Jan Ness, Encyclopedia of Chemical Technology, New York: John Wiley and Sons, 1981.

[37] R. Datta, S. Tsai, P. Bonsignore, S. Moon and J. Frank, "Technological and economic potential of poly(lacic acid_ and lactic acid derivatives," *FEMS Microbiology Reviews,* vol. 16, pp. 221-231, 1995.

[38] M. Hartmann, Biopolymers from Reneable Resources, Berlin: Springer-Verlag, 1998.

[39] G. Kharas, F. Sanchez-Riera and D. Severson, Platics From Microbes, Munich: Hanser-Gardner, 1994.

[40] R. Conn, J. Kolstad, D. Bornezelleca, L. Dixler, B. Filer, B. LaDu and M. Pariza, "Safety assessment of polylactic for the use as a food-contact poymer," *Food and Chemical Toxicology,* vol. 33, no. 4, pp. 273-283, 1995.

[41] D. Garlotta, "A literature Review of Poly(Lactic Acid)," *Journal of Polymers and the Environment,* vol. 9, pp. 63-84, 2002.

[42] M. Holm, S. Saravanamurugan and E. Taarning, "Conversion of Sugars to Lactic Acid Derivatives Using Heterogeneous Zeotype Catalysts," *Science,* vol. 328, pp. 602-605, 2010.

[43] M. Bicker, S. Endres, L. Ott and H. Vogal, "Catalytic conversion of carboydrates in subcrittical water: A new chemical process for lacti acid production," *Journal of moclecular catalysis,* vol. 239, pp. 151-157, 2005.

[44] E. Taarning, S. Saravanmurugan, M. Holm, J. Xiong, R. West and C. Christensen, "Zeolite-Catalyzed Isomerization of Triose Sugars," *ChemSusChem,* vol. 2, no. 7, pp. 625-627, 2009.

[45] R. West, M. Holm, S. Saravanamurugan, S. Xiong, Z. Beversdorf, E. \. Taarning and C. Christensen, "Zeolite H-USY for the production of lactic acid and methyl lactate from C3 surages," *Journal of Catalysis,* vol. 269, pp. 122-130, 2010.

[46] M. Moliner, Y. Roman-Leshkov and M. Davis, "Tin-containing zeolites are highly active catalyst for the isomerization of glucose in water," *PNAS,* vol. 107, no. 14, pp. 6164-6168, 2010.

[47] M. Holm, Y. Pagan-Torres, S. Saravanamurugan, A. Riisager, J. Dumisic and E. Taarning, "Sn-Beta catalysed converstion of hemicellulosic sugars," *Green Chemisrty,* Vols. 702-706, no. 14, p. 2012, 2012.

[48] E. Taarning, S. Saravanamurugan and M. Holm, "Zeolite-catalyzed prepeation of alpha-hydroxy carboxylic acids and esters thereof". United States Patent 8,143,439, 27 March 2012.

[49] X. Yang and L. Liu, "Improved preperation of lactide from lactic acid using microwave irradation," *Polmer Bulletin,* vol. 61, pp. 177-188, 2008.

[50] D. Esposito and M. Antonietti, "Chemcial Conversion of Sugars to Lactic Acid by Alkaline Hydrothermal Processes," *ChemSusChem,* vol. 6, pp. 989-992, 2013.

[51] F. Chambon, N. Essayem, F. Rataboul, C. Pinel, A. Cabiac and E. Guillon, "Process for converting cellulose or lignocellulosic biomass using stable non-zeolite solid lewis acid based on tin or antimony alone or as a mixture". United States Patent 2013/0291734 A1, 24 October 2013.

[52] K. Tominaga, K. Satoh, A. Mori, S. Shimada, H. Tsuneki and Y. Hirana, "Method for productions lactic acids from carbohydrate-containting raw materials". United States Patent 2013/0204069 A1, 8 Aug 2013.

[53] M. Holm, S. Saravanamurugan and E. Taaring, "Supporting online material for conversion of sugars to lacti acid derivatieve using heterogenious zeotype catalysts," *Science,* vol. 328, p. 602, 2010.

[54] J. Bozell and G. Petersen, "A review on the production of levulinic acid and furanics from sugars.," *Green Chemistry,* vol. 12, no. 4, pp. 539-554, 2010.

[55] A. Meyers, M. Seefeld, B. Lefker, J. Blake and P. Williard, "Stereoselective alkylations in rigid systems," *Journal of American Chemistry Society,* vol. 120, pp. 7429-7438, 1998.

[56] A. Bitonti, I. McDonald, F. Salituro, J. Whitten, E. Farvi and P. Wright, "Novel indole derivatives useful to treat estrogen-related newplasms and disorders". World patent Patent 9522524, 1995.

[57] J. Jang and P. Rogers, "Effect of levulinic acid on cell growth and poly-beta-hydroxalkanoate production by Alcaligenes," *Biotechology Letters,* vol. 18, pp. 219-224, 1996.

[58] H. Aert, M. Genderen, G. Steenpaal, L. Nelissen, E. Meiger and J. Liska, "Modified poly(2,6-dimethyl-1,4-phenylene) ethers prepared by redistribution," *Macromolecules,* vol. 30, pp. 6056-6066, 1997.

[59] T. Taylor, W. Kielmeyer and C. Golino, "Emulsified furan resin-based binding compositions for glass fibers". World Patent Patent 9426677, 1995.

[60] J. Lai, "Preparation of mixed symmetrical azonitrile polyerization initiators". United States Patent 5010179, 1991.

[61] J. Bush, "Acylated nitrogen-based fouling conrol agents by reaction of amines with acylcarboxylic acids and alkenes". United States Patent 5851377, 1998.

[62] J. Tsucha and K. Yochida, "Skin cosmetics containing levulinates, glycyrisates, and resorcinol or isopropylmethylphenol". Japan Patent 05320023, 1994.

[63] P. Adams, R. Lange, R. Yodice, M. Baker and J. Kietz, "Intermediates useful for preparing dispersant-viscosity improvers for lubricating oils". Europe Patent 882745, 1998.

[64] M. Raidel and F. Aschenbrenner, "Absorbent item". World Patent Patent 9843684, 1998.

[65] K. Gundlach, L. Sanchez, C. Hanzlik, K. Brodsky, R. Colt and A. Montes, "Ink compositions for thermal ink-jet printing". United States Patent 5769929, 1998.

[66] M. Nakozato and Y. Konishi, "Bakable composition for blackening metal surface". Japan Patent 06280041, 1995.

[67] T. Oono, S. Saito, S. Shinohara and K. Takakuwa, "Fluxes for electric circuit board soldering and electic circuit boards". Japan Patent 08243787, 1996.

[68] A. Shimizu, S. Nishio, Y. Wada and I. Metoki, "Photographic processing method for processing silver halide photograhic light-sensitive matial". Europe Patent 704756, 1996.

[69] Y. Maekawa and Y. Miyaki, "Nonaueous secondary batteries with anodes containing amorphous chalcogen compounds or oxides". Japan Patent 09190820, 1997.

[70] T. Hille, "Transdermal resorption of pharmaceuticals from cupercooled melts". German Patent 4446600, 1996.

[71] W. Armstrong and E. Phillips, "Corrosion-inhibiting coatings compositions containing metal or amine salkts of ketoacids". Europe Patent 496555, 1993.

[72] K. Lourvanig and G. Rorrer, "Dehydration of glucose to organic acids in micropouous pillared clay catalyst," *Applied Catalyst A,* vol. 109, pp. 147-165, 1994.

[73] J. Jow, G. Rorrer, M. Hawley and D. Lamport, "Dehydration of D-fructose to levulinic acid over LZY zeolite catalyst," *Biomass,* vol. 14, pp. 185-194, 1987.

[74] J. Dahlmann, "Preparation of levulinic acid," *Chem. Ber.,* vol. 101, pp. 4251-4253, 1964.

[75] S. Fitzpatrick, "Manufacture of furfual and levulinic acid by acid degradation of legnocellulosic". World patent Patent 8910362, 1990.

[76] S. Fitzpatrick, "Production of levulinic acid by the hydroysis of carbohydrate-containing materials". World patent Patent 9640609, 1997.

[77] S. Saha and S. Sivasanker, "Influence of Zn- and Ga-doping on the conversion of ethanol to hydrocarbons over ZSM-5," *Catalysis Letters,* vol. 15, pp. 413-418, 1992.

[78] K. Nahid and W. Seames, "Seperation and Purifciation of Aromatics from Cracke Crop Oils using Sulfolate," Univiersity of North Dakota, Grand Forks, ND, 2009.

[79] M. Khambete and W. Seames, "Study of decarboxylation and alklation of catalyltically cracked soybean oil," University of North Dakota, Grand Forks, ND, 2005.

[80] J. Šťávová, J. Beránek, E. Nelson, B. Diep and A. Kubátová, "Limits of detection for the determination of mono- and dicarboxylic acids using gas and liquid chromatographic methods coupled with mass spectrometry," *J. Chrom. B: Analytical Techologies in the Biomedical and Life Sciences,* no. 879, pp. 1429-1438, 2011.

[81] J. Šťávová, D. Stahl, W. Seames and A. Kubatova, "Method Development for the Characterization of Biofuel Intermediate Products Using Gas Chromatography with Simultaneous Mass Spectrometric and Flame Ionization Detections," *J. Chrom. A,* no. 88, pp. 79-88, 2012.

[82] S. Bithi, "Process for lead free avgas octane enhancers from crop oils," University of North Dakota, Grand Forks, 2008.

[83] K. Jamshidi, S. Hyon and Y. Ikada, "Thermal characterization of polylactides," *Polymer,* vol. 29, pp. 2229-2234, 1988.